Applications of Spin-Coupled Valence Bond Theory

DAVID L. COOPER*

Department of Chemistry, University of Liverpool, P.O. Box 147, Liverpool L69 3BX, U.K.

JOSEPH GERRATT*

School of Chemistry, University of Bristol, Cantocks Close, Bristol BS8 1TS, U.K.

MARIO RAIMONDI*

Dipartimento di Chimica Fisica ed Elettrochimica, Università di Milano, Via Golgi 19, 20133 Milano, Italy

Received November 5, 1990 (Revised Manuscript Received May 13, 1991)

Contents

I. Introduction

Recent years have seen a very significant resurgence of interest in ab initio valence bond approaches. A major role in this renaissance has been played by spin-coupled valence bond (SCVB) theory. The SCVB approach is capable of yielding not only accurate potential energy surfaces for ground and *many* excited states but also provides crucial new insights into the structure and bonding in whole series of molecular systems of central significance in chemistry.

The many-electron problem cannot be solved exactly, and consequently there will always be several distinct approaches to this subject. Tensions between molecular orbital and valence bond approaches have existed since the early days of quantum theory, and it is certainly neither our purpose nor our ambition to engage in a sterile attempt to supplant the current impressive level of sophistication of MO-based methods. Nevertheless, the ideas and concepts of VB theory continue to underlie a very large part of modern molecular physics and of contemporary chemistry at the molecular level. The present degree of development of VB-based methods should be seen as enriching the field of quantum chemistry as a whole.

The SCVB approach is based on the single-configuration spin-coupled wave function, which provides a clear-cut physical picture of *correlated* electronic structure and constitutes an excellent starting point for more sophisticated multiconfiguration (SCVB) calculations. One key to the success of the spin-coupled wave function, and thus of the entire SCVB strategy, lies in the realization that all the orbitals must be allowed sufficient freedom to deform, including the possibility of delocalization onto other nuclear centres. Further important aspects include the complete optimization of all the orbitals, without *any* constraints on the overlaps between them, and the consideration of the full spin space.

The main purpose of this Review is to provide a survey of representative recent applications of the SCVB approach, which may be considered the proper generalization and modern development of the ideas of Heitler and London[1] and of Coulson and Fischer[2] to molecular electronic structure. Particular emphasis is placed on the physical interpretation of *correlated* electronic structure, as revealed by the simple single-configuration spin-coupled wave function. Representative multiconfiguration VB calculations are also described, in order to demonstrate that it is now possible to obtain highly accurate results while retaining a clear-cut visuality of each particular physical and chemical situation.

In addition to describing the capabilities of this modern form of VB theory, a subsidiary goal of this Review is to try to persuade those whose business is state-of-the-art MO-CI calculations that there is much to be gained from projecting highly correlated wave functions onto SCVB configurations. Such a procedure could be an important route to obtaining at least some physical and chemical insight from MO-based wave functions with as many as 10^6–10^9 determinants.

In view of the theme of this volume, namely applied quantum chemistry, as well as the availability of a number of recent reviews of the SCVB approach,[3-7] this Review is concerned mostly with recent *applications* of the approach, rather than with theoretical aspects. A characteristic feature of the method has been rapid advances in the range of systems that can be treated. We have tried to strike a balance in this Review be-

0009-2665/91/0791-0929$09.50/0

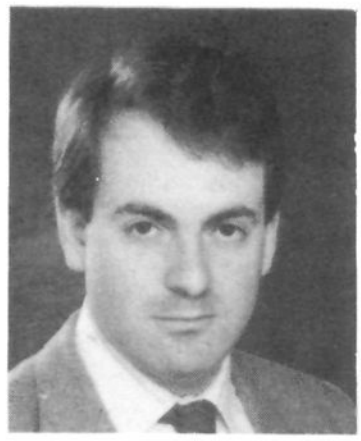

David L. Cooper was born in Leeds (UK) in 1957. He graduated in Chemistry from Oxford University (UK) in 1979 and obtained his D.Phil. in 1981 with W. G. Richards in Oxford. From 1981 to 1983 he held a Smithsonian Fellowship at the Harvard-Smithsonian Center for Astrophysics, before returning to Oxford for a further two years as a Royal Society University Lecturer. David moved to Liverpool University (UK) in 1985, where he is now a senior lecturer in Physical Chemistry.

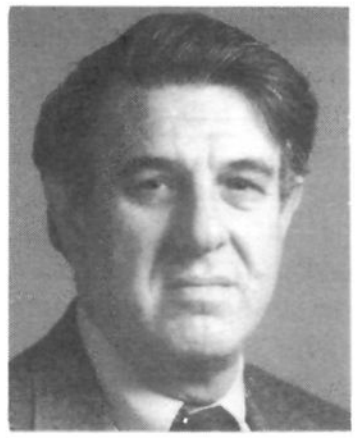

Joseph Gerratt, born in 1938, was brought up in Northampton (UK). He graduated in Chemistry from the University of Oxford in 1961 and obtained his Ph.D. in 1966 with I. M. Mills in Reading (UK). He was a post-doctoral fellow with W. N. Lipscomb at Harvard from 1966 to 1967, during which time he laid the foundations of spin-coupled theory, leading to a major paper published in *Advances in Atomic Molecular Physics* in 1971. After a lectureship at the University of East Anglia (UK), Joe moved to Bristol University (UK) in 1968, where he is now a Reader in Theoretical Chemistry.

Mario Raimondi was born in Gravedona (Como), Italy, in 1939. He graduated in Chemistry from the University of Milan (Italy) in 1963. From 1964 to 1967 he worked as a Research Assistant at Catania University (Sicily). He moved back to Milan in 1967, where he has developed sophisticated algorithms for carrying out valence bond calculations. Mario is now an Associate Professor of Physical Chemistry at Università di Milano.

Joe and Mario met one another at CECAM, Paris (France) in 1975. The ensuing cooperation led to the first publication on the spin-coupled valence bond method in *Proceedings of the Royal Society of London, A* in 1980. They were subsequently joined in 1982 by David, with the first joint paper published in 1984. The "Gang of Three" now collaborate very closely on a wide range of projects.

tween a general overview of various studies which may have been reviewed before, although not all in one place, and an account of "new" applications. Indeed, at the time of writing, a number of the latter have not yet appeared in print.

II. Theoretical Aspects

It is useful to view the SCVB approach in the wider context of quantum chemistry and so this section starts with very brief accounts of some of the salient features of MO and classical VB theory. This discussion also serves to highlight the similarities and differences in the two approaches, and to establish some of the notation to be used later.

A. Features of MO Theory

Electrons are fermions, and this means that in spite of the strong Coulombic repulsions between them, there are several important properties of many-electron systems that can be understood on the basis of an independent-particle model. For example, the aufbau principle for atoms is remarkable for its success in rationalizing the structure of the periodic table.

In its simplest form, the SCF molecular orbital theory wave function Ψ_{MO} for a closed-shell system consisting of $2n$ electrons can be written in the form of a Slater determinant based on n doubly occupied MO's, $\phi_1 - \phi_n$. However, for present purposes it is more useful to write it instead as

$$\Psi_{MO} = (2n!)^{-1/2}\,\mathcal{A}\,[\phi_1(\mathbf{r}_1)\phi_1(\mathbf{r}_2)\cdots\phi_n(\mathbf{r}_{2n-1})\phi_n(\mathbf{r}_{2n})\Theta^{2n}_{00;f}] \equiv \{\phi_1{}^2\phi_1{}^2\cdots\phi_n{}^2\} \quad (1)$$

where $\mathcal{A}$ is the usual antisymmetrizer, and $\Theta^{2n}_{00;f}$ is a $2n$-electron spin function of the form

$$\Theta^{2n}_{00;f} = (1/\sqrt{2})[\alpha(1)\beta(2) - \beta(1)\alpha(2)]\cdots (1/\sqrt{2})[\alpha(2n-1)\beta(2n) - \beta(2n-1)\alpha(2n)] \quad (2)$$

and describes n singlet pairs of electron spins.

The fundamental interpretation of MO theory in terms of bonding, nonbonding and antibonding orbitals arises most clearly when the MOs are expressed in terms of a *minimal* set of atomic orbitals. The interpretation of the MO's resulting from modern calculations using much more realistic basis sets can become exceedingly awkward. In addition, there is usually nothing for polyatomic molecules in the canonical MO's (i.e. those which form bases for irreducible representations of the molecular point group) which can be recognized as a chemical bond between different atoms. In general, MO wave functions are invariant to any unitary transformations of orbitals which remain doubly occupied in all configurations. It may be possible to choose transformations which result in more localized orbitals, but such manipulations correspond to imposing our preconceptions as to the nature of the electron distribution in a particular molecule.

One of the most serious shortcomings of the SCF wave function is its inability to describe correctly the making and breaking of chemical bonds, processes which lie at the very heart of chemistry. A very significant improvement in this respect is provided by the use of MCSCF wave functions, consisting of several distinct configurations Ψ_I constructed from a common set of orthonormal orbitals

$$\Psi_{MCSCF} = \sum_I c_I \Psi_I \quad (3)$$

MCSCF calculations involve full optimization of the coefficients c_I and of all the orbitals occurring in the Ψ_I. In practice, it usually turns out to be most convenient

to employ the "complete active space" or CASSCF expansion consisting of all possible orbital products which can be generated from the chosen set of active orbitals and of active electrons. With appropriate choices of the active space, any required process of molecular dissociation can be described correctly.

The number of configurations which occur in such a CASSCF expansion increases very rapidly both with the number of active electrons and with the number of active orbitals. Nevertheless, with modern algorithms[8] calculations with, say, 12 electrons distributed in 12 orbitals are becoming routine. The total number of configurations for this example is 2.3×10^5 for a singlet state, and 1.1×10^6 for a triplet, neglecting any simplifications which may arise from using the molecular point group symmetry. The interpretation of such a wave function, which typically consists of significant contributions from many configurations, now presents serious problems.

It has become fairly common to refer, albeit rather loosely, to dynamical and nondynamical electron correlation effects. The distinction is far from clear but, *in general terms*, nondynamical correlation effects are those which must be included to ensure correct dissociation, and these are relatively easy to treat. For an N-electron system, it is useful for the purposes of this Review to *define* the "nondynamical correlated energy" as that obtained using a CASSCF wave function with an active space consisting of N electrons and N orbitals. Dynamical correlation effects, which are in general more difficult to treat, then account for the further difference between this nondynamical correlated (NDC) wave function and the exact solution of the usual electronic structure problem.

A typical recipe for constructing a CASSCF wave function which ensures correct dissociation is first to decide which electrons are to be considered as valence electrons and then to distribute these in all the valence orbitals in all possible ways which give the appropriate molecular symmetry. For a system with N valence electrons, such a procedure typically involves less than N valence orbitals, so that the NDC wavefunction is something of a special case. It does, however, represent the best that one can do without "going outside the valence space". Of course, many CASSCF calculations are much more extensive than this and include more orbitals than just those required for proper dissociation, and thus already take some account of dynamical correlation.

In general, further quantitative refinement of the CASSCF description, i.e. the inclusion of (further) dynamical correlation, is achieved via the introduction of additional configurations, without further optimization of the orbitals. Unfortunately, the resulting CI expansions are very slowly convergent, as everyone is aware. The *initial* slow convergence of the expansion is due, at least in part, to the unsuitability of the unoccupied or virtual orbitals. In the case of a neutral molecule, for example, these virtual orbitals are typically too diffuse and are instead more suitable for describing the molecular negative ion. Ultimately, of course, the slow convergence can be traced to the difficulties inherent in any attempt to describe properly the r_{12} cusp without explicit consideration of terms linear in the interelectronic coordinates.

B. Classical VB Theory

Whereas MO theory was originally developed to explain the electronic spectra of molecules, rather than the nature of bonding, the classical VB approach was chiefly concerned with problems of valency and with the associated *stability* (or otherwise) of molecular states.

Chemistry is replete with regular patterns, some of which are of great subtlety. Nearly all of the observed regularities, at least among molecules, can be understood on the basis that they are formed from atoms or from smaller fragments with characteristic properties. Consequently, it seems obvious that our theoretical description of molecular electronic structure should reflect this fact. Furthermore, if we do so, then we necessarily include in a direct way at least a proportion of the type of electron correlation that is most important to the chemical properties of molecules.

This is expressed in the approach of Heitler and London,[1] or of "classical" valence bond theory, in which the wave function for a molecule is constructed from wave functions for the constituent atoms:

$$\Phi_{HL} = 1s_a(1)1s_b(2) + 1s_b(1)1s_a(2) \qquad (4)$$

A central concept in classical VB theory is that of the exchange interaction, which arises from the requirement that the wave function must be antisymmetric with respect to the interchange of electrons formally associated with the different atoms (or fragments). The magnitude of this exchange energy depends critically on the degree of overlap (i.e. nonorthogonality) between the different orbitals.

As is well known, the role of the exchange integral in covalent bonding can be generalized to give a consistent, but always qualitative, explanation of a whole range of phenomena, including valence itself, the saturation of valency, the shapes of simple molecules, the properties of multiple bonds, and the avoided intersections between "zeroth-order" potential curves.

Although the concepts of VB theory possess a compelling clarity and simplicity, any straightforward attempt to translate them into quantitative form turns out to be very disappointing, quite apart from the inherent technical difficulties. The most obvious remedy, as for MO-based approaches, is to include further configurations or structures. However, it is then greatly disconcerting to discover that even in preeminently covalent systems, such as hydrocarbons, the most important contributions can arise from ionic structures. In general, the number of ionic structures that must be included increases rapidly with size of system and, as a result, the original clarity of the VB approach is lost.

Even in the case of H_2, classical VB theory suggests significant contributions from ionic structures. However, the true role of ionic structures in this case was first revealed by Coulson and Fischer[2] who rewrote the wave function in the form

$$\Phi_{CF} = \phi_1(1)\phi_2(2) + \phi_2(1)\phi_1(2) \qquad (5)$$

The orbitals ϕ_1 and ϕ_2 are now to be regarded as *deformed* hydrogenic 1s functions

$$\phi_1 = 1s_a + \lambda 1s_b$$

$$\phi_2 = 1s_b + \lambda 1s_a \qquad (6)$$

in which the deformation takes the form of a slight *delocalization* from one center onto the other. Substituting eq 6 into eq 5 we obtain

$$\Phi_{CF} = (1 + \lambda^2)\Phi_{HL} + (2\lambda)\,\Phi_{ION} \tag{7}$$

where Φ_{HL} is the covalent contribution defined in eq 4, and Φ_{ION} is the corresponding ionic contribution

$$\Phi_{ION} = 1s_a(1)1s_a(2) + 1s_b(1)1s_b(2) \tag{8}$$

The parameter λ plays two equivalent roles. On the one hand, λ determines the extent of the deformation of the orbitals ϕ_1 and ϕ_2. On the other, it determines the degree of mixing of the ionic structure Φ_{ION} with the covalent structure Φ_{HL}.

In other words, the presence of ionic structures in the classical VB description of H_2 can be interpreted as the deformation of the atomic orbitals, resulting from molecule formation. Furthermore, the extent of the deformation in H_2 varies in a perfectly reasonable way with interatomic separations. For values of the internuclear distance R close to the equilibrium separation R_e, orbitals ϕ_1 and ϕ_2 in eq 5 have a considerable overlap, and this gives rise to a large negative exchange interaction, which in turn is necessary to furnish a good description of the bond. As R increases toward infinity, λ tends to zero, and so ϕ_1 and ϕ_2 assume pure atomic form, as one would expect.

At this stage, a choice has to be made between orbitals which are strictly localized on individual centres and orbitals which are allowed to delocalize onto other centers. In general, it turns out that a very small amount of delocalization of an essentially localized orbital onto neighboring centers can correspond to a fairly large total weight from classical VB ionic structures. The price to be paid for *insisting* that the valence bond description of a molecule is based on strictly localized orbitals can be a high one. Realistic descriptions in this case usually require a large perturbation to the original picture, typically in the form of many ionic structures. On the other hand, if one allows the orbitals complete freedom to deform toward neighboring centers, the perturbation to the original picture can be very small. Although there might be particular instances in which it is useful to insist on purely localized orbitals, it is clear that the modern development of VB theory should be based on orbitals which are not constrained in this way.

Finally, it is perhaps worthwhile to emphasize the quality of the simple Coulson–Fischer wave function for H_2. Optimizing only the single parameter λ, it is possible to obtain ca. 85% of the observed binding energy. The calculated value of R_e is within 0.015 Å of the experimental value, and the potential curve remains qualitatively correct over the entire range of R.

C. Spin-Coupled Theory

In extending to an N-electron system the ideas of Heitler and London,[1] and particular those of Coulson and Fischer,[2] we are led to the following form of wave function

$$\Psi_{SM} = (N!)^{1/2} \sum_{k=1}^{f_S^N} c_{Sk}\mathcal{A}[\phi_1\phi_2\cdots\phi_N\Theta_{SM;k}^N]$$
$$\equiv \{\phi_1\phi_2\cdots\phi_N\} \tag{9}$$

which we call the *spin-coupled wave function*. Each electron is described by a distinct orbital ϕ_μ, which is determined by expanding it in a set of basis functions χ_p, which are usually simple analytical representations (of Gaussian or Slater type) of atomic orbitals centered on *all* the nuclei of the molecule:

$$\phi_\mu = \sum_{p=1}^{m} c_{\mu p}\chi_p \tag{10}$$

In general, all of these singly occupied orbitals are nonorthogonal.

It turns out that the optimal orbitals are usually very localized with immediately recognizable parentage. The fact that the orbitals are both singly occupied and highly localized means that the electrons are able to avoid one another, so that the spin-coupled wave function necessarily incorporates a considerable degree of electron correlation. At the same time, the overlap between the orbitals allows for the necessary quantum interference effects which give rise to the various types of bonding interactions.

An important feature of the spin-coupled wave function is the occurrence in it of linear combinations of N-electron spin functions $\Theta_{SM;k}^N$, each of which is an eigenfunction of $\hat{S}^2$ and of $\hat{S}_z$. It follows that the spin-coupled configuration is also an eigenfunction of $\hat{S}^2$ and of $\hat{S}_z$. The index k denotes the particular mode of coupling the individual electron spins to produce the required resultants S and M. The total number of such distinct modes of coupling for each value of M is given by

$$f_S^N = \frac{(2S + 1)N!}{(\frac{1}{2}N + S + 1)!(\frac{1}{2}N - S)!} \tag{11}$$

There are many different ways of constructing the $\Theta_{SM;k}^N$, with the most appropriate choice being dictated to a large extent by the nature of the problem being studied, and also by computational convenience. Provided we use the *full* spin space of f_S^N functions, as is usually the case in spin-coupled calculations, then it is relatively straightforward to transform between different bases. For an account of different spin bases, and of the relationships between them, see, for example, ref 9.

A commonly used method of constructing the $\Theta_{SM;k}^N$ is to couple together the individual electron spins, one at a time, according to the usual rules for combining angular momenta, such that each partial spin function is an eigenfunction of $\hat{S}^2$. A particular mode of coupling the spins of N electrons to give a resultant S is then fully defined by a vector of $N - 1$ partial spins. This successive coupling is conveniently visualized by means of the *branching diagram* in Figure 1, whereby the vectors of partial spins may be interpreted as rightwards paths across the diagram; the figures in the circles are the values of f_S^N. The set of functions formed in this way is known by various names, including the "standard" basis, the genealogical basis, and the Yamanouchi–Kotani basis. The $\{\Theta_{SM;k}^N, k = 1, 2, \cdots, f_S^N\}$ constitute a complete orthonormal set and form a basis for an irreducible representation (irrep) of $\mathcal{S}_N$, the symmetric group of degree N.

In the case of molecular dissociation, it is often possible to obtain much additional insight by considering also nonstandard bases. For example, if a system with

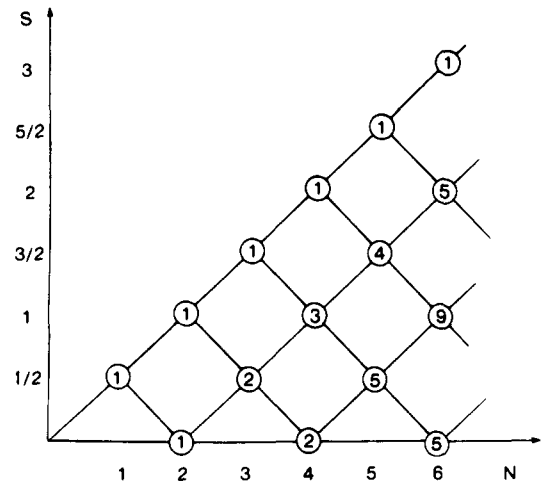

Figure 1. Branching diagram representation of the standard genealogical basis of spin functions.

$N' + N''$ electrons breaks up into two fragments A and B with N' and N'' electrons, respectively, then it is appropriate to form spin functions $\Theta^{N'}_{S'M';k'}$ and $\Theta^{N''}_{S''M'';k''}$ characteristic of the two subsystems, and then to couple these together to form the total spin function. Such a set of spin functions, which is sometimes described as an $N_A \times N_B$ basis, can reveal in a very direct way which states of the fragments are important as the molecule is formed.

A basis of central importance in classical VB theory is the Rumer basis, which highlights the significance of bonded pairs of electrons in molecules. These spin functions are constructed by coupling together the spins of pairs of electrons to form singlets, except for the last $2S$ electrons (if $S > 0$). Of course, it is then possible to couple together these pairs in a large number of ways and thereby produce an overcomplete set, but well-established procedures are available for selecting a complete linearly independent set of f^N_S functions. The Rumer functions are nonorthogonal.

Another basis of some utility is obtained by coupling together the spins of pairs of electrons to form either singlets or triplets. These pairs are then coupled together sequentially, in much the same way as for the genealogical functions, so as to give the overall resultant spin, S. This set of spin functions, which is known as the Serber basis, is orthonormal, but it does not correspond to standard representations of $\mathcal{S}_N$. The Serber basis is a useful, but much less used, alternative to the standard basis, to which it is connected by an orthogonal transformation.

In the spin-coupled wave function, all the orbital coefficients $c_{\mu p}$ in eq 10 and all the spin-coupling coefficients c_{Sk} in eq 9 are fully optimized simultaneously. The means by which this is achieved is described very briefly later. It is worth emphasizing that the orbitals which result from a spin-coupled calculation are unique in the sense that there is usually *no* freedom whatsoever to subject them to linear transformations (so as to produce delocalized orbitals, for example) without at the same time changing the entire wave function.

The use of a linear combination of spin functions, and the simultaneous optimization of all the orbitals, ensures that any process of molecular dissociation can be described correctly. The spin-coupling coefficients c_{Sk} are sensitive indicators of the behavior of the wave function and describe the processes of spin uncoupling and recoupling as the atoms move about on the potential surface. In many cases, the dominant mode of spin coupling remains characteristic of separated fragments over an unexpectedly wide range of internuclear distances. Not until the interacting systems approach within a critical distance, typically 4–5 bohr for processes involving first-row atoms, do the values of the spin-coupling coefficients begin to alter. They then change to values characteristic of the newly formed molecule with surprising abruptness.

The expectation value of the energy of the wave function in eq 9 can be written

$$E = \frac{1}{\Delta}\left[\sum_{\mu,\nu}^{N} \mathbf{D}(\mu|\nu)h_{\mu\nu} + \tfrac{1}{2}\sum_{\mu,\nu,\sigma,\tau}^{N} \mathbf{D}(\mu\nu|\sigma\tau)g_{\mu\nu\sigma\tau}\right] \qquad (12)$$

where Δ is the normalization integral

$$\Delta = \langle \Psi_{SM} | \Psi_{SM} \rangle \qquad (13)$$

and $h_{\mu\nu}$ and $g_{\mu\nu\sigma\tau}$ are the usual one- and two-electron integrals transformed to the spin-coupled orbital basis. The $\mathbf{D}(\mu|\nu)$ and $\mathbf{D}(\mu\nu|\sigma\tau)$ are, respectively, elements of the one-electron and two-electron spinless density matrices, and contain all the effects of the nonorthogonality of the orbitals. The scheme used to optimize the orbitals requires density matrices up to order four, and the efficient determination of all the required orders of density matrices plays a central role in current implementations of the spin-coupled approach.

We should mention a useful procedure which lies part way between the SCF and spin-coupled approaches, namely the so-called "generalized valence bond" or GVB method. According to this approach, each doubly occupied orbital ϕ_i in the SCF wave function is replaced by two distinct orbitals ϕ_i and ϕ_i' which overlap with one another, but each pair of orbitals is required to remain orthogonal to all the other orbital pairs of the system. In general, only the perfect-pairing (PP) spin function is retained. The "strong orthogonality" (SO) constraint removes much of the computational complexity of the spin-coupled approach, while still providing for a significant part of the (nondynamical) correlation energy of the singlet-coupled pairs of electrons.

The "GVB-SOPP" model can furnish a correct description of the dissociation of an electron-pair bond, but it is not particularly suitable for the description of more complex processes. As a very simple example, it is useful to consider the reaction $H + H_2 \rightarrow H_2 + H$, for which the spin-coupled description is based on three fully optimized nonorthogonal orbitals and both modes of spin coupling for $N = 3$ and $S = {}^1/_2$. This leads to a description which is of a uniform quality over the entire potential surface. However, in the GVB-SOPP approach, the strong orthogonality constraint allows only *two* of the orbitals to overlap, and so a uniform description of the simultaneous making and breaking of the H–H bonds requires the introduction of further configurations.

Two basic computational strategies are currently used by our group to calculate all the various orders of density matrices required for optimizing spin-coupled wave functions. The first of these is known as the "symmetric group approach", and the more recent

scheme, which has distinct advantages when dealing with larger numbers of electrons, is known as the "super-cofactor approach". Another efficient strategy for optimizing wave functions constructed from nonorthogonal orbitals has been described recently by Verbeek, van Lenthe, and co-workers.[10]

The symmetric group approach has been described in some considerable detail in previous reviews.[3,6] It can be shown that the Nth-order density matrix for an N-electron system is related to purely group-theoretical quantities, namely the representation matrices for the irrep of $\mathcal{S}_N$ labeled by S and N. The full set of $N!$ $f_S^N \times f_S^N$ dimensional matrices, plus the c_{Sk} coefficients, are sufficient to calculate the Nth-order (spinless) density matrix, $\mathbf{D}(\mu_1\mu_2\cdots\mu_N|\nu_1\nu_2\cdots\nu_N)$, without any knowledge of the form of the orbitals.[11] The different orders of density matrices are related to one another by a hierarchy of relations reminiscent of the Laplace expansion of a determinant. For example,

$$\mathbf{D}(\mu_1\mu_2\mu_3|\nu_1\nu_2\nu_3) = \sum_{\nu_4}\mathbf{D}(\mu_1\mu_2\mu_3\mu_4|\nu_1\nu_2\nu_3\nu_4)\langle\mu_4|\nu_4\rangle \quad (14)$$

where it is understood in the notation for the density matrices that orbital indices which occur on the same side of a vertical bar may never be equal to one another. In actual practice, the fourth-order density matrix is computed directly from the Nth-order density matrix by means of the relation

$$\mathbf{D}(\mu_1\mu_2\mu_3\mu_4|\nu_1\nu_2\nu_3\nu_4) = \sum_{\nu_5\cdots\nu_N}\mathbf{D}(\mu_1\cdots\mu_N|\nu_1\cdots\nu_N)\langle\mu_5|\nu_5\rangle\cdots\langle\mu_N|\nu_N\rangle \quad (15)$$

and the lower order density matrices are obtained successively by means of eq 14, and its analogues.

In the super-cofactor approach,[12] the spin-coupled wave function is first expressed as a linear combination of Slater determinants U_i constructed from nonorthogonal spin-orbitals:

$$\Psi_{SM} = \sum_I b_I U_I \quad (16)$$

For each pair of determinants, U_I and U_J, we can construct $\mathbf{D}_{IJ}$, the matrix of overlap integrals between the orbitals appearing in the two determinants. Cofactors of first to fourth order, i.e. $\mathbf{D}_{IJ}(\mu_1|\nu_1)$ to $\mathbf{D}_{IJ}(\mu_1\mu_2\mu_3\mu_4|\nu_1\nu_2\nu_3\nu_4)$, can be generated from $\mathbf{D}_{IJ}$ by striking out appropriate rows and columns. It is useful to define the symbol $\delta_{IJ}(\mu\nu)$ which is unity if the spin of the μth spin-orbital in U_I matches the spin of the νth spin-orbital in U_J, but is zero otherwise. The fourth-order density matrix, for example, can then be written in the form

$$\mathbf{D}(\mu_1\mu_2\mu_3\mu_4|\nu_1\nu_2\nu_3\nu_4) = \sum_{I,J} b_I b_J \delta_{IJ}(\mu_1\nu_1)\delta_{IJ}(\mu_2\nu_2)\delta_{IJ}(\mu_3\nu_3)\delta_{IJ}(\mu_4\nu_4) \times \mathbf{D}_{IJ}(\mu_1\mu_2\mu_3\mu_4|\nu_1\nu_2\nu_3\nu_4) \quad (17)$$

It is important to note that the same fourth-order cofactor can arise from the deletion of rows and columns from the overlap matrices associated with different pairs of Slater determinants. The number of *unique* cofactors of a given order remains fairly small, even for relatively large numbers of electrons. The number of cofactors of different orders which must be processed in the super-cofactor approach are listed in Table I. It is clear that the total amount of information which must be processed increases in a very acceptable way with increasing N. Further simplifications arise from the fact that the cofactors can be factorized into α- and β-spin blocks of smaller dimensions.

TABLE I. The Various Numbers n_i of ith-Order Cofactors (i = 1,2,3,4) Which Must Be Computed for Singlet Systems

N	n_1	n_2	n_3	n_4
6	120	21	0	0
8	1596	406	36	0
10	22155	7260	1035	55
12	314028	122760	24310	2211

The density matrices, computed by either strategy, are then used to build the gradient vector $\mathbf{g}$ of the energy with respect to all the variational parameters ($c_{\mu p}$ and c_{Sk}), and the corresponding second derivative or hessian matrix $\mathbf{G}$. In MCSCF codes, the dimension of the hessian is usually rather large; usual approaches involve constructing directly the action of $\mathbf{G}$ on the vector of variational parameters $\mathbf{c}$. In the case of spin-coupled theory, $\mathbf{G}$ is usually relatively small, and so it is convenient to compute it explicitly. Exactly as in MCSCF approaches, the various coefficients are updated by a Newton–Raphson-type scheme, with modifications of diagonal elements to ensure a positive-definite hessian.

The particularly efficient strategy used to update the variational parameters in the current versions of the spin-coupled programs is known as the "stabilized Newton–Raphson procedure". In general, this scheme, which is based on the analysis of Goldfeld, Quandt, and Trotter,[13] has excellent convergence characteristics. Let $\delta\mathbf{c}$ denote the vector of corrections to all the orbital and spin-coupling coefficients, and let $\mathbf{d}$ denote the actual corrections made at the previous iteration. The stabilized Newton–Raphson procedure, also known as GQT2, can then be summarized:

$$(\mathbf{G} + \alpha\mathbf{Q})\delta\mathbf{c} = -\mathbf{g}$$

$$\alpha = |\epsilon_0| + R|\mathbf{g}|$$

$$Q_{ij} = \delta_{ij} + (\beta^2 - 1)d_i d_j / \sum_i d_i^2 \quad (18)$$

where R plays the role of a step length, ϵ_0 is the most negative eigenvalue of $\mathbf{G}$, and β is a parameter which controls the significance attached to the particular direction defined by the previous set of corrections. The initial value of R is 0.1, and this is modified according to an algorithm which involves the ratio of the expected (second-order) energy improvement to that actually achieved. Similar considerations apply to β, which takes an initial value of 0.9. When the gradients are sufficiently small and ϵ_0 is positive, i.e. $\mathbf{G}$ is positive definite, α is set to zero and the "pure" Newton–Raphson procedure is used.

In many applications we wish to describe only a part of an N-electron system by spin-coupled wave functions, and accordingly we divide the electrons into active and inactive sets, in much the same way as in CASSCF calculations. The spin-coupled wave function now assumes the form

$$\Psi_{SM} = (N!)^{1/2}\sum_{k=1}^{f_S^N} c_{Sk}\mathcal{A}(\psi_1^2\psi_2^2\cdots\psi_n^2\,\phi_1\phi_2\cdots\phi_N\Theta_{00;f}^{2n}\Theta_{SM;k}^{N}) \equiv \{\psi_1^2\psi_2^2\cdots\psi_n^2\,\phi_1\phi_2\cdots\phi_N\} \quad (19)$$

in which $2n$ "core" electrons are accommodated in n orthogonal doubly occupied orbitals $\psi_1, \psi_2, \cdots, \psi_n$ and N active electrons are accommodated in N distinct nonorthogonal singly occupied spin-coupled orbitals $\phi_1, \phi_2, \cdots, \phi_N$. The total number of electrons is, of course, $2n + N$. Orbitals $\phi_1 \cdots \phi_n$ may always be orthogonalized to all of the "core" orbitals $\psi_1 \cdots \psi_n$ without changing the total wave function.

In practice, molecular orbitals are usually determined by carrying out an SCF or an appropriate CASSCF calculation with an atom-centered basis set $\{\chi_p, p = 1, 2, \cdots, m\}$. From this one selects n orbitals $\psi_1 \cdots \psi_n$ on the basis of orbital energy, or after first localizing the orbitals, or on some other chemical grounds. The remaining $m - n$ occupied and virtual molecular orbitals are then used as basis functions for the N spin-coupled orbitals. This use of molecular orbitals is entirely equivalent to the use of the original χ_p basis functions, but it greatly simplifies the incorporation of the orthogonality between the "core" orbitals and the spin-coupled orbitals.

D. Spin-Coupled Valence Bond Wave Functions

It is useful first to define two terms, namely configuration and structure. We use the term *configuration* to denote a particular orbital product, with all possible modes of coupling together the electron spins. On the other hand, *structure* is used to denote a particular orbital product together with a particular mode of spin coupling. The spin-coupled configuration in eq 9, for example, corresponds to f_S^N structures.

By allowing double occupancy of the orbitals $\phi_1 \cdots \phi_N$ optimized in the spin-coupled wave function, it is possible to generate many additional configurations, which we call spin-coupled ionic configurations. In classical VB theory it is conventional to refer to structures with doubly occupied orbitals as singly ionic, doubly ionic, etc. In spite of the changed significance of such orbital products in spin-coupled theory, where orbitals need not be strictly localized on individual centers, we continue to adhere to this nomenclature.

The SCVB wave function consisting of the N-electron spin-coupled configuration and of *all* spin-coupled ionic configurations coincides exactly with our definition in section II.A of the NDC wave function, i.e. the CASSCF wave function with an active space consisting of N electrons and N orbitals. The NDC wave function corresponds to a "full-VB" or a "full-CI" calculation *in this space*. Note that the numbers of structures, in the first case, and of configuration state functions, in the other, necessarily coincide.

The spin-coupled wave function can be considered to provide the best single-configuration representation of the NDC wave function. In general, we find that the spin-coupled model accounts for most of the energy difference between the Hartree–Fock and NDC wave functions. An equivalent statement is that the contributions from spin-coupled ionic configurations are small. This is a direct consequence of fully optimizing the orbitals without insisting on strict localization. Indeed, for up to six electrons, the spin-coupled energy is usually within 1 or 2 mhartree of the NDC value obtained with the same basis set. Furthermore, an analogue of Brillouin's theorem applies, so that singly ionic configurations cannot interact directly with the spin-coupled configuration. In most circumstances, the role of spin-coupled ionic configurations can simply be ignored when interpreting the SCVB wave function.

We now consider the further refinement of the spin-coupled wave function by the addition of structures which include orbitals that are not occupied in the ground state. This procedure gives rise to a "nonorthogonal configuration interaction" scheme, and the multiconfiguration VB wave functions constructed in this way are known as SCVB wave functions.[14] This same procedure also produces excited states of the N-electron system, and one of the great surprises in this work has been the large number of states that can be obtained to a worthwhile accuracy.

When the spin-coupled calculation has converged, the gradient vector $\mathbf{g}$ is essentially null (and the second derivative matrix $\mathbf{G}$ is positive definite). The orbitals then satisfy equations which can be cast in the form

$$\hat{F}_\mu^{(\mathrm{eff})} \phi_\mu = \epsilon_\mu \phi_\mu \tag{20}$$

Each operator $\hat{F}_\mu^{(\mathrm{eff})}$ ($\mu = 1, 2, \cdots, N$) is hermitian, and possesses a complete set or "stack" of orthonormal solutions which we denote $\phi_\mu^{(i)}$ ($i = 1, 2, \cdots, m$). In general, orbitals in different stacks are not orthogonal to each other. One solution in each stack, $\phi_\mu^{(1)}$ for example, coincides with the occupied orbital ϕ_μ already found, and the others are termed virtual orbitals.

Although eq 20 is reminiscent of Hartree–Fock orbital equations, the $\hat{F}_\mu^{(\mathrm{eff})}$ are in fact *very* different from a Fock operator. Each $\hat{F}_\mu^{(\mathrm{eff})}$ is constructed from quantities in which occupied orbital ϕ_μ is missing. Consequently, the $\phi_\mu^{(i)}$ correspond to the motion of one electron in the field of the other $N - 1$ electrons, which is a reasonably realistic representation of the actual physical situation. The energies $\epsilon_\mu^{(i)}$ represent the average energy of the electron in the corresponding orbital in the presence of all the other electrons. Spin-coupled theory is not an independent particle model and so there is no simple relation between the $\epsilon_\mu^{(i)}$ and the total energy of the molecule or the first ionization potential, as in MO theory.

Additional configurations may be generated by replacing one, two, or more occupied orbitals by virtual orbitals from their respective stacks. Such replacements may be termed "vertical" excitations. It is usual also to consider ionic structures, with double occupancy of one or more orbitals, as the inclusion of these generally introduces relatively little additional computational expense. The final SCVB wave functions are very compact, and consist of a linear combination of the structures derived from the spin-coupled configuration and of those derived from typically 10^2–10^3 excited configurations:

$$\Psi_{SM} = (N!)^{1/2} \sum_{i_1 \cdots i_N} \sum_k c_{Sk}(i_1 \cdots i_N) \mathcal{A}[\phi_1^{i_1} \phi_2^{i_2} \cdots \phi_N^{i_N} \Theta_{SM;k}^N] \tag{21}$$

In actual calculations, we choose a set of orbitals $\phi_\mu^{(i)}$ from each stack according to the nature and extent of the states we wish to describe. The coefficients $c_{Sk}(i_1 \cdots i_N)$ for each state, and the corresponding total energies, are determined by constructing the matrix of the hamiltonian over the chosen set of structures, and diagonalizing.

The SCVB wave function in eq 21 represents the simultaneous expansion of the total electronic wave

function in N distinct orthonormal sets of orbitals. The different sets or stacks are not orthogonal to one another. The $\phi_\mu^{(i)}$ are obtained by solving for the motion of the electron in fairly realistic potentials, and so the set can be regarded as providing a reasonably optimal expansion for electron coordinate r_μ in the total wave function. It is reasonable, therefore, to expect that the expansion in eq 21 will converge more rapidly than traditional MO-CI expansions, at least initially.

The construction of the hamiltonian matrix, and of the corresponding overlap matrix, is carried out by means of a very flexible "cofactor-driven" nonorthogonal CI program. The cofactor-driven algorithm is based upon the Löwdin expression for matrix elements between Slater determinants constructed from nonorthogonal spin–orbitals. Not only can the same cofactor of dimension $N - 2$ arise from different pairs of Slater determinants but each Slater determinant can occur in the expansion of numerous structures. A single pass through the list of unique cofactors is sufficient to compute all the matrix elements between structures. In actual fact, the cofactors have block diagonal form, because of the orthogonality of α and β spin–orbitals, and so the program deals only with determinants of fairly small dimension.

The nonorthogonal CI stage of the SCVB calculation enables us to refine the spin-coupled description as much as is desired. In actual practice, the ground state is usually described sufficiently well by the addition of a number of singly and doubly excited structures. Some triple or quadruple excitations are necessary to obtain good accuracy for spectroscopic constants, and to ensure size consistency of the final wave function.

The resulting ground state potential energy surfaces are closely parallel to those yielded by very extensive CASSCF-CI calculations, and the corresponding SCVB wave functions provide accurate values of one-electron properties, such as dipole moments. Further improvements could undoubtedly be gained by including larger numbers of configurations in the calculations, but, so far at least, this has not appeared to be a worthwhile effort.

It is important to emphasize that the spin-coupled configuration by itself reproduces with very reasonable accuracy all the features of a ground state potential energy surface. This configuration plays a dominant role in the SCVB wave function for the ground state, and its contribution varies relatively little with nuclear geometry. In no case so far has the addition of further structures brought about any significant qualitative change in the description of the molecule provided by the single-configuration spin-coupled wave function. Indeed, one of the chief uses of the nonorthogonal CI calculations has been to confirm that this is indeed the case.

Analogous statements hold for excited states. As a result of the manner in which the orbitals $\phi_\mu^{(i)}$ are obtained, almost all excited states of interest are described well by just one or two configurations. The dominant configurations for these excited states typically correspond to single excitations from the spin-coupled configuration. The qualitative interpretation of these states, and the identification of dissociation limits, is thus very straightforward. It usually turns out that the description of the excited states is refined by many of the structures already involved in the SCVB expansion of the ground state. In some cases, it is useful also to include configurations generated by single, double, etc. excitations from the "reference" configurations for the low-lying excited states.

Using large, well-chosen basis sets, it is usually possible with compact SCVB wave functions to obtain a consistently high level of accuracy over the entire range of nuclear geometry for large numbers of widely differing states spanning a wide range of energy. Examples are given in section IV.

The SCVB approach is thus a flexible and very powerful procedure. The method incorporates characteristic concepts and ideas (such as fairly localized orbitals which are allowed to deform, and the recoupling of electron spins as the nuclear geometry varies) which have a direct and appealing interpretation in terms of the actual physics and chemistry of the systems under study.

III. Applications of Spin-Coupled Theory (Single Spatial Configuration)

It is expedient at this stage to restate, very briefly, some of the assertions made in section II. For an N-electron system, it is useful for the purposes of this Review to *define* the "nondynamical correlated energy" as that obtained using a CASSCF wave function with N active electrons and N active orbitals. Dynamical correlation effects then account for the further difference between this nondynamical correlated (NDC) wave function and the exact solution of the usual electronic structure problem. From this viewpoint, the spin-coupled wave function can be considered to be the best single-configuration representation of the NDC wave function. In general, the spin-coupled model accounts for most of the energy difference between the Hartree–Fock and NDC wave functions. An equivalent statement is that the contributions from spin-coupled ionic configurations are small.

From the point of view of *interpretation*, the spin-coupled model has obvious advantages over a CASSCF wave function which has significant contributions from many configurations. Furthermore, the spin-coupled configuration provides an excellent reference function for the inclusion of dynamical correlation effects, and all of our experience to date suggests that the spin-coupled configuration dominates the final multiconfiguration spin-coupled VB wave function for all nuclear geometries.

As a consequence of these considerations, we may claim that the spin-coupled model provides an excellent description of the *correlated* motion of electrons in molecules, and that the physical picture is not significantly altered by further refinement of the wave function. The purpose of this section is to examine the correlated electronic structure of a diverse range of molecules as revealed by applications of spin-coupled theory. In section IV we consider the inclusion of dynamical correlation effects.

A. Hybridization and the C–H Bond

The deduction of the tetrahedral arrangement of four equivalent bonds in methane was of fundamental importance to the whole of organic chemistry, long before

modern experimental techniques for structure determination became available or the advent of quantum mechanics. The Hartree–Fock description, based on the configuration $(1a_1)^2(2a_1)^2(1t_2)^6$, bears little relationship to the traditional view of four localized bonds between carbon and hydrogen. Indeed, according to Coulson,[15] "such a description presents more problems than it solves, for it is well known that the C–H bond has characteristic properties, such as its length, force constant and polarity, which, while not exactly constant, vary only relatively little from molecule to molecule". Of course, it is possible to take linear combinations of the canonical MO's so as to obtain new orbitals which are essentially localized in each C–H bond, but the criteria which lie behind such a procedure are somewhat arbitrary and correspond to imposing our preconceptions as to the nature of the bonding.

The classical VB description, as introduced by Pauling,[16] is much more appealing in this respect. Each of the four equivalent covalent bonds is taken to arise from the overlap of a 1s function on a hydrogen atom and one of four (orthogonal) sp^3 hybrids on carbon, with singlet coupling of the associated electron spins. Unfortunately, actual ab initio implementations of this simple idea are very disappointing. In order even to match the SCF energy in a given basis set, it is necessary to include large numbers of ionic configurations.[17] This all but destroys the conceptual appeal of the original model, which rapidly becomes very muddled.

It turns out that the spin-coupled description of the valence electrons of CH_4, in which the eight valence electrons are described by eight distinct nonorthogonal *fully optimized* orbitals, closely resembles Pauling's pioneering view, but there are also important differences.[18] However, it is more instructive for our present purposes to start with a consideration of methylene, CH_2, for which the $^1A_1$–$^3B_1$ excitation energy has been a testing ground for many theoretical approaches. Compact multiconfiguration spin-coupled VB calculations for CH_2 predict[19] a value for the singlet–triplet splitting which compares favorably with the full-CI value obtained with the same basis set. These calculations, in which both states are treated on an equal footing with 202 spatial configurations derived from a single reference configuration in each case, are described in section IV, and we concentrate here on the single-configuration spin-coupled reference configuration.

Spin-coupled orbitals for the six valence electrons of the $^3B_1$ ground state and the $^1A_1$ excited state of CH_2 are shown in Figures 2 and 3. For the $^3B_1$ state, orbitals ϕ_1 and ϕ_3 take the form of distorted sp^2-like hybrids on carbon. Contrary to the assumptions of classical VB theory, these two orbitals are not orthogonal but have an overlap of $\Delta_{13} \approx 0.5$. However, each of these orbitals overlaps most strongly ($\Delta_{12} \approx 0.8$) with one of a pair of distorted H(1s) functions, orbitals ϕ_2 and ϕ_4, to which it points.[20] The two remaining orbitals accommodate the two nonbonding electrons, and take the form of the remaining lobe of the sp^2-like hybrid, pointing away from the hydrogen atoms, and of a p function with its principal axis perpendicular to the molecular plane. The dominant mode of spin coupling (94.7% in the Kotani basis) corresponds to two C–H bonds and to triplet coupling of the spins of the nonbonding electrons.

TABLE II. Overlap Integrals between the Spin-Coupled Orbitals for the Valence Electrons of CH_2 (For the labeling of the orbitals see Figures 2 and 3)

$^1A_1$

	ϕ_1	ϕ_2	ϕ_3	ϕ_4	ϕ_5	ϕ_6
ϕ_1	1	0.80	0.49	0.17	0.42	0.00
ϕ_2		1	0.17	−0.08	0.21	0.00
ϕ_3			1	0.80	0.42	0.00
ϕ_4				1	0.21	0.00
ϕ_5					1	0.00
ϕ_6						1

$^3B_1$

	ϕ_1	ϕ_2	ϕ_3	ϕ_4	ϕ_5	ϕ_6
ϕ_1	1	0.80	0.32	0.12	0.19	0.19
ϕ_2		1	0.12	−0.06	0.13	0.13
ϕ_3			1	0.80	0.19	0.19
ϕ_4				1	0.13	0.13
ϕ_5					1	0.68
ϕ_6						1

The C–H bonds in the singlet state are composed of sp^3-like hybrids on carbon and distorted H(1s) functions. The description of the nonbonding electrons is very different from that just described for the triplet state, and differs markedly from the expectations of a standard single-configuration RHF calculation, in which both electrons occupy an sp^2-like hybrid pointing along the C_2 axis. In the spin-coupled wave function for the $^1A_1$ state, each of the remaining lobes of the sp^3-like hybrid accommodates one electron. The dominant mode of spin coupling (98.8% in the Kotani basis) corresponds to two C–H bonds, with singlet coupling of the spins of the nonbonding electrons. The overlap integrals between the various orbitals are collected in Table II, and show a significant overlap between the two nonbonded hybrids ($\Delta_{56} \approx 0.7$).

The form of the nonbonding orbitals for the $^1A_1$ state of CH_2 has important consequences for understanding the mechanisms of a number of reactions involving this molecule. Consider, for example, the class of cycloaddition reactions

$$CH_2 + RR'C{=}CR''R''' \rightarrow \text{products} \qquad (22)$$

which produces both stereoisomers in the case of the triplet state of the carbene but only one in the case of the singlet state.[21] The orbital description of CH_2 ($^1A_1$) suggests a preference for an asymmetric path in which the carbene first approaches one carbon center of the alkene, with the CH_2 plane twisted in order to maximize the overlap of one sp^3-like nonbonding hybrid with one $C(2p_\pi)$ function of the alkene. In this way, the attack of the soft electrophile, methylene, is concentrated on a single position of the alkene, a soft nucleophile. As the two molecules approach, the CH_2 system swings around to allow the formation of the two new C–C bonds of the cyclopropane ring in a single step. The form of the nonbonding orbitals of CH_2 ($^1A_1$) is already well suited to the simultaneous formation of these two bonds, and only one stereoisomer is formed. In the case of the $^3B_1$ state, only the sp^2-like nonbonding hybrid is directly suited to formation of a new C–C bond. The resulting triplet diradical allows for much rotation during the relatively slow ring-closing step, which involves a triplet to singlet conversion, and so both stereoisomers are produced.

This simple qualitative argument appears to be confirmed by spin-coupled calculations for the approach

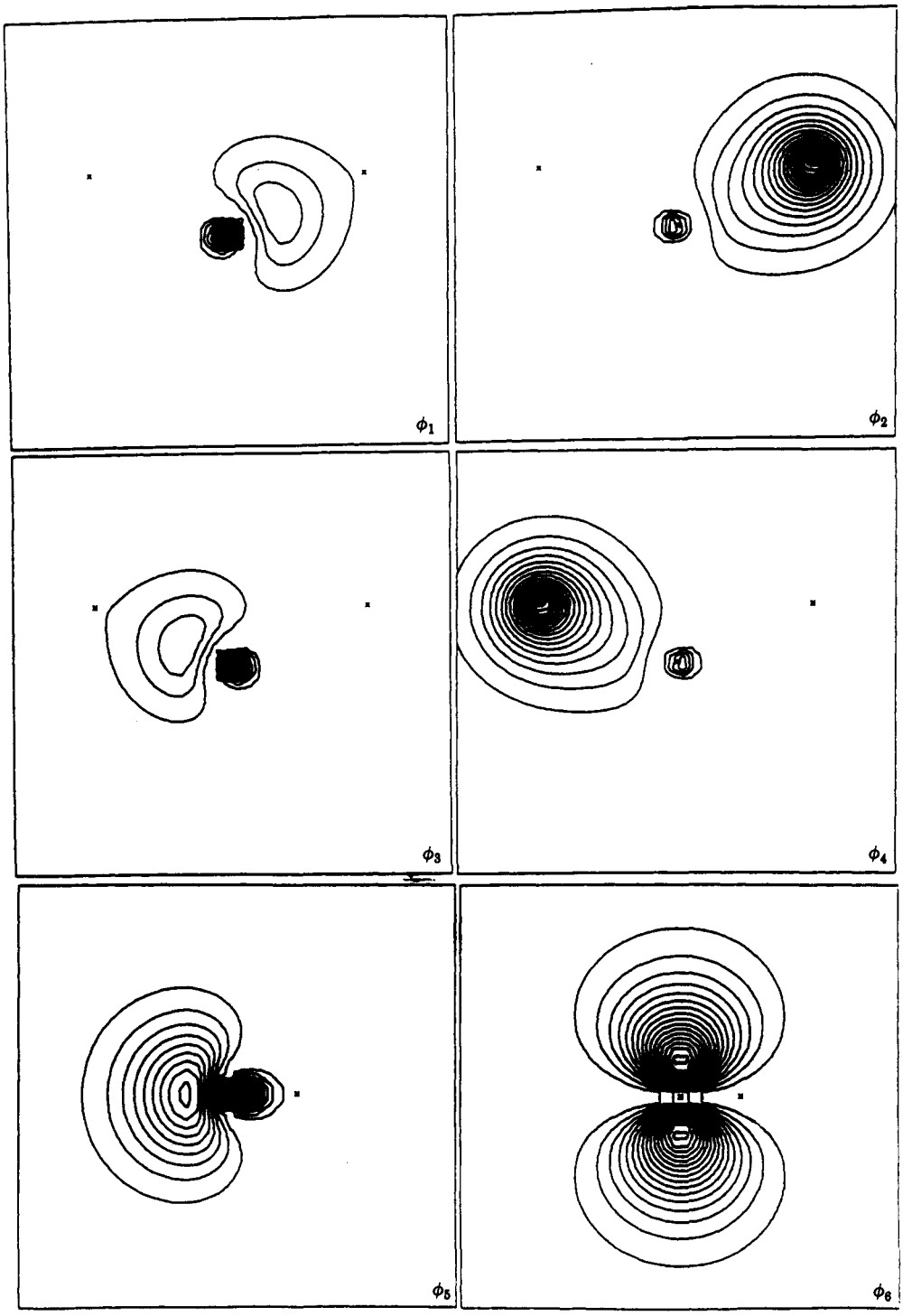

Figure 2. Contour plots of $|\phi_\mu|^2$ for CH_2 ($^3B_1$). Spin-coupled orbitals ϕ_1–ϕ_4 are shown in the σ_v' (molecular) mirror plane, and ϕ_5–ϕ_6 in the σ_v mirror plane.

of singlet and triplet CH_2 to ethene along symmetric and asymmetric paths.[19] A similar scenario can be envisaged for the simple singlet methylene insertion reaction

$$CH_2\ (^1A_1) + H_2 \rightarrow CH_4 \qquad (23)$$

which involves the complex process of forming two new C–H bonds while breaking the strong bond in H_2. Using the spin-coupled description of CH_2 ($^1A_1$) to predict a favorable pathway for this process, we would expect the initial approach of H_2 to be with its bond axis pointing along the direction of one of the nonbonding sp^3-like hybrids. As the molecules come together, the H atom furthest from CH_2 swings round toward the second nonbonding hybrid. Detailed calculations confirm that this reaction can occur along this path with *zero* barrier.[22]

According to the usual Woodward–Hoffmann rules, the direct approach of H_2 to CH_2 ($^1A_1$) is forbidden. This insertion reaction is known to proceed experimentally with little or no activation barrier. It is worthwhile to recall also that the least motion pathway for the cycloaddition of singlet methylene and ethene is also forbidden by these rules, but that such reactions are common. At the end of the day, the singlet state of CH_2 is described rather badly by a single RHF

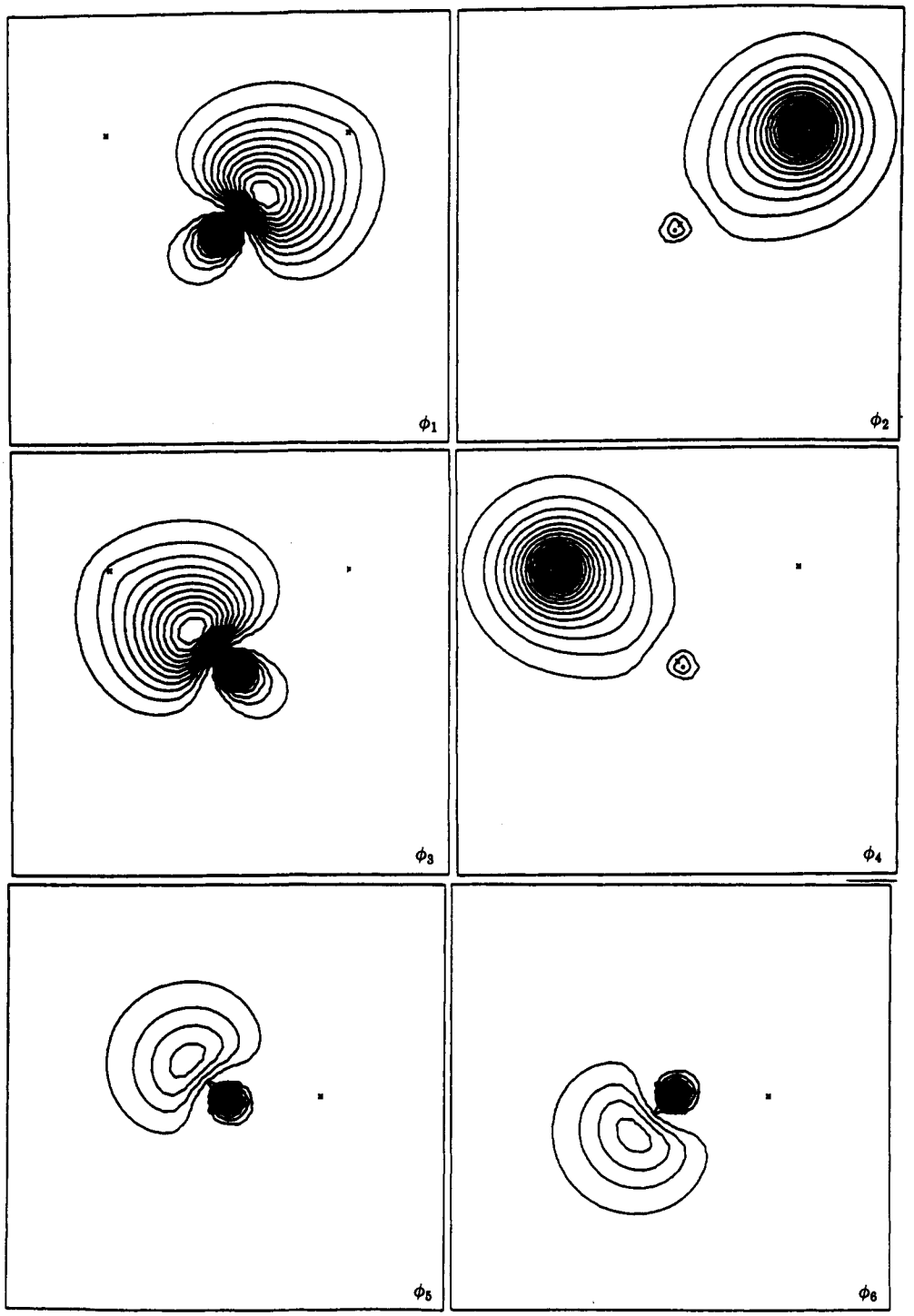

Figure 3. Contour plots of $|\phi_\mu|^2$ for CH_2 ($^1A_1$). Spin-coupled orbitals ϕ_1–ϕ_4 are shown in the σ_v' (molecular) mirror plane, and ϕ_5–ϕ_6 in the σ_v mirror plane.

configuration—a reliable description requires at least a two-configuration description of the type[23]

$$(\cdots)(3a_1)^2 - \mu(\cdots)(1b_1)^2 \qquad (24)$$

so that Woodward–Hoffmann-type arguments based on the MO's from a single RHF configuration are of very limited value. Furthermore, such arguments concentrate only on the spatial symmetry of the wave function, and tend to ignore the important role played by spin recoupling. From the spin-coupled investigations of the reaction of singlet CH_2 with ethene and with H_2, we can conclude that the changes in the mode of spin coupling, in the transition region from reactants to products, turn out to be the most important aspect in characterizing what might be termed "the act of reaction".

In view of the spin-coupled descriptions for singlet and triplet methylene, and reactions involving these species, the form of the spin-coupled orbitals for CH_4 and CH_3 present no surprises. Each C–H bond in CH_4 is described by the overlap ($\Delta \approx 0.7$) of a slightly distorted sp^3-like hybrid orbital with a slightly distorted H(1s) function, with singlet coupling of the associated electron spins. The four carbon hybrids are completely equivalent (as are also the four hydrogen orbitals) and can be permuted into one another by operations of the T_d point group. Although the perfect-pairing spin

function dominates, there are also small contributions from the other modes, and contrary to the usual assumptions of classical VB theory, the carbon hybrids are not orthogonal ($\Delta \approx 0.5$). Nonetheless, it is very pleasing to find that intuitive concepts such as directed covalent bonds, formed from the overlap of sp^x-like hybrids on C and 1s functions on H, arise naturally in all of these studies simply by minimizing the total energy without preconceptions.

Using a basis set of DZP quality, a frozen-core CASSCF calculation with all distributions of eight electrons in eight orbitals (1764 configurations) results in an energy improvement of 202 kJ mol^{-1} over the SCF description. The spin-coupled wave function, although based on just a single spatial configuration, provides an energy improvement over the SCF wave function of 170 kJ mol^{-1}, i.e. 84% of the nondynamical correlation energy, as *defined* above. The contrast with classical VB theory, in which ionic structures are essential even to match the SCF energy, is very clear indeed.

The determination of minimum-energy paths, and the location of any barriers along them, usually calls for extensive search procedures. A key feature of our studies of the reactions of singlet methylene, for example, is the *guidance* provided by the orbital descriptions of the reactants and products as to which portions of the potential surface should be searched.

We turn now to the question of the vertical ionization potentials of methane. Spin-coupled theory is not an independent particle model and it turns out that there is no simple relationship between the orbital energies, ϵ_μ in eq 20, and the ionization potentials. Furthermore, unless such a situation happens to correspond to the lowest energy, there is no a priori reason for the optimized orbitals of CH_4^+ to resemble those of CH_4. In general, accurate values for the ionization potentials require separate calculations for the neutral species and for the ion.

Nonetheless, in the spirit of Koopmans' theorem, it is straightforward to obtain simple estimates of the ionization potentials using the orbitals of the neutral species: an approximate wave function for CH_4^+ can be constructed from the eight possible products of seven orbitals which result from removing one valence orbital from CH_4. A small nonorthogonal CI (spin-coupled VB) calculation using these eight "hole" configurations yields a triply degenerate $^2T_2$ ground state and a $^2A_1$ excited state, as expected from the SCF description. These "invariant orbital" spin-coupled estimates[18] of the vertical ionization potentials are of a similar accuracy to those from Koopmans' theorem.

In the case of CH_4, comparison of estimated vertical ionization potentials with experiment is confused by strong Jahn–Teller effects in the $^2T_2$ state. It is thus not surprising that direct spin-coupled calculations for CH_4^+ lead to a symmetry-broken solution. The total wave function for the $^2T_2$ state at the tetrahedral geometry emerges directly from a small nonorthogonal CI calculation, using only the four equivalent symmetry-broken components.[18]

The spin-coupled description of the process

$$CH_4 \rightarrow CH_3(^2A_1') + H \qquad (25)$$

is very straightforward: the sp^3-like hybrids on methane evolve into the sp^2-like hybrids of CH_3 as the H atom departs and the umbrella angle of the CH_3 fragment changes to that characteristic of products. At the same time, the sp^3-like hybrid which points toward the departing H atom evolves into a C(2p) function. This type of process is essentially trivial to treat with the spin-coupled method—an important asset of the approach is the correct description of dissociation processes. As a somewhat more severe test of the single spatial configuration of spin-coupled theory, we have also examined the process

$$HCN \rightarrow CH(a^4\Sigma^-) + N(^4S) \qquad (26)$$

in which the strong C≡N triple bond is broken.[24] It is notable that not only does the simple spin-coupled configuration provide a correct description of the process HCN → CH + N, and a simple physical picture of the changes occurring as the N atom is removed, but the calculated dissociation energy (with a TZVP basis set) is 74% of the experimental value. In general, the spin-coupled orbitals for the 10 valence electrons of this system closely resemble those postulated by classical VB theory, except for the usual small, but crucial, distortions. However, near the equilibrium geometry of HCN, two of the spin-coupled orbitals take the form of two-center (CN) localized MO's. As the N atom is removed, these two-center orbitals evolve into essentially localized orbitals characteristic of the two fragments.

In addition to the changes in the form of many of the orbitals, which are easy to interpret in terms of familiar chemical concepts, the spin-coupled description of this process is characterized by an extensive recoupling of the electron spins. The change of the dominant mode of spin coupling from that of the molecular singlet state to that characteristic of the two quartet fragments is found to occur over a relatively narrow range of bond lengths. As is indeed the case for many of the processes which have been studied with the spin-coupled approach, the recoupling of the electron spins plays an essential role.

B. Aromatic Molecules

Most organic chemicals subscribe to a rather ambivalent view of the relative merits of MO and VB approaches to molecular electronic structure, particularly with regard to aromatic systems. On the one hand, it is customary to represent reaction mechanisms in terms of resonance between classical VB structures with localized bonds and lone pairs. In the case of aromatic substitution, for example, very simple VB ideas usually lead naturally to correct predictions of the reaction products. At the same time, most organic chemistry textbooks foster the view that MO theory is in some sense "more fundamental" than VB theory, and that the latter is somewhat "old-fashioned".

It is the experience of chemistry that the chemical properties of planar benzenoid aromatic molecules are dominated by the "π" electrons, and as such, it is easy to justify working within the usual approximation of σ–π separation. We use the labels σ and π in this context to distinguish between electrons occupying orbitals which are symmetric and antisymmetric, respectively, with respect to reflection in the molecular plane. A description of aromatic molecules which concentrates only on the π electrons cannot be

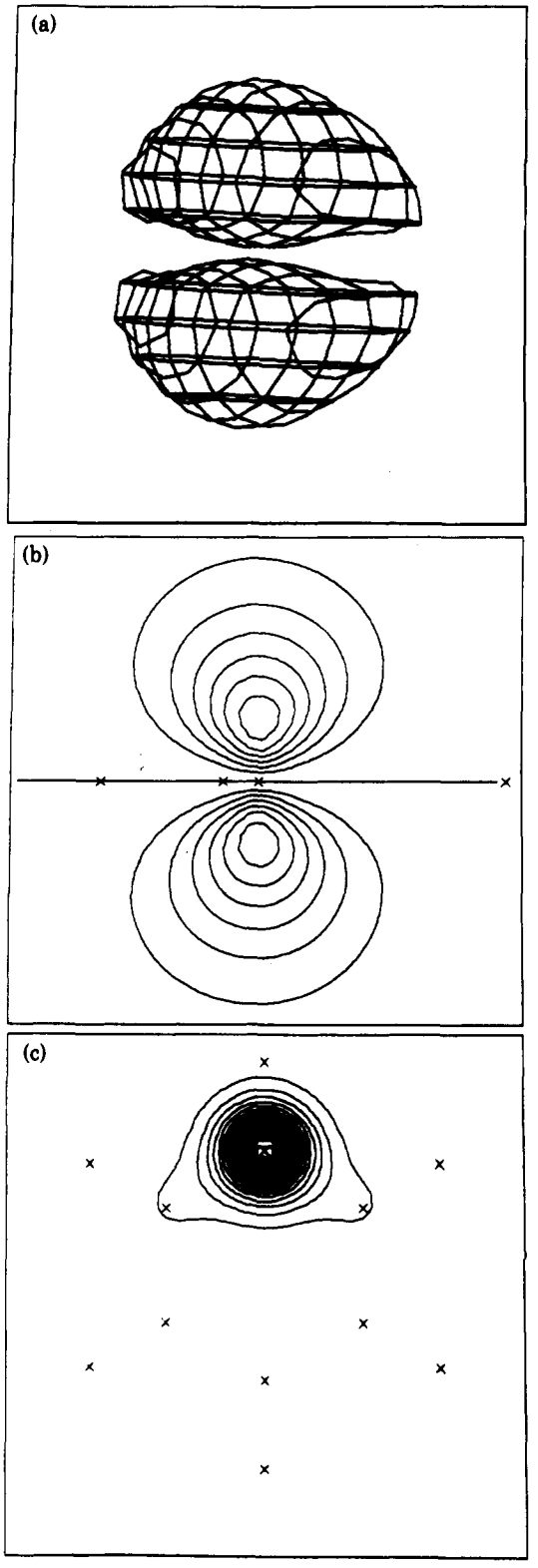

Figure 4. One of the six equivalent spin-coupled π orbitals of benzene: (a) "wire mesh" representation; (b) contours of ϕ_μ in a σ_v mirror plane (i.e. a plane perpendicular to the molecular frame and containing two C–H bonds); (c) contours of $|\phi_\mu|^2$ in the plane 1 bohr above the σ_h molecular plane. The projected positions of the nuclei are marked with crosses.

"complete", not least because it can be shown that the regular hexagon structure of benzene arises primarily from the σ-bonded framework and not from the π electrons.[25] Nonetheless, the enhanced stability of aromatic molecules relative to comparable conjugated

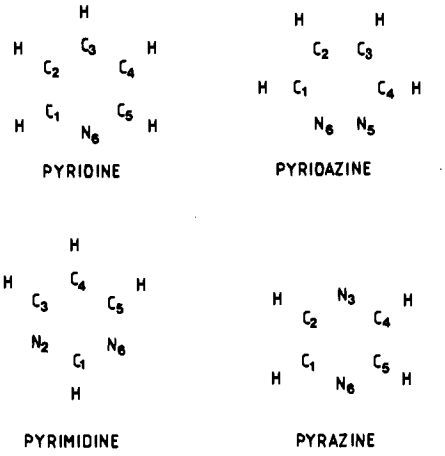

Figure 5. Structural formulae of the heteroaromatic molecules pyridine, pyridazine, pyrimidine, and pyrazine. The molecules have been drawn to scale.

alkenes can be ascribed primarily to special features of the π-electron systems.

According to the SCF description of a molecule such as benzene, the special stability is linked to the occurrence of delocalized π orbitals. In classical VB theory, on the other hand, the enhanced stability is associated with resonance between Kekulé and para-bonded or Dewar structures. In spite of the obvious differences between these two descriptions, many organic chemists tend to use interchangeably the terms "delocalization energy", "resonance energy", and "aromatic stabilization energy".

Spin-coupled theory has now been applied to benzene[26] and naphthalene,[27] to heteroaromatic molecules based on five- and six-membered rings,[28] to inorganic analogues of benzene,[26c] and to cyclobutadiene and 2,4-dimethylenecyclobutane-1,3-diyl.[29] A general account of the results for benzenoid aromatic systems has appeared elsewhere.[5] The main finding is that the π-electron systems of all the aromatic molecules considered are much better described in terms of localized, nonorthogonal, singly occupied orbitals than in terms of the doubly occupied, orthonormal, delocalized canonical MO's of SCF molecular orbital theory. In the spin-coupled description of these systems, the characteristic stability of the π-electron systems arises from the particular modes of coupling the electron spins rather than from any supposed delocalization of the orbitals.

At convergence, the spin-coupled wave function for the six π electrons of benzene is found to consist of six distinct highly localized nonorthogonal orbitals which can be transformed into one another by successive $\hat{C}_6$ rotations. One of these six equivalent orbitals is shown in Figure 4. It is clear that each of the orbitals takes the form of a $C(2p_z)$ function, slightly distorted in a symmetrical fashion toward the neighboring carbon centers. The distortion effects are no larger than has been found for the C–C π bonds in conjugated alkenes. Similar descriptions arise for pyridine, pyridazine, pyrimidine, and pyrazine, for which structural formulae are collected in Figure 5. The degree of distortion of the spin-coupled orbitals is consistent with usual notions of electronegativity differences.

With the use of a basis set of TZVP quality for benzene, the difference in energy between the SCF and

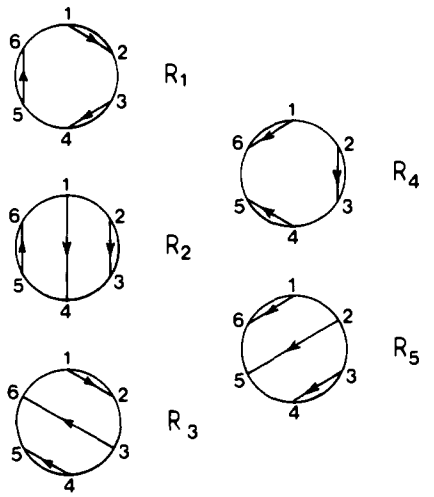

Figure 6. Rumer diagrams for $N = 6$ and $S = 0$.

CASSCF wave functions (six π electrons in six π orbitals and relaxation of the doubly occupied σ orbitals) is ca. 190 kJ mol^{-1}. A spin-coupled calculation[26c] in the same basis set (and with the same description of the σ electrons) provides an energy improvement over the SCF wave function of ca. 170 kJ mol^{-1}, i.e. 90% of the nondynamical correlation energy, as defined earlier. The remaining 10% can be attributed to spin-coupled ionic configurations.

It is useful to contrast these findings with the conclusions of a direct implementation of classical VB theory by Norbeck and Gallup.[30] The total classical VB wave function, consisting of all covalent and ionic structures for the six π electrons was found to be dominated by singly ionic structures with adjacent charges. Indeed, the wave function based on only the covalent Kekulé and para-bonded structures gave an energy inferior to that from an SCF calculation in the same basis set. Of course, it is relatively straightforward to project the spin-coupled wave function onto a basis of VB structures in which each orbital is restricted to use basis functions associated with only one carbon atom. Although it is likely that the total weight of singly ionic structures for benzene would be somewhat smaller than suggested by Norbeck and Gallup, this projection procedure would again emphasize the net importance of such structures. As described earlier, spin-coupled orbitals are fully optimized in a multicenter basis set; even orbitals which are essentially localized on one center do make some use of the basis functions on other centers. It turns out that these relatively *small* deformations of the spin-coupled orbitals can correspond to fairly *large* weights for classical VB ionic structures.[31]

The spin-coupled calculations employed the full spin space, which consists of five functions for the case of six electrons with a net spin of zero, and it is straightforward to transform between different representations. It is important to stress once more that the same flexibility does not exist in the form of the orbitals: in general the spin-coupled wave function is not invariant to linear transformations of the orbitals. The relative importance of the different modes of spin coupling is most easily visualized in terms of the Rumer basis. The Rumer diagrams for $N = 6$ and $S = 0$ are depicted in Figure 6, in which an arrow $i \rightarrow j$ signifies that electrons i and j are singlet coupled, and this

TABLE III. Occupation Numbers (expressed as percentages) of the Different Spin Couplings in the Rumer Basis for Heteroaromatic Molecules with Six-Membered Rings[a]

	R_1	R_2	R_3	R_4	R_5
benzene	40.5	6.5	6.5	40.5	6.5
pyridine	40	7.5	5.5	40	7.5
pyridazine	20.5	8.5	8.5	54	8.5
pyrimidine	40	8.5	6	40	6
pyrazine	40	8	4.5	40	8

[a] The Rumer diagrams (R_i) are numbered as in Figure 6, and the ordering of the orbitals is indicated in Figure 5. In each case, R_1 and R_4 are the Kekulé-type structures.

corresponds to the occurrence in the total spin function of a factor of

$$2^{-1/2}[\alpha(i)\beta(j) - \beta(i)\alpha(j)] \qquad (27)$$

Occupation numbers of the different spin couplings in the Rumer basis are collected in Table III for various six-membered aromatic ring systems and show the expected dominance of Kekulé-type structures. In addition, the heterocycles show a marked preference for C=N bonds, as we might have expected.

The spin-coupled description of naphthalene is very similar to that of benzene, both in terms of the orbitals and of the weights of the different modes of spin coupling. It is straightforward to define resonance energies for all of these systems. In the case of benzene, for example, this is taken as the difference between the energy of the full spin-coupled wave function and that from a calculation using the same orbitals but just spin function R_1.

Analogous descriptions arise for five-membered rings, such as furan, pyrrole, and thiophene, except that the heteroatom now contributes two π electrons. In the spin-coupled model, one of these electrons occupies a highly localized orbital, while the other shows significant delocalization onto neighboring carbon centers to a degree which is consistent with the electronegativity of the heteroatom. The weights of the different modes of spin coupling and the computed resonance energies are consistent with the traditional organic chemistry views of these systems. In addition, simple VB estimates of the ionization potentials for these systems are at least as good for the lowest states of the ion as those derived from Koopmans' theorem, while the higher ones appear to be considerably more reliable.[28b]

Spin-coupled calculations for inorganic analogues of benzene, such as borazine ($B_3N_3H_6$) and boroxine ($B_3O_3H_3$), lead to rather different conclusions.[26c] Each N or O atom contributes two π electrons, one of which occupies a very localized orbital. The other shows significant delocalization onto the neighboring B centers. In this sense, there are marked similarities to the five-membered heterocycles. However, the perfect-pairing spin function dominates and we find that resonance energies are negligible, if defined as for the organic ring systems. The spin-coupled descriptions of borazine and boroxine are very similar, and suggest that neither molecule has significant aromatic character.

In spite of its great utility in organic chemistry, formal definitions of the concept of aromaticity in terms of chemical or physical properties have proved somewhat elusive.[32] One criterion, which proves useful for many benzenoid systems, is the observation of aniso-

tropic magnetic susceptibilities—the so-called "ring currents". In the case of benzene, preliminary spin-coupled calculations of the magnetic properties of this molecule reproduce the expected anisotropy (see also section IV.C).

It is now well established that the simple Hückel $4n + 2$ rule exaggerates the differences between "aromatic" and "antiaromatic" π-electron systems such as cyclobutadiene. For C_4H_4 with a square-planar nuclear configuration (D_{4h} symmetry), the ground electronic state is $^1B_{1g}$ with a $^3A_{2g}$ excited state lying more than 40 kJ mol^{-1} above it. The square-planar geometry is unstable for the ground state, and the molecule distorts to a rectangular geometry. In the triplet excited state, on the other hand, the square-planar geometry is stable with respect to geometrical distortion. As we would expect, all of these features are faithfully reproduced by a straightforward application of spin-coupled theory, employing just a single optimized spatial configuration for each state. Of greater significance is the physical picture revealed by these calculations.

In that the characteristic stability of benzenoid molecules is linked in spin-coupled theory to the particular mode of coupling the electron spins, we might expect the orbital descriptions of cyclobutadiene and of benzene to be very similar, but the mode of spin coupling to be very different. Consider first the singlet ground state at a square-planar configuration, and suppose that the spin-coupled orbitals for C_4H_4 are very similar to those described earlier for benzene. In this case, it turns out that the mode of spin coupling would be completely determined by the overall B_{1g} symmetry. For the orbitals ordered a, b, c, d around the ring, this mode of coupling the electron spins is best envisaged in the Serber basis as *triplet* coupling of the electron spins associated with each diagonal (i.e. a/c and b/d), and then coupling of these two triplet subsystems to a net singlet.

In the special case of electron spins which are *strictly* triplet coupled, the spin-coupled wave function is not altered by taking the sum and difference of the corresponding orbitals, i.e. (a + c) and (a − c) (neglecting normalization). In this sense, two seemingly rather different descriptions are actually equivalent. In the first, there are orbitals essentially localized at each corner with triplet coupling on each diagonal. In the other there are in-phase and out-of-phase combination orbitals on each diagonal, again triplet coupled. The term "anti-pairs" has been coined for this latter description (cf. antiferromagnetic coupling).

It is possible to show for the "anti-pair description" of C_4H_4 that the spatial wave function already corresponds to the required B_{1g} symmetry, and so the mode of spin coupling is no longer determined purely by the spatial symmetry.[29b] This introduces an extra degree of freedom into the wave function over the "localized orbital description" of this molecule, and thus the possibility of a lower total energy. Not surprisingly, the converged single-configuration spin-coupled wave function for C_4H_4 turns out to correspond to this anti-pair description, although the weight of the "additional" spin degree of freedom is very small.

For a square-planar geometry, the spin-coupled descriptions of the $^1B_{1g}$ and $^3A_{2g}$ states of C_4H_4 are found to be very similar indeed, except that the two triplet subsystems are coupled to a net singlet in one case and to a triplet in the other. The converged spin-coupled orbitals for the $^3A_{2g}$ state at its equilibrium geometry (D_{4h} symmetry) are shown in Figure 7. As mentioned earlier, distortion of the triplet state to rectangular geometry is energetically unfavorable: we find that the same orbital description pertains. The singlet state, on the other hand, becomes more stable at a rectangular geometry: the orbitals change into slightly distorted C($2p_\pi$) functions analogous to those in alkenes, and the dominant mode of spin coupling corresponds to C–C π bonds along the short sides of the ring.

It is clear that benzene and cyclobutadiene differ markedly in terms of the particular mode of coupling the electron spins. As a further example, spin-coupled theory has been applied to the triplet ground state and to the lowest singlet excited state of 2,4-dimethylenecyclobutane-1,3-diyl. This molecule can be envisaged as arising from C_4H_4 by substitution of CH_2 groups for the H atoms at opposite corners of the ring. The $^3B_{2u}$ ground state is found to possess one anti-pair, although the triplet character is not entirely confined to the ring and there is significant triplet character in the two exocyclic C=C bonds, consistent with the observed proton hyperfine coupling. In keeping with other theoretical studies,[33] the lowest singlet state is found to possess ^1A_g symmetry rather than the $^1B_{2u}$ symmetry expected from Hückel theory. For the ^1A_g state, four orbitals are involved in exocyclic C–C π bonds, as is the case for the triplet state, but the remaining two orbitals do not constitute an anti-pair.[29] Instead, these last two orbitals take the form of localized, slightly distorted C($2p_\pi$) functions with an overlap of only 0.3. In order to increase this overlap to a value more typical of a normal chemical bond, the molecule would need to distort from planar geometry. Indeed, it is now clear that the planar structure is not a true minimum for the singlet state, but is instead a transition state for the formation of (nonplanar) 3,4-dimethylenebicyclo[1.1.0]butane, via the development of a long transannular bond.[34]

An important outcome of these spin-coupled calculations for the π-electron systems of aromatic and antiaromatic molecules is the internal *consistency* of the descriptions. It has proved possible, for example, to *predict* with acceptable accuracy the form of the orbitals and the weights of the different Rumer functions for thiazole before carrying out spin-coupled calculations. The transferability of the description between related systems strongly recommends its use to construct representations of larger and more complex π-electron systems, perhaps within a semiempirical formalism. Indeed, Li and Paldus have recently utilized orbitals analogous to those from ab initio spin-coupled calculations to implement a VB approach for PPP-type hamiltonians, within the Clifford algebra unitary group approach.[35] This PPP-VB approach provides very good total π-electron energies for a wide variety of conjugated systems, even when only covalent Kekulê-type structures are included.

C. 1,3-Dipoles

The large class of molecules known as 1,3-dipoles, which includes diazoalkanes, nitrones, carbonyl ylides, and fulminic acid, presents particularly awkward problems for classical theories of valency, as also do the

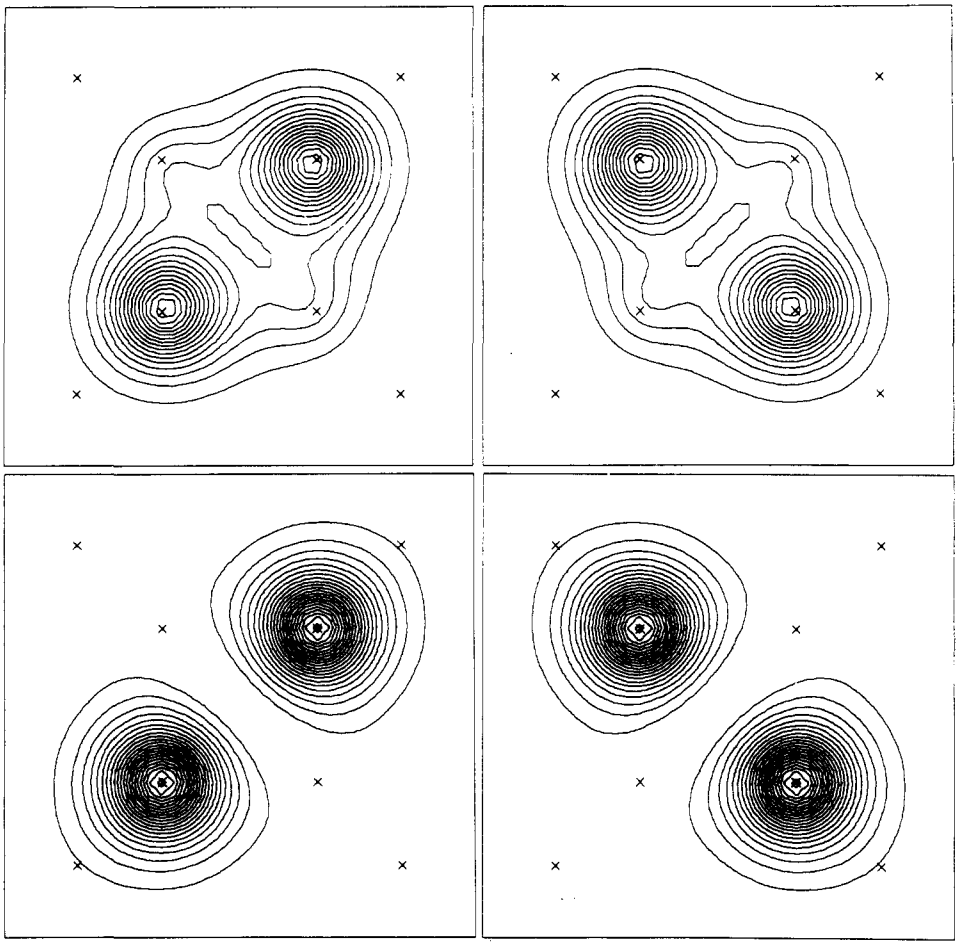

Figure 7. Spin-coupled π orbitals for the $^3A_{2g}$ state of C_4H_4 at the square-planar geometry. Contours of $|\phi_\mu|^2$ are shown in the plane 1 bohr above the σ_h molecular plane. The projected positions of the nuclei are marked with crosses.

triatomics ozone and nitrous oxide. The usual representation of diazomethane (CH_2N_2), for example, invokes resonance between a number of zwitterionic and diradical structures:

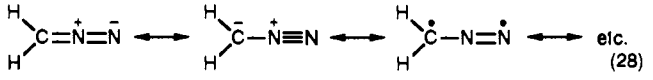

(28)

In general, theoretical studies have done little to clarify the interpretation of the bonding in these molecules, and there have been widely different estimates of the relative weights of the different bonding schemes.

It is usual to interpret 1,3-dipolar cycloaddition reactions in terms of four "π" electrons from the 1,3-dipole and two from the dipolarophile (typically a substituted ethene). In this spirit, spin-coupled calculations have been carried out[36] for the π-electron systems of a number of 1,3-dipoles, including diazomethane, fulminic acid (HCNO), and nitrone (CH_2NHO), and for the inorganic species O_3, NNO, and NO_2. A consistent picture emerges for all of these systems, in which the central heavy atom takes part in more covalent bonds than would normally be expected from the usual "octet rule".

The four spin-coupled π-orbitals for diazomethane are illustrated in Figure 8 as contours in the σ_v mirror plane perpendicular to the molecular plane. Each orbital takes the form of a $2p_x$ function, slightly distorted toward one of the neighboring centers, with one orbital on each of the terminal heavy atoms and two on the central N atom. Although the two orbitals on the central N atom have a high overlap (0.79 in a TZVP basis set), the associated electron spins are *not* coupled to a singlet. The overwhelmingly dominant mode of spin coupling (99% in the Kotani basis) corresponds to fully formed C–N and N–N π_x bonds. If we include now also the bonding in the σ framework and the "in-plane" π_y bond between the N atoms, we find that the central N atom takes part in *five* covalent bonds.

Using a TZVP basis set for CH_2N_2, the difference in energy between the RHF and CASSCF wave functions (four π_x electrons in four π_x orbitals and relaxation of the doubly occupied σ and π_y orbitals) is ca. 120 kJ mol^{-1}. The analogous spin-coupled wave function affords an energy within 1 kJ mol^{-1} of the CASSCF description. It is clear that the NDC wave function for diazomethane is approximated very well by a single spatial configuration, and indeed by a single mode of spin coupling, corresponding to a hypervalent N atom. This hypervalency is the result of subtle electron correlation effects incorporated in the NDC wave function.

Of course, none of this suggests that the classical VB picture is in any way incorrect—merely that it is unnecessarily complicated. If the spin-coupled description of diazomethane were projected onto a basis of classical VB structures, then significant contributions would arise for a number of very different canonical structures. The utility of these seemingly different, but fundamentally equivalent, descriptions depends on how they can be used to understand the chemistry of 1,3-dipoles and related systems. Both schemes are of use in this

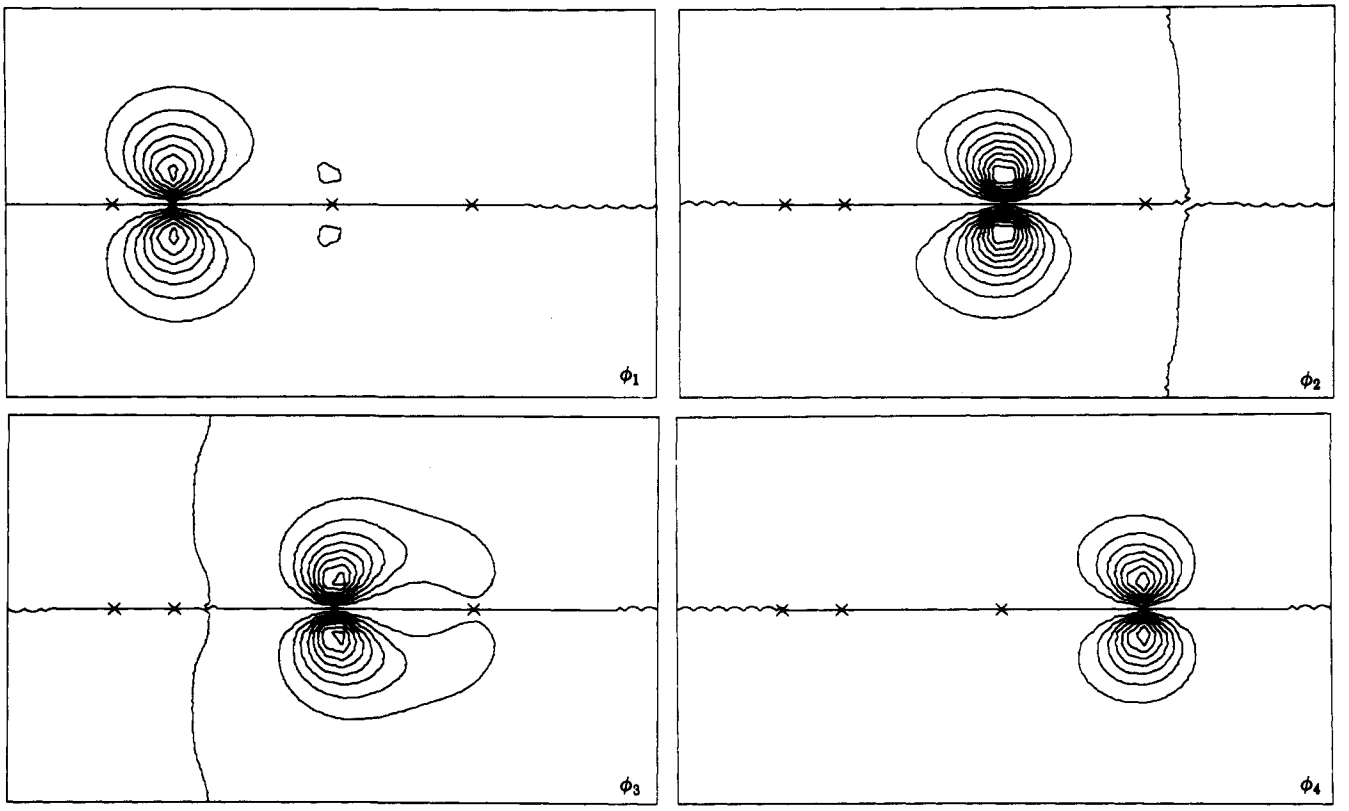

Figure 8. Contour plots for CH_2N_2 of $|\phi_\mu(\mathbf{r})|^2$ in the σ_v mirror plane perpendicular to the molecular plane. The crosses mark the projected positions of the nuclei.

respect, but the simplicity of the very compact spin-coupled description is particularly appealing.

Certainly, the very short bond lengths between the heavy atoms in diazomethane are entirely consistent with fully formed C=N and N≡N multiple bonds, and it is easy to understand why the molecule should exhibit a relatively small dipole moment (ca. 1.5 D). Furthermore, in that the central N atom of CH_2N_2 is utilizing *all* of its valence electrons in bonding, it is not surprising that this atom shows a high resilience to attack by electrophiles or nucleophiles, particularly when compared to the reactivity of its neighbors or of N atoms in other π-electron systems. Similar structural and reactivity considerations apply for other 1,3-dipoles.

For CH_2N_2, the only reaction which the central N atom will undergo readily is cleavage of the bonds to the carbon atom, and it is tempting to suggest that the explosive nature of this process might be linked in some way to the hypervalent nature of the bonding. Certainly, the nitro group also features a hypervalent atom and it is likely that azides, nitrate esters, and many other shock-sensitive materials also fit into this category. The products, N_2 and methylene in the case of diazomethane, do not involve any hypervalency and it is interesting to examine where along the reaction coordinate this change occurs.

Spin-coupled calculations have been carried out for a number of systems to examine the sensitivity of the hypervalent character to small geometric distortions. For each case studied, the hypervalency is "switched off" over a remarkably narrow range of bond lengths. For a shock-sensitive material such as diazomethane, these changes occur very close to the equilibrium geometry, i.e. after a relatively small elongation of the $H_2C\cdots N_2$ separation. For more stable systems, such as CH_2NHO, these transformations to the nature of the bonding require very much larger geometrical changes.

A key feature of the spin-coupled description of 1,3-dipoles is its *simplicity*, provided we are able to overcome the long-established prejudices against hypervalent first-row atoms.[37]

D. Clusters of Lithium Atoms

Theoretical studies of small clusters of lithium atoms have been reported by a number of research groups, employing a wide variety of different approaches. Koutecký, Fantucci, and co-workers[38,39] have addressed themselves mostly to the problem of determining the most stable geometrical conformations and atomicities using MO-CI techniques. Fully optimized geometries are also available from the MBPT calculations of Rao and Jena.[40] Ray and Hira[41] have determined optimal geometries for various clusters by optimizing, at the UHF level of theory, the "lattice constant" of a lithium crystal lattice.

McAdon and Goddard have applied the GVB approach, albeit with the usual restrictions of strong orthogonality and perfect pairing, to investigate the nature of the bonding in numerous small clusters of lithium atoms.[42] Their studies suggest a scheme based on singly occupied orbitals localized at *interstitial* sites, and led directly to a new "generalized valence bond model of metallic bonding".[43] The GVB-SOPP calculations suggest a differentiation of the orbitals into different classes, localized in triangular faces or in tetrahedral hollows.

Malrieu and co-workers[44] have also addressed the important problem of elucidating the nature of the bonding in such systems. They used concepts typical

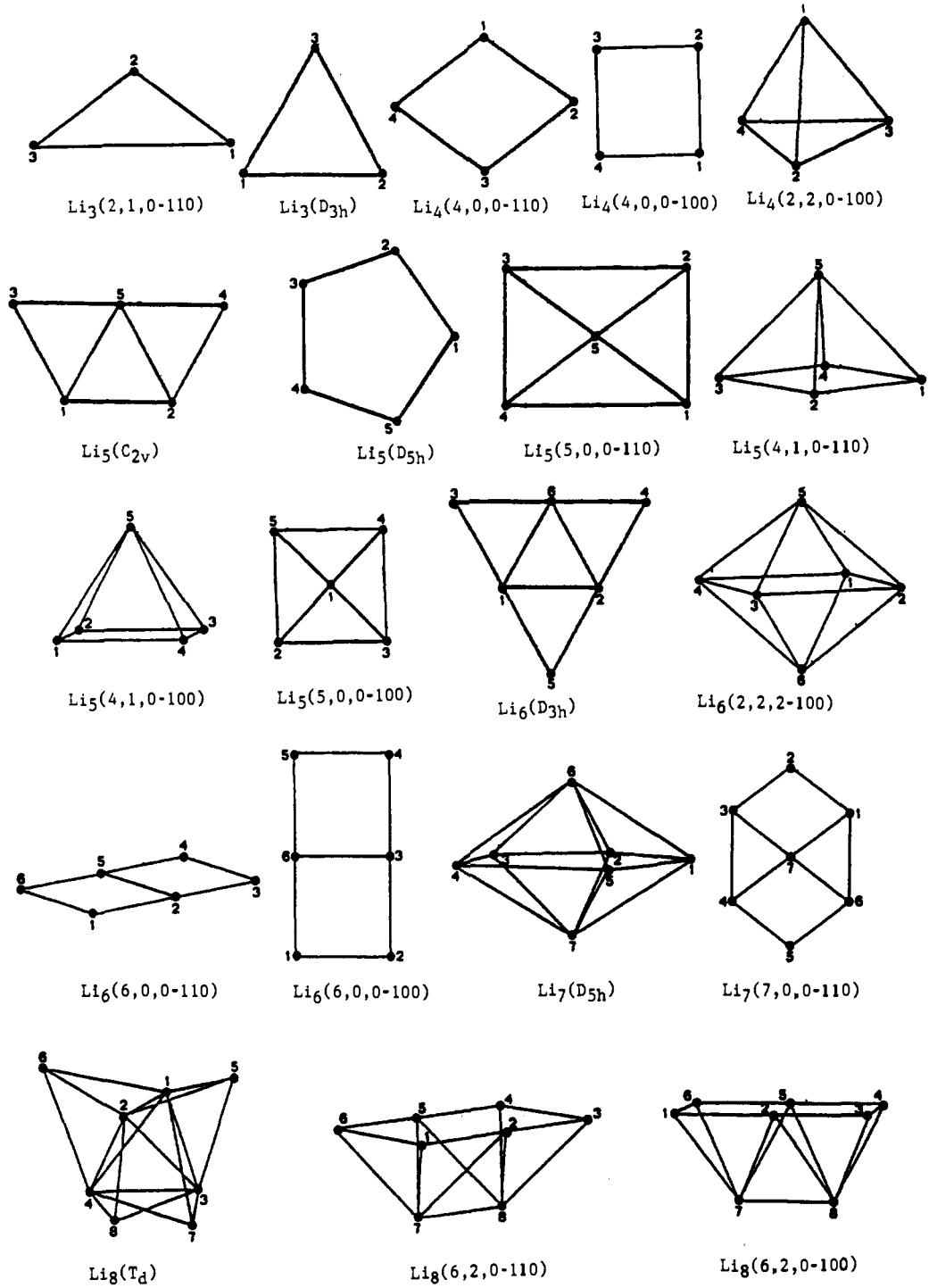

Figure 9. Geometries of the lithium clusters listed in Table IV. $Li_4(D_{2h})$ has the same shape as Li4(4,0,0-110), but different nuclear separations (and angles).

of classical valence bond theory to analyze wave functions based on localized MO's resulting from UHF calculations.

Spin-coupled calculations have been carried out for two series of clusters.[45] All of these clusters are shown in Figure 9. The first set comprises clusters for which the geometries, fully optimized in the previous work listed above, correspond to the most favored arrangement for the particular atomicity. We denote these systems $Li_n(G)$ (n = 4–8), where G is the relevant molecular point group. All the clusters in this set were studied with the same [9s5p/3s2p] basis set[46] as frequently used in previous studies. In addition we performed calculations on $Li_3(D_{3h})$ (equilateral triangle) and $Li_5(D_{5h})$ (regular pentagon), which represent fragments of clusters of higher atomicity.

The second set of clusters represents portions of a body-centered cubic (bcc) lattice, cut according to (100) and (110) planes. These clusters may be denoted $Li_n(n_1,n_2,n_3\text{-}P)$, where n_i is the number of lithium atoms in the ith layer (i = 1, 2, 3) and P labels the plane (100 or 110). We used the same geometries and 6-21G basis set[47] for these systems as in the previous work of Ray and Hira.[41]

The spin-coupled calculations for a general cluster consisting of n lithium atoms were carried out explicitly

TABLE IV. Results of Spin-Coupled Calculations for Small Clusters of Lithium Atoms[a]

system		$2S+1$	f_S^N	total energy, hartree: spin-coupled	total energy, hartree: SCF	BE, kcal/mol
Li_3						
	D_{3h}	2	2	-22.318 18	-22.301 16	4.81
	2,1,0-110	2	2	-22.310 22	-22.297 35	3.84
Li_4						
	D_{2h}	1	2	-29.784 93	-29.752 73	9.08
		3	3	-29.763 91	-29.738 53	5.74
	4,0,0-110	1	2	-29.778 21	-29.736 36	8.74
		3	3	-29.767 28	-29.740 70	7.02
	4,0,0-100	1	2	-29.771 00	-29.711 22	7.61
		3	3	-29.766 23	-29.738 51	6.86
	2,2,0-100	3	3	-29.761 53	-29.745 18	6.12
		1	2	-29.760 82	-29.717 00	6.01
Li_5						
	C_{2v}	2	5	-37.236 31	-37.206 59	9.74
	D_{5h}	2	5	-37.225 89	-37.170 22	8.44
	5,0,0-110	2	5	-37.211 37	-37.186 04	7.31
		4	4	-37.180 08		3.38
	4,1,0-110	2	5	-37.209 79	-37.175 43	7.11
		4	4	-37.208 87	-37.191 37	7.00
	4,1,0-100	2	5	-37.206 56	-37.180 10	6.70
		4	4	-37.172 03		2.37
	5,0,0-100	2	5	-37.194 84	-37.170 39	5.23
		4	4	-37.170 13	-37.153 37	2.13
Li_6						
	D_{3h}	1	5	-44.693 29	-44.653 97	10.75
		3	9	-44.661 83		7.47
	2,2,2-100	1	5	-44.674 82	-44.631 94	9.52
		3	9	-44.658 14	-44.633 87	7.78
	6,0,0-110	3	9	-44.671 16	-44.635 55	9.14
		1	5	-44.669 14	-44.603 20	8.93
	6,0,0-100	1	5	-44.663 61	-44.603 13	8.35
		3	9	-44.655 05	-44.606 45	7.46
Li_7						
	D_{5h}	2	14	-52.131 29	-52.102 27	9.78
	7,0,0-110	2	14	-52.113 82	-52.063 34	8.91
		4	14	-52.100 18		7.69
Li_8						
	T_d	1	14	-59.600 51	-59.558 76	11.50
	6,2,0-100	1	14	-59.555 76	-59.497 55	8.69
		3	28	-59.552 67		8.44

[a] The shapes of these clusters are shown in Figure 9. BE is the binding energy per atom.

for the n valence electrons. These are described by n distinct singly occupied nonorthogonal orbitals ϕ_μ. The core electrons were accommodated in n doubly occupied orthogonal orbitals ψ_1 taken from a prior SCF calculation. The general strategy is exactly the same as that described in section II.C (cf. eq 19). In our usual short-hand notation, the spin-coupled configuration can thus be written $\{\psi_1^2\psi_2^2\cdots\psi_n^2\ \phi_1\phi_2\cdots\phi_n\}$. All the spin-coupled orbitals were fully optimized without any constraints on the overlaps between them. The full spin space was employed in each case.

The numerical results, summarized in Table IV, highlight the importance for these systems of the (nondynamical) correlation effects introduced by the spin-coupled wave function. The agreement with previous studies concerning the ordering of the different spin multiplicities is very satisfactory, and the relative stabilities of the different classes of structures, as indicated by the binding energies, are in very good agreement with the other theoretical treatments listed above.

The form of the spin-coupled wave functions for these lithium clusters reveals a great deal about the electronic structure of such systems. In addition, the nature of the spin-coupled orbitals, which can be interpreted as nonorthogonal Wannier functions in the limit of a very extended system, has consequences for the validity of the approximations usually introduced in the most popular methods for studying extended systems. The "tight binding" approximation, for example, relies on the assumption that the (orthogonal) one-particle states are localized around the nuclear centers.

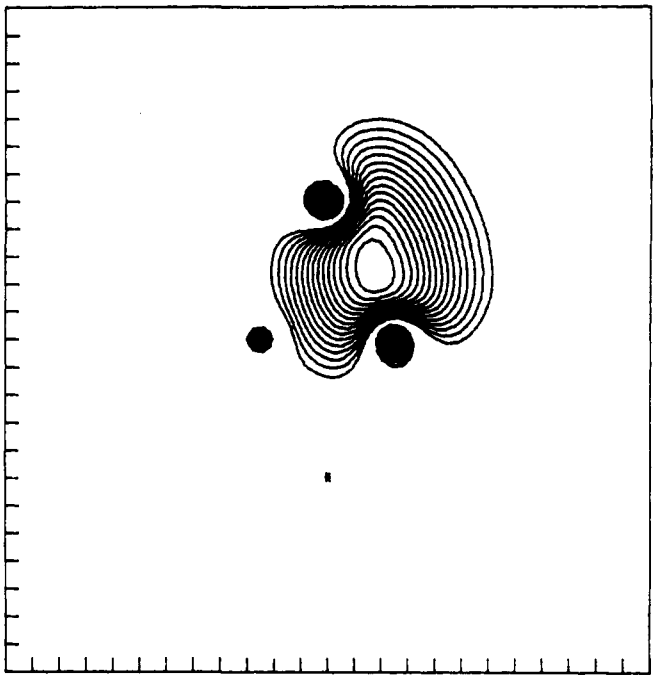

Figure 10. One of the four equivalent spin-coupled orbitals for the valence electrons of the $Li_4(D_{2h})$ rhombus. The other orbitals can be generated from this one by symmetry operations of the molecular point group.

In almost all of the cases considered, we find that the spin-coupled orbitals are both localized and *interstitial*. The only atomic-like orbital occurs for Li_5(4,1,0-110), in which one orbital is localized on the vertex of the rhomboid pyramid. Almost all of the orbitals link pairs of atoms belonging to the perimeter (in the case of the two-dimensional clusters) or to the external edges (in the three-dimensional systems). Orbitals for a typical example, $Li_4(D_{2h})$, are illustrated in Figure 10. In some cases, these interstitial orbitals form in-phase and out-of-phase combinations, analogous to those described in section III.B for antiaromatic hydrocarbons. This additional feature is observed for energetically less favored geometries with special symmetry, such as (square) Li_4(4,0,0-100) and (irregular tetrahedral) Li_4(2,2,0-100).

The most important building block when moving toward forms of increasing complexity turns out to be the rhombus subunit, followed by the triangle and the tetrahedron.

The relaxation of the strong orthogonality and perfect-pairing constraints inherent in the earlier GVB-SOPP calculations[42] leads to significant changes in the form of the orbitals in a number of systems. From the general form of the matrices of overlap integrals between the spin-coupled orbitals, it is difficult to justify the strong orthogonality constraint, except, perhaps, on the grounds of computational convenience. In general, all of the f_S^N spin functions contribute to the spin-coupled wave functions for these clusters, but a very small

number of the $\Theta^N_{SM;k}$ dominate (in the Rumer basis). In some cases, it would not be too serious to impose the perfect-pairing approximation, at least from the point of view of the qualitative features of the orbital picture, but this constraint is probably best avoided.

We find that the spin-coupled description of the Li_4 rhombus, for example, is entirely consistent with the picture of nonnuclear maxima (or "pseudo-atoms") that arises from the topological partitioning of correlated electron densities.[48] Work is underway to examine the consequences of the form of the spin-coupled orbitals, as well as the properties and locations of nonnuclear maxima in the total density, for developing a highly visual correlated-orbital alternative to the usual form of band theory for extended systems. Returning to considerations of small molecules, there are also consequences for understanding the bonding in the oligomers of methyllithium, and in other systems for which somewhat naive considerations might suggest that the lithium atoms are hypervalent.

E. Boron Hydrides

As is well known, conventional accounts of the electronic structure of boranes such as B_2H_6, B_4H_{10}, and B_5H_{11} rely on just four main structural units: (a) the two-center two-electron (2c-2e) B–H terminal bond, formed by the overlap of an sp^x hybrid on boron and a 1s function on hydrogen; these terminal B–H bonds occur in BH_2 units; (b) the 2c-2e B–B terminal bond; (c) three-center two-electron (3c-2e) B–H–B bridge bonds, formed by the overlap of a hydrogen 1s orbital and of two boron sp^x hybrids pointing toward H; and (d) "closed" (or "central") 3c-2e BBB bonds, formed by the overlap of three B(sp^x) hybrids, one from each center, each pointing toward the middle of the boron triangle. Diborane, for example, can be assigned the "styx" number (2002) where the four integers denote, respectively, the numbers of 3c-2e B–H–B bonds, of 3c-2e closed BBB bonds, of 2c-2e B–B bonds, and of BH_2 groups. It is possible to rationalize the structures of a wide range of boranes using just these four simple units. Note that for carboranes and other heteroboranes it is sometimes useful to consider also 3c-2e "open" B–B–B bridge bonds, analogous to the B–H–B bridges.

The utility of the widely used 2c-2e and 3c-2e localized orbital bonding scheme for boranes is unequivocal, but its theoretical foundations are somewhat less definitive. Certainly, a straightforward application of MO theory to B_2H_6, for example, leads to orbitals which are delocalized throughout much of the molecule. Of course, using the invariance of the SCF wave function with respect to unitary transformations of the orbitals, it is possible to use various localization schemes, of differing expense, efficiency, and objectivity, to obtain localized molecular orbitals (LMO's) which show the desired B–H–B and terminal B–H character. Such procedures have been followed with considerable success by Lipscomb and co-workers.[49]

Two series of spin-coupled calculations have been carried out for diborane. In the first of these, our preconceptions as to the nature of the terminal B–H bonds were retained.[50] The canonical MO's for B_2H_6 were localized by using an implementation of the population localization scheme described by Pipek and Mezey:[51] the LMO's are generated by maximizing the quantity

$$Z = \sum_A \sum_i [P_A(i)]^2 \qquad (29)$$

where $P_A(i)$ is the contribution made by each electron in MO ψ_i to the Mulliken population on center A. The resulting LMO description of the 12 valence electrons corresponds closely to the conventional picture of four terminal B–H bonds and of two B–H–B bridges. Spin-coupled calculations were then carried out explicitly only for the four "bridging" electrons.

The second series of calculations for B_2H_6 was more elaborate in that all 12 valence electrons were considered directly in the spin-coupled wave function.[52] Eight of the resulting nonorthogonal orbitals take the form of B(sp^3-like) hybrids and of distorted H(1s) functions, with singlet coupling of the associated electron spins, so as to form rather "ordinary" B–H bonds. The remaining four nonorthogonal orbitals resemble very closely those from the simpler calculation in which the B–H bonds were described by LMO's. In this sense, the full 12-electron calculation appears to confirm the validity of using our preconceptions as to the nature of the terminal BH_2 units to reduce the effective size of the problem. As will become apparent, it is most convenient for our present purposes to concentrate on the results of this simpler calculation.

In the spin-coupled description of B_2H_6, each B–H–B bridge involves the overlap of two singly occupied orbitals. One of these (ϕ_1 in Figure 11) resembles the superposition of two B(sp^3-like) hybrids, but is distorted toward the B···B axis. The other (ϕ_2 in Figure 11) is a distorted H(1s) function and overlaps strongly with ϕ_1 ($\Delta_{12} \approx 0.85$). The dominant mode of spin coupling (99.3% in the Kotani basis) corresponds to singlet coupling of the associated electron spins. ϕ_3 and ϕ_4 are the counterparts in the other B–H–B bridge. The picture that emerges from spin-coupled theory for the bridging region of B_2H_6 has much in common with the conventional view of 3c-2e "banana" bonds, but there are important differences also, such as the distortion of ϕ_1 and ϕ_3 toward the B···B axis, and the relatively large overlap between these two orbitals ($\Delta_{13} \approx 0.4$).

In view of the close similarity for B_2H_6 between the full spin-coupled calculation and the simpler treatment concentrating only on the bridging region, it seems worthwhile to pursue this simpler approach for larger boron hydride systems. We describe here preliminary results for the $B_3H_8^-$ ion (see Figure 12). Application of the population localization scheme to the canonical MO's of this ion results in three LMO's which describe the interactions between the boron atoms and the bridging hydrogen atoms and a further six LMO's which describe the terminal B–H bonds in the BH_2 units.

Spin-coupled calculations have been carried out explicitly for the six valence electrons of $B_3H_8^-$ not involved in terminal B–H bonds. Three of the resulting orbitals (ϕ_1, ϕ_2, and ϕ_5) are depicted in Figure 13; the other three (ϕ_3, ϕ_4, and ϕ_6) can be obtained from these simply by reflection in the σ_v mirror plane. Orbital ϕ_1 is composed mostly of an sp^3-like hybrid on B_1 and an sp^3-like hybrid on B_2, both pointing toward H_1, but the contribution from the B_1 center is only approximately one half of that from the B_2 center. Orbital ϕ_2 is a distorted H(1s) function, similar to that observed in

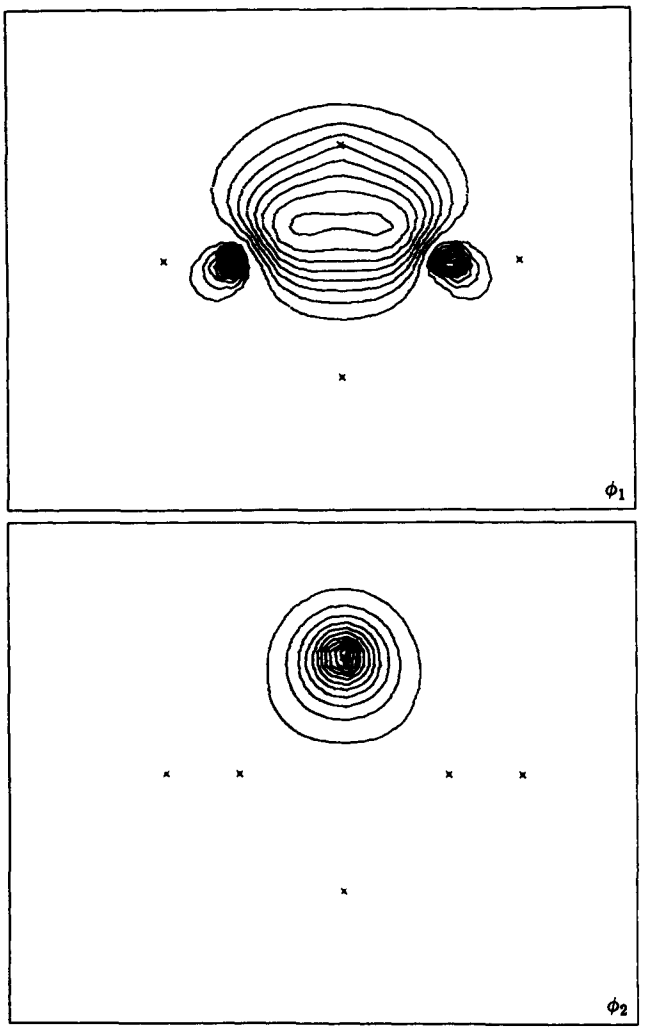

Figure 11. Contour plots for B_2H_6 of $|\phi_1|^2$ and of $|\phi_2|^2$ in the plane containing the two B–H–B bridges.

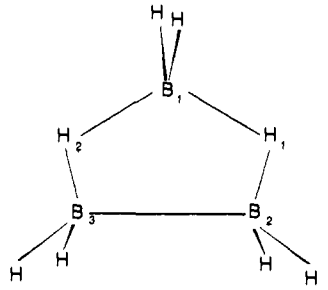

Figure 12. Structure of the $B_3H_6^-$ ion (C_{2v} symmetry). The $B_2 \cdots B_3$ separation is slightly larger than $B_1 \cdots B_2$ (or $B_1 \cdots B_3$). H_1 (H_2) is considerably closer to B_2 (B_3) than to B_1. The lines between the atoms are not meant to convey any information about the nature of the bonding.

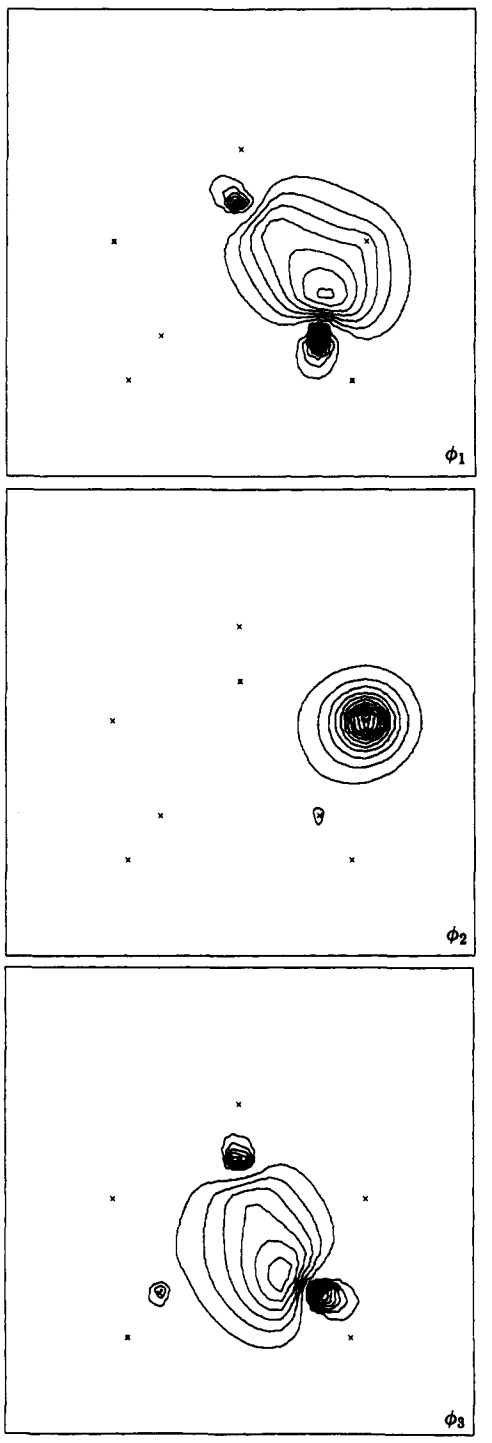

Figure 13. Three of the six spin-coupled orbitals involved in B–H–B bridges and closed BBB bonding. Contours of $|\phi_\mu|^2$ are shown in the plane containing the three boron atoms. The orientation of the molecule is the same as in Figure 12.

B_2H_6. Orbital ϕ_5 is composed mostly of an sp^3-like hybrid on B_1 and an sp^3-like hybrid on B_2, now pointing *into* the BBB triangle, but the contribution from the B_1 center is only approximately one half of that from B_2. Thus, after consideration of the terminal bonds, each of the sp^3-like lobes on B_1 is involved in *two* spin-coupled orbitals, ϕ_1 and ϕ_5 (or ϕ_3 and ϕ_6). The pairs (ϕ_1,ϕ_2) and (ϕ_3,ϕ_4) describe the B–H–B bridges. Orbitals ϕ_5 and ϕ_6 describe a closed 3c-2e BBB unit.

In view of the partial utilization of the $B_1(sp^3\text{-like})$ hybrids in orbital ϕ_1 (and ϕ_3), it is straightforward to rationalize the highly asymmetric positions of the bridging H atoms in $B_3H_8^-$. Furthermore, the two electrons not involved in B–H–B bridges or terminal B–H bonds form a closed BBB unit rather than a 2c-2e bond between B_2 and B_3. As a consequence of these considerations, we would expect a relatively large $B_2 \cdots B_3$ separation, as is indeed observed for this ion.[53]

A particular pleasing feature of this description of $B_3H_8^-$ is its "add-on" nature, whereby the B–H–B bridges resembles those in B_2H_6 and the closed BBB linkage simply appears as an additional characteristic. It is to be hoped that analogous studies of larger boranes will reveal a small number of such essentially

additive principles. For clusters based on complete, closed polyhedra of boron atoms (*closo*-boranes) and for the larger open-cluster boranes, the conventional localized "styx" approach becomes very cumbersome, and it is then more usual to consider a description based on canonical MO's. It will be very interesting indeed to examine the spin-coupled descriptions of such systems.

F. Bonding to Transition-Metal Atoms in Low Oxidation States

The experimental study of the structures and reactivity of systems containing transition-metal atoms in low oxidation states remains one of the most active areas of inorganic chemistry. The formal oxidation states of the transition-metal atoms are typically zero or one, or possibly even negative values. The chemistry of such systems usually differs markedly from that of the more traditional compounds involving higher oxidation states.

Progress in characterizing, understanding, and predicting the nature of the bonding to transition-metal atoms in low oxidation states has been very slow, even for small molecules containing just one or two transition-metal atoms. The basic problem, for any theoretical method, is the fine balance between the strong d–d coupling in the separated atoms and the process of bond formation, which necessitates the breakdown of at least some of this coupling. In addition, it appears that the calculated properties for some systems can be very sensitive to subtle electron correlation effects.

Spin-coupled calculations have concentrated so far on MH diatomics and on the corresponding MH^+ ions.[54] Our main interest is in the similarities and differences in the electronic structure of these various systems, as revealed by spin-coupled theory. Calculations for ground and low-lying excited states of MH and MH^+ species (M = Sc–Cr, Y–Mo) have been carried out typically for three values of the nuclear separation R: $R \approx R_e$, large R, and an intermediate value. These calculations used contracted GTO basis sets of triple-ζ (TZV) quality, with the addition of p polarization functions on hydrogen.

For a system with N valence electrons, we first carried out a CASSCF calculation with an active space of N electrons in N orbitals. In some cases, it was necessary to use a slightly larger number of active orbitals, so as to avoid problems of symmetry breaking. All the doubly occupied "inactive" orbitals were allowed to relax in the field of the improved description of the valence electrons. The inactive, active, and virtual CASSCF natural orbitals were then used as the basis set for all subsequent calculations. The spin-coupled calculations were carried out explicitly for the valence electrons, in the manner described in section II.C, with the remaining electrons accommodated in the inactive orbitals from the CASSCF calculation.

Spin-coupled calculations for a state of a given spin multiplicity are usually carried out without any restrictions on the spatial symmetry of the final wave function. However, it is often appropriate in the studies of MH and MH^+ systems to constrain certain orbitals to be of σ, π, or δ symmetry, particularly when dealing with excited states of the same spin multiplicity as the ground state. In most cases, the numbers of σ, π, and δ orbitals is self-evident from the overall spatial symmetry. For the small number of cases in which there was any ambiguity, all of the various possibilities have been examined so as to find the "assignment" of lowest energy. In all cases, orbitals of the same symmetry were fully optimized without any constraints on the overlaps between them. The *full* spin space was used in each case, with no restrictions.

TABLE V. Spin-Coupled Results for MH and MH^+ Systems[a]

system	state	R_e, bohr	D_e, eV	T_e, eV
ScH^+	$^2\Delta$	3.54 (3.46)	1.87 (2.34)	
	$^2\Sigma^+$	3.43 (3.38)	1.62	0.22 (0.21)
TiH	$^4\Phi$	3.56 (3.44)	1.94 (2.06)	
	$^2\Delta$	3.53 (3.35)	1.62 (1.78)	0.32 (0.28)
VH	$^5\Delta$	3.44 (3.25)	1.95 (2.33)	
CrH^+	$^5\Sigma^+$	3.15 (3.03)	0.76 (1.21)	

[a] A range of MCPF results is reported in ref 55. The values quoted in brackets in this table relate to MCPF calculations in which only the valence electrons are correlated. For the cations, the MCPF dissociation energies listed here are values of D_0 rather than values of D_e.

For a small number of states, we have calculated complete potential energy curves and so we are able to report values of R_e, D_e, and T_e. All of the results obtained in this way are collected in Table V. Of course, it would be unrealistic to expect spectroscopic accuracy for single-configuration frozen-core calculations in a limited basis set.

On the whole, this has not been an area in which applications of conventional CASSCF-CI methods have fared particularly well. The most reliable theoretical results for these systems have been obtained by Langhoff, Bauschlicher, Partridge, and co-workers[55] using a modified coupled pair functional (MCPF) formalism with more extensive basis sets. The MCPF-based wave functions take into account a significant proportion of the dynamical correlation effects for the valence electrons. The authors of the MCPF work also examined the importance of correlating larger numbers of electrons and, in some cases, of including relativistic effects. It is instructive to compare the MCPF and spin-coupled results; the MCPF values quoted in Table V are those which *exclude* core–valence correlation and relativistic effects, as in the spin-coupled calculations.

It can be seen from Table V that the values of R_e from the spin-coupled calculations are too large by 0.1–0.2 bohr. In each case, the spin-coupled configuration accounts for a large proportion of the dissociation energy (80–95%, except 63% for CrH^+). The similarity between the spin-coupled and MCPF estimates of T_e for ScH^+ ($^2\Sigma^+$) and for TiH ($^2\Delta$) is striking. Of course, all of these values could be improved by including additional configurations in a SCVB treatment, and by using larger basis sets, but this is most unlikely to modify the essential physical picture. A further series of calculations, with a smaller GTO basis set, has been carried out at $R \approx R_e$ for MH systems (M = Sc–Cu, Rh), describing the "core" with the SCF MO's for the ground state or for a suitable low-lying excited state.

We describe here the valence orbitals in the spin-coupled configuration for VH ($^5\Delta$). At large R, we observe a $4s^23d^3$ configuration on vanadium and a 1s orbital on hydrogen. The form of the orbitals for $R \approx R_e$ is shown in Figure 14. As the atoms are brought together, the H(1s) orbital, ϕ_3, distorts slightly toward

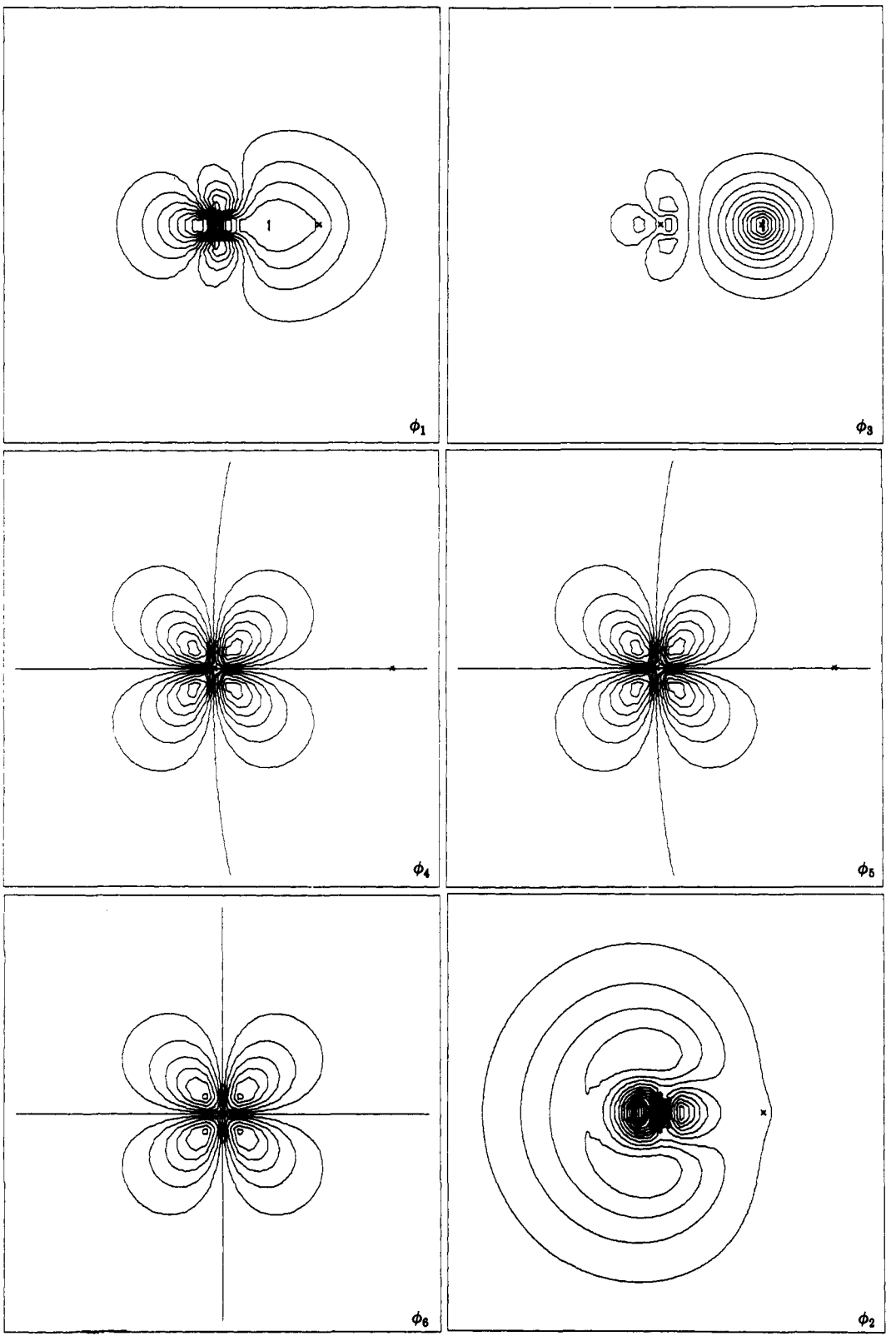

Figure 14. Spin-coupled orbitals ϕ_1–ϕ_6 for the valence electrons of VH ($^5\Delta$).

vanadium. The d orbitals on the transition metal center, ϕ_4–ϕ_6, change remarkably little. Much more marked changes occur in the two essentially 4s orbitals on vanadium, which take on characteristic forms at shorter R, to which we refer as the "bonding hybrid" and the "nonbonding hybrid". Orbital ϕ_1 (the bonding hybrid) distorts toward hydrogen and appears to take on substantial d_{z^2} character. The other orbital, ϕ_2 (the nonbonding hybrid), retains the same basic shape but starts to point away from hydrogen.

The covalent bond in this system arises from the high overlap of orbitals ϕ_1 and ϕ_3, with singlet coupling of the associated electron spins. As the internuclear distance increases, a complicated reorganization of the electron spins takes place, in which the pairing characteristic of the molecule gives way to coupling associated with the $4s^23d^3$ configuration in the isolated transition-metal atom. For all nuclear separations we

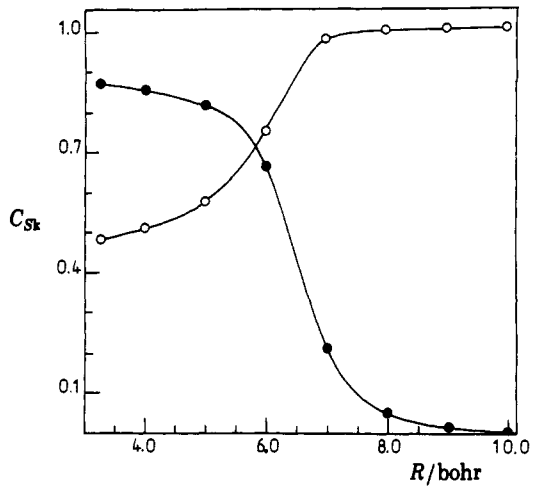

Figure 15. Variation with R of the spin-coupling coefficients c_{S4} (●) and c_{S5} (○) for VH ($^5\Delta$).

TABLE VI. Overlap Integrals Δ_{ij} between the Spin-Coupled Orbitals for the Valence Electrons of VH ($^5\Delta$) (At short range, ϕ_1 is the "bonding hybrid", ϕ_2 is the "nonbonding hybrid", and ϕ_3 is the distorted H(1s) function)

R, bohr	Δ_{12}	Δ_{13}	Δ_{23}
3.263	0.40	0.80	0.16
4.0	0.42	0.74	0.12
5.0	0.48	0.63	0.07
6.0	0.53	0.50	0.05
7.0	0.64	0.23	0.03
8.0	0.64	0.12	0.02
9.0	0.64	0.07	0.01
10.0	0.64	0.03	0.01

have considered, the wave function is dominated (in the standard basis) by just two of the five spin functions:

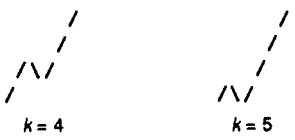

The variation with R of the spin-coupling coefficients c_{S4} *and* c_{S5} is shown in Figure 15. The most dramatic changes in the spin-coupling coefficients occur between 5 and 7 bohr. The overlap integral (Δ_{13}) between orbitals ϕ_1 and ϕ_3 also changes very rapidly in this region of R. All the non-zero overlap integrals are listed in Table VI. Although Δ_{23} remains small for all geometries considered, it does begin to increase at short R. It would not be easy in the present case to justify the use of strong orthogonality and perfect-pairing restrictions.

The spin-coupled description of VH^+ ($^4\Delta$) is very similar to that of VH ($^5\Delta$), except for the absence of the nonbonding hybrid. Pictures analogous to those for VH (and VH^+) emerge for all the MH and MH^+ systems based on first-row atoms. The variation of the dipole moment (at R_e) with the identity of the transition metal is similar to that found in the MCPF-based calculations.[55] We find that it is possible to formulate simple rules, based on the availability of empty d_{z^2} orbitals at large R, to rationalize the ordering of electronic states in these systems.

We turn now to the spin-coupled description of the valence electrons in NbH ($^5\Delta$). At large R, we observe a $5s^14d^4$ configuration on niobium and a 1s orbital on hydrogen, as indeed should be the case. The form of the orbitals for $R \approx R_e$ is shown in Figure 16. This system is typical of all the MH and MH^+ systems, based on second-row transition-metal atoms, which we have studied. The "bonding hybrid", ϕ_1, is similar to that for VH, but appears to include more d_{z^2} character. The "nonbonding hybrid", ϕ_2, is significantly different from that described for VH. For the second-row transition-metal systems, the nonbonding hybrid most closely resembles the out-of-phase $5s\text{-}4d_{z^2}$ combination. Orbital ϕ_3, which is based on H(1s), is fairly similar to the corresponding orbital in VH, but shows greater deformation.

The spin-coupled approach is currently being applied to a wide range of more complex molecules with metal–metal bonding, and with carbonyl, alkene, and phosphine ligands. The model systems being studied[56] are relatively small by the usual standards of inorganic chemistry, but they should be sufficiently complex to exhibit many of the general features. It is important to exercise some care in the choice of model systems, paying particular attention to the known chemistry. For example, scandium and titanium atoms in a formal oxidation state of zero do not in general form stable complexes with carbonyl ligands except, for example, for various $M(CO)_x$ species which can be studied in inert gas matrices. Ti^{II} does form some stable complexes with CO, such as $Ti(CO)_2(Cp)_2$, but it is not clear that the Ti^{II}–CO bonding is similar to the $M^{(0)}$–CO bonding envisaged for the later transition metal atoms.

Inorganic chemists usually consider CO to be a two-electron ligand. With the use of the population localization technique described in section III.E, it is possible to treat a system such as V–CO as a seven-electron problem—five from the transition metal and two from the carbonyl—and this seems a very reasonable approximation, at least for preliminary work. Such approximations are useful because the *total* number of valence electrons in these systems rapidly becomes too large to treat with the current versions of the spin-coupled programs. A significant number of systems have now been studied in this way.

Spin-coupled orbitals are shown in Figure 17 for linear V–CO ($^6\Sigma^+$), and lend further support to the familiar model of σ donation to the metal and of π back-donation onto the carbonyl (see also ref 57). The expected forward σ donation from the carbonyl to the metal in V–CO occurs via orbital ϕ_1, which takes on some of the "bonding hybrid" character, analogous to that described above for VH. The second orbital on the carbonyl, ϕ_2, is much more compact and shows less deformation toward the metal. Orbital ϕ_7 takes the form of a nonbonding hybrid on the transition metal. The associated π back-donation from the metal to the carbonyl occurs via the vanadium d orbitals ϕ_3 and ϕ_4, which distort toward the carbonyl and populate the vacant $CO(\pi^*)$ orbital. The remaining orbitals (ϕ_5 and ϕ_6) are of δ symmetry. The total wave function is dominated by one mode of spin coupling: the spins of the two electrons on the carbonyl are singlet coupled, with the spins of the electrons on the vanadium center coupled to the maximum value ($S = 5/2$).

Preliminary calculations have been carried out for the complex $Cr(CO)_5(H_2)$, again using the population localization scheme to reduce the effective size of the

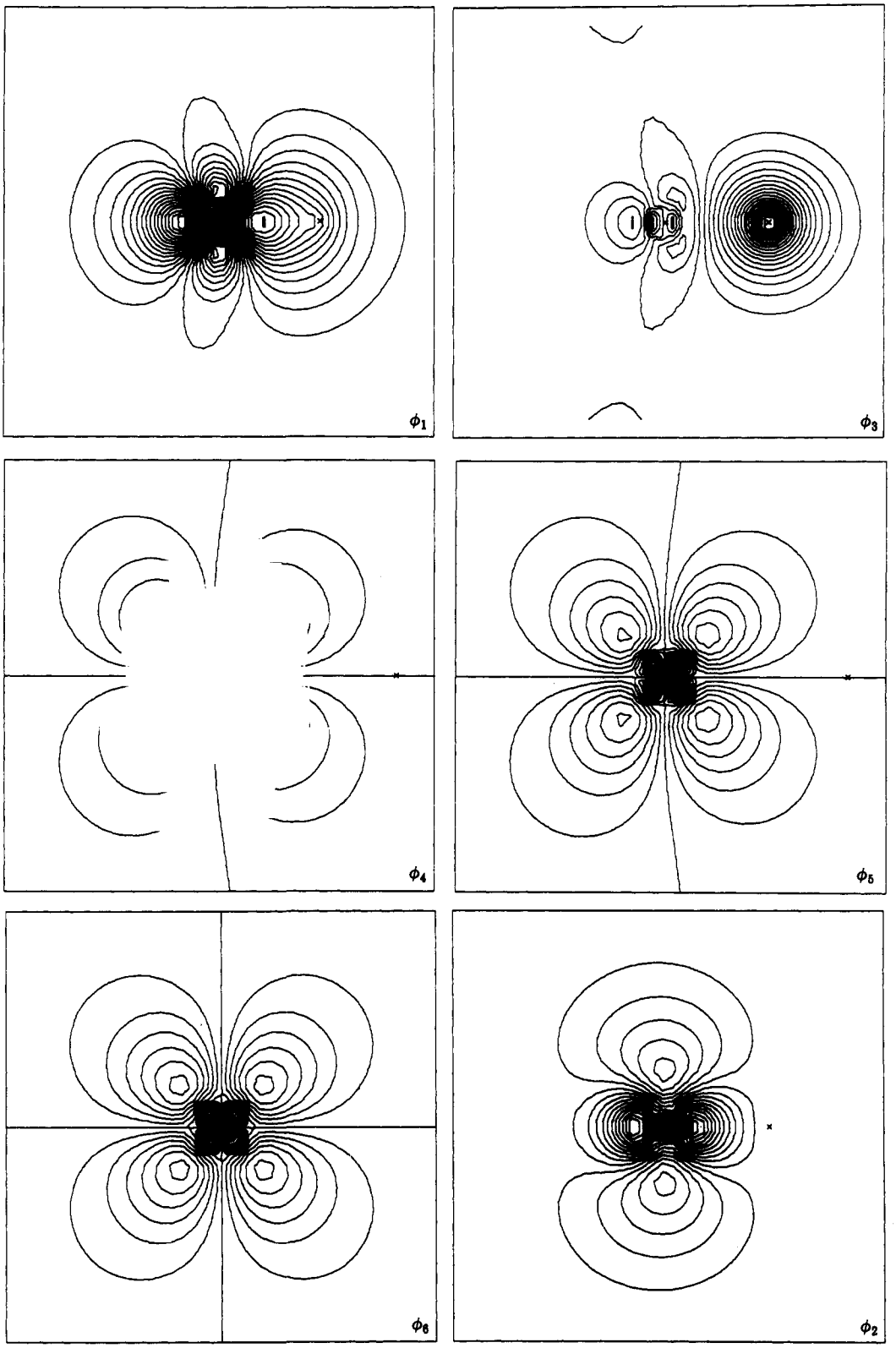

Figure 16. Spin-coupled orbitals ϕ_1–ϕ_6 for the valence electrons of NbH ($^5\Delta$).

problem. Spin-coupled orbitals are shown in Figure 18 for a six-electron calculation which concentrated on the two electrons of the H_2 moiety, two electrons from the metal, and two from the "lone pair" of the carbonyl *trans* to H_2. The overall nature of the Cr–CO bonding is essentially the same as that just described for the monocarbonyl V–CO, but the π back-donation occurs via only one (ϕ_3) of the two available metal orbitals, with the other (ϕ_4) retaining essentially pure atomic form. Orbitals ϕ_5 and ϕ_6 (not shown in Figure 18) are derived from the carbonyl. The orbitals of the H_2 unit (ϕ_1 and ϕ_2) show much more delocalization than do the corresponding orbitals in the isolated H_2 molecule. The perfect-pairing spin function dominates. The metal orbitals which might lead to dissociation of H_2, i.e. oxidative addition, are either compact atomic functions or are already heavily involved in back-donation into all available CO(π^*) orbitals. Consequently, this particular complex incorporates molecular H_2 rather than two M–H bonds.

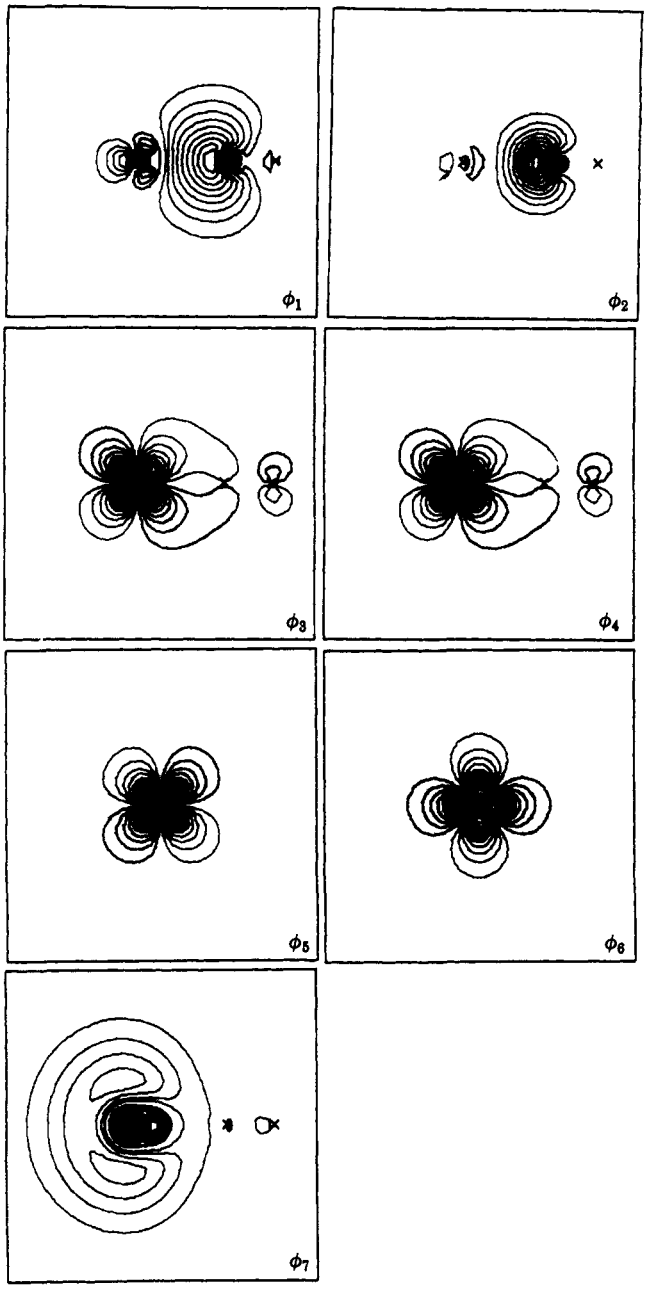

Figure 17. Spin-coupled orbitals for V–CO ($^6\Sigma^+$). The molecule points across the page with the vanadium atom, which defines the origin of the coordinate system, located on the left. Contours of ϕ_1, ϕ_2, ϕ_3, and ϕ_7 are shown in the plane $y = 0$, of ϕ_4 in the plane $x = 0$, and of ϕ_5 and ϕ_6 in the plane $z = 0$.

Much work remains to be done, but there are already clear indications that the spin-coupled description of systems such as these will lead to significant progress toward understanding the nature of the bonding to transition-metal atoms in low oxidation states.

IV. Applications of SCVB Theory (Multiconfiguration Valence Bond)

A. Diatomic Systems

The SCVB approach has been used to study ground and excited states of numerous neutral and charged diatomic systems. In particular, there has been a number of SCVB studies of potential energy curves for charge-transfer processes. The systems considered include low-lying states[58] of $LiHe^+$ and the processes[59,60]

$$C^{3+}(2l) + H(1s) \rightarrow C^{2+}(nln'l';^1L) + H^+$$

$$C^{3+}(2s) + Li(2p) \rightarrow C^{2+}(nln'l';^1L) + Li^+(1s^2) \qquad (30)$$

Collisions involving multiply charged atomic ions and neutral atomic targets (such as H, He, and Li) play an important role in establishing the ionization structure of a wide range of terrestrial and astrophysical plasmas. In general, electron capture by slow ion projectiles from neutral atomic targets takes place preferentially (and often very selectively) into excited states which can then emit high-energy photons, thus leading to cooling of the plasma. In addition, these photon emissions are potentially useful as a diagnostic probe, yielding information on the plamsa environment and on the generation and transport of impurity ions.

It appears to be a general feature of such charge-transfer collisions that it may be necessary to consider all the avoided crossings between several states. It is necessary to describe each state with uniform accuracy over the entire range of R. In addition, it is essential to describe well the asymptotic splittings, since these determine to a very large extent the location and the nature of the avoided crossings. We concentrate here on two fairly representative applications of SCVB to diatomic species. We describe in some detail calculations for the system C^{4+} + H(1s), in order to give an indication of the general procedures used to select virtual orbitals and to select the classes of excitations to be included in the SCVB wave function. Our second example is the N^{5+} + $He(1s^2)$ system, for which we describe the simultaneous determination of more than 40 adiabatic states, and the calculation of matrix elements of $\partial/\partial R$ (nonadiabatic couplings).

Spin-coupled calculations for the $^2\Sigma^+$ ground state of the "simple" system CH^{4+} have been carried out for 18 nuclear separations (R) between 2 and 30 bohr, using a univeral even-tempered (UET) basis set consisting of 9s/6p/3d Slater functions on each center. Over the entire range of R considered, the spin-coupled orbitals correspond to $C^{3+}(1s1s'2s)$ + H^+. The dominant mode of spin coupling is that in which the two core electrons are singlet coupled, and the overlap between the core orbitals varies little with nuclear separation ($\Delta_{12} = 0.97$ at $R = 30$ bohr). In the case of the $^2\Sigma^+$ states, the smallest SCVB wave functions consisted of just nine spatial configurations, namely the spin-coupled configuration plus the eight additional configurations which may be generated from it by single excitations of the "valence" orbital (ϕ_3) into the eight lowest σ virtual orbitals from stack number three. In SCVB theory, these singly excited configurations are usually very good representations of the low-lying excited states. Note that these configurations cannot interact directly with the reference configuration. The calculated total energies for three representative values of R are collected in Table VII, and the asymptotic energies are listed in Table VIII. It is clear that each of the $^2\Sigma^+$ states is represented well by just one spatial configuration.

It is convenient to use the symbol $X_\mu^{(i)}$ to denote the ith orbital of symmetry X = σ, π, or δ in stack μ. The occupied orbitals are $\sigma_1^{(1)}$, $\sigma_2^{(1)}$, and $\sigma_3^{(1)}$. As might be expected, the two "core" stacks turn out to be very similar—the overlap between $\sigma_1^{(3)}$ and $\sigma_2^{(3)}$, for example, is $\Delta = 0.999$ at $R = 30$ bohr. It was found that taking only alternate virtuals from the first two stacks, in a

TABLE VII. Total Energies (in hartree) for the Lowest $^2\Sigma^+$ and $^2\Pi$ States of CH^{4+} at Three Representative Nuclear Separations, R

$^2\Sigma^+$ States

		no. of spatial configurations				
R, bohr	state	1	9	132	157	182
30	1	-34.639 74	-34.639 74	-34.642 70	-34.643 36	-34.643 46
	2		-34.342 03	-34.343 74	-34.345 66	-34.346 16
	3		-33.262 50	-33.263 15	-33.263 34	-33.263 82
	4		-33.182 07	-33.182 27	-33.182 76	-33.182 89
	5		-33.160 46	-33.160 69	-33.160 87	-33.160 87
	6		-32.875 11	-32.875 13	-32.875 13	-32.875 13
7	1	-34.311 91	-34.311 91		-34.315 46	
	2		-34.014 42		-34.019 15	
	3		-32.962 69		-34.963 21	
	4		-32.890 86		-32.890 95	
	5		-32.846 40		-32.847 06	
	6		-32.820 03		-32.821 24	
3	1	-33.766 82	-33.766 83		-33.769 99	
	2		-33.455 30		-33.461 00	
	3		-32.778 38		-32.779 22	
	4		-32.272 62		-32.273 19	
	5		-32.163 33		-32.164 67	
	6		-31.985 52		-31.986 15	

$^2\Pi$ States

		no. of spatial configurations			
R, bohr	state	4	50	63	76
30	1	-34.341 98	-34.346 32	-34.346 38	-34.346 58
	2	-33.181 84	-33.182 71	-33.183 60	-33.183 73
	3	-33.160 45	-33.160 57	-33.160 70	-33.161 35
	4	-32.534 30	-32.535 67	-32.535 72	-32.535 75
7	1	-34.011 91			-34.016 71
	2	-32.860 75			-32.862 64
	3	-32.820 10			-32.821 38
	4	-32.452 74			-32.452 85
3	1	-33.430 86			-33.434 58
	2	-32.321 87			-32.323 38
	3	-32.166 84			-32.168 07
	4	-31.856 19			-31.856 46

TABLE VIII. Relative Asymptotic Energies (in electron volts) for Low-Lying $^2\Sigma^+$ and $^2\Pi$ States of CH^{4+}[a]

$^2\Sigma^+$ States

	no. of spatial configurations				
asymptote	9	132	157	182	exp
$C^{3+}(2s) + H^+$	-8.10	-8.14	-8.10	-8.09	-8.00
$C^{3+}(2p) + H^+$	0	0	0	0	0
$C^{3+}(3s) + H^+$	29.38	29.41	29.45	29.45	29.55
$C^{3+}(3p) + H^+$	31.56	31.61	31.64	31.65	31.68
$C^{3+}(3d) + H^+$	32.15	32.19	32.24	32.25	32.28
$C^{4+} + H(1s)$	42.64	42.68	42.74	42.75	42.88

$^2\Pi$ States

	no. of spatial configurations				
asymptote	4	50	63	76	exp
$C^{3+}(2p) + H^+$	-31.57	-31.66	-31.64	-31.64	-31.68
$C^{3+}(3p) + H^+$	0	0	0	0	0
$C^{3+}(3d) + H^+$	0.58	0.60	0.62	0.61	0.60

[a] The calculated values are obtained by removing the coulombic repulsion at 30 bohr in the $C^{3+} + H^+$ states from the corresponding SCVB energies. The experimental values are based on Moore's tables of atomic energy levels.[81]

TABLE IX. Asymptotic Forms of the Orbitals Used in SCVB Calculations for $^2\Sigma^+$ and $^2\Pi$ States of CH^{4+}

$^2\Sigma^+$

$\sigma_1^{(1)} \approx$ C(1s)	$\sigma_2^{(1)} \approx$ C(1s)	$\sigma_3^{(1)} \approx$ C(2s)
$\sigma_1^{(2)} \approx$ C(2s)	$\sigma_2^{(3)} \approx$ C(2p)	$\sigma_3^{(2)} \approx$ C(2p)
$\sigma_1^{(4)} \approx$ C(3s)	$\sigma_2^{(5)} \approx$ C(3p)	$\sigma_3^{(3)} \approx$ C(1s)
$\sigma_1^{(6)} \approx$ C(3d)	$\sigma_2^{(7)} \approx$ H(1s)	$\sigma_3^{(4)} \approx$ C(3s)
$\pi_1^{(1)} \approx$ C(2p)	$\pi_2^{(2)} \approx$ C(3p)	$\sigma_3^{(5)} \approx$ C(3p)
$\sigma_2^{(1)} \approx$ C(1s)	$\delta_2^{(1)} \approx$ C(3d)	$\sigma_3^{(6)} \approx$ C(3d)
		$\sigma_3^{(7)} \approx$ H(1s)
		$\pi_3^{(1)} \approx$ C(2p)
		$\pi_3^{(2)} \approx$ C(3p)
		$\pi_3^{(3)} \approx$ C(3d)
		$\delta_3^{(1)} \approx$ C(3d)

$^2\Pi$

$\sigma_1^{(1)} \approx$ C(1s)	$\sigma_2^{(1)} \approx$ C(1s)	$\sigma_3^{(1)} \approx$ C(2s)
$\sigma_1^{(2)} \approx$ C(2s)	$\sigma_2^{(3)} \approx$ C(2p)	$\sigma_3^{(2)} \approx$ C(2p)
$\pi_1^{(1)} \approx$ C(2p)	$\pi_2^{(1)} \approx$ C(2p)	$\sigma_3^{(3)} \approx$ C(1s)
	$\pi_2^{(2)} \approx$ C(3p)	$\pi_3^{(1)} \approx$ C(2p)
	$\delta_2^{(1)} \approx$ C(3d)	$\pi_3^{(2)} \approx$ C(3p)
		$\pi_3^{(3)} \approx$ C(3d)
		$\pi_3^{(4)} \approx$ C(4p)
		$\pi_3^{(5)} \approx$ C(4d)
		$\delta_3^{(1)} \approx$ C(3d)
		$\delta_3^{(2)} \approx$ C(4d)

staggered arrangement, had very little effect on the spin-coupled VB energies. This allowed us to go higher in each stack without encountering problems of linear dependence, and thus leads to a good description of a larger number of states. The orbitals listed in Table IX were chosen after several numerical experiments. Note that $\sigma_3^{(3)}$ is a little unusual in that it has the form of a C(1s) orbital and has a high overlap with $\sigma_1^{(1)}$ and $\sigma_2^{(1)}$ ($\Delta = 0.92$ at $R = 30$ bohr). Virtuals from separate stacks are eigenfunctions of different operators, and so there is nothing to prevent virtual orbitals for valence electrons taking the same form as occupied core orbitals. The configurations involving $\sigma_3^{(3)}$ were found to lower the energy of a number of states.

Three series of SCVB calculations were carried out using the chosen set of virtuals. The first consisted of

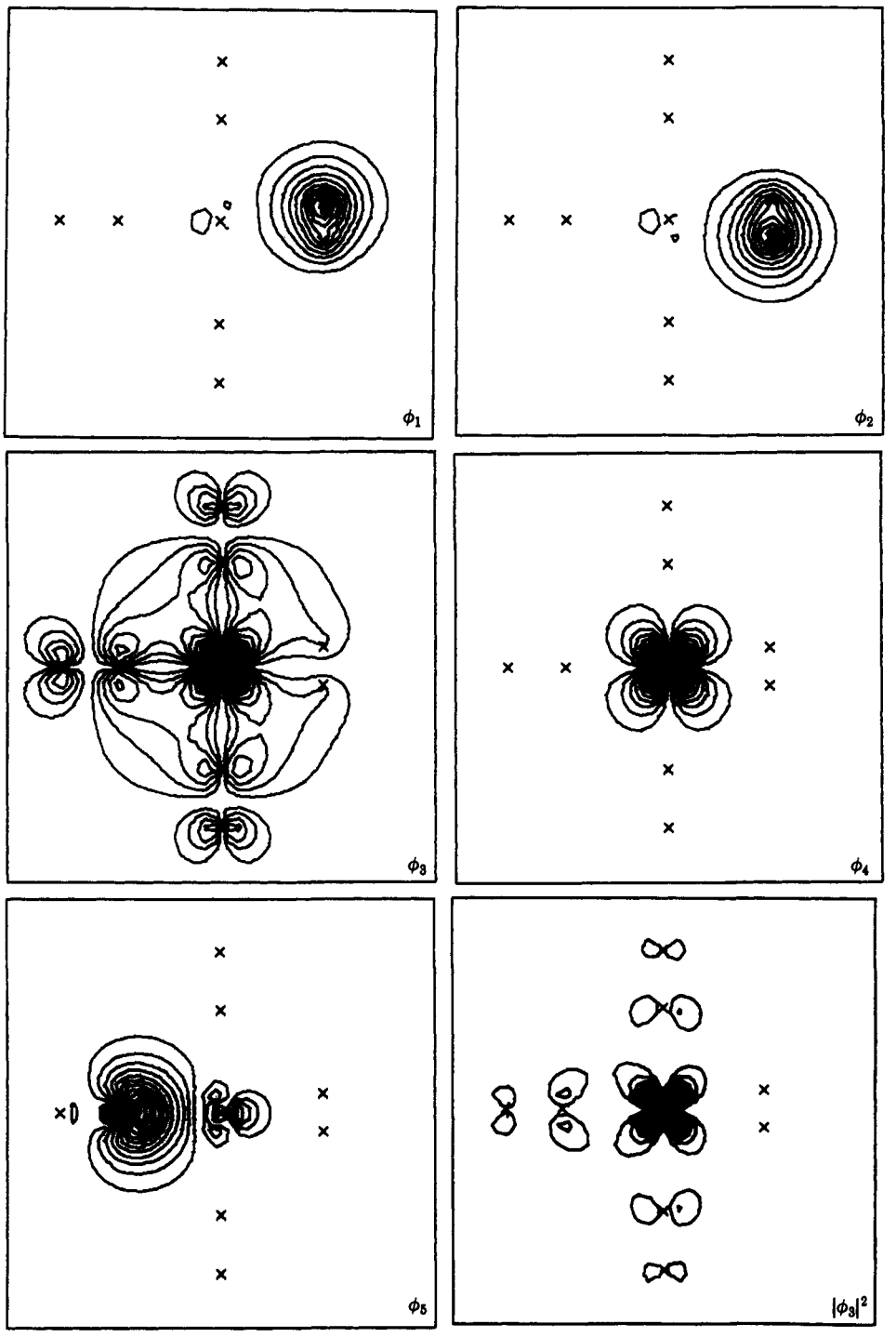

Figure 18. Spin-coupled orbitals from a six-electron calculation on $Cr(CO)_5(H_2)$. Contours of ϕ_1–ϕ_5 are shown in the plane containing the Cr–H_2 unit. The contours of ϕ_3 tend to exaggerate the degree of back-donation, and so we also show $|\phi_3|^2$.

132 spatial configurations, corresponding to the spin-coupled configuration plus all single and double excitations of the occupied orbitals into virtual solutions from their own stacks. The 132-configuration calculation also included all those "ionic" configurations in which one orbital is doubly occupied, in order to improve the description of charge-transfer effects. It can be seen from Tables VII and VIII that the improvements at 30 bohr over the nine-configuration calculation are fairly modest, with the largest change occurring for the ground state. With this in mind, a list of 157 spatial configurations was constructed which included double excitations both from the spin-coupled configuration and from the dominant configuration for the first excited state. In addition to these, the largest calculation (182 configurations) also included double excitations from the "reference" configuration for the second excited state. Double excitations from the dominant configuration for the first excited state do result in a small improvement, but the further changes arising from the inclusion of excitations from the reference configuration for the second excited state are very small.

A full set of potential curves was computed for the first six states of $^2\Sigma^+$ symmetry with the list of 157 spatial configurations. Each state is overwhelmingly dominated by just one spatial configuration for all nuclear separations, the coefficients for the other configurations being almost negligible. More than one mode

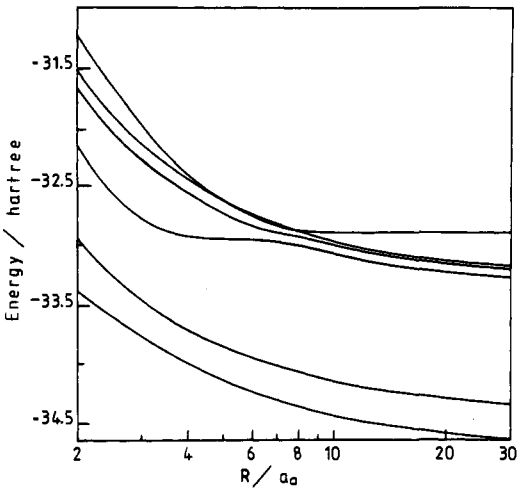

Figure 19. SCVB potential energy curves for the first six $^2\Sigma^+$ states of CH^{4+}.

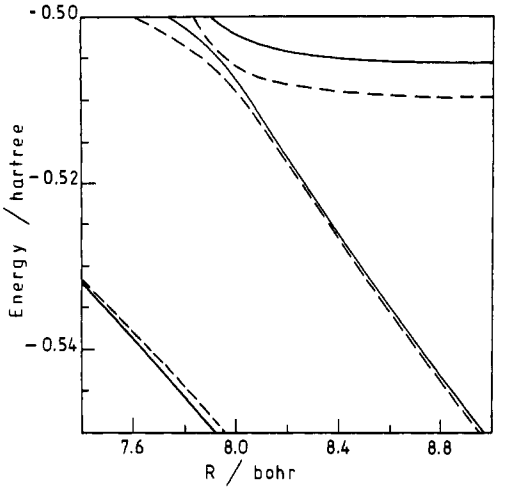

Figure 20. Comparison of SCVB potential curves (broken line) for $^2\Sigma^+$ states of CH^{4+} with those from the model potential calculations (full line) of Gargaud et al.[61] See also Figure 19.

of spin coupling is possible for many of the configurations and so the list of 157 spatial configurations actually corresponds to a total of 208 VB structures.

Analogous calculations have been carried out for low-lying states of $^2\Pi$ and $^2\Delta$ symmetry, using occupied and virtual orbitals taken from the spin-coupled calculations for the $^2\Sigma^+$ ground state. The calculations exhibit the same excellent convergence with respect to the number of spatial configurations, and the final potential energy curves for the first four $^2\Pi$ states, for example, were calculated by using SCVB wave functions consisting of just 76 spatial configurations (122 VB structures).

The SCVB potential energy curves for the $^2\Sigma^+$ states are shown in Figure 19 and these are compared in Figure 20 with those from the model potential calculations of Valiron and co-workers.[61] It remains to be seen whether quantal scattering calculations using the SCVB potential curves will significantly reduce the existing discrepancies between calculated and experimental cross sections. Certainly, the calculated cross sections are very dependent on the location and nature of the avoided crossing with the $C^{3+}(3d)$ channel, and it is likely that they will also prove to be very sensitive to the relative locations of the $^2\Pi$ and $^2\Sigma^+$ states.[62]

We turn now to our second example, the NHe^{5+} system, for which the most important charge-transfer processes are

$$N^{5+} + He \rightarrow N^{4+}(3l) + He^+$$

$$N^{5+} + He \rightarrow N^{3+} + He^{2+} \qquad (31)$$

with a fairly high probability for the two-electron capture. SCVB calculations have been carried out by using exactly the same GTO basis set as used by Bacchus[63] in CIPSI calculations. The final SCVB wave functions, consisting of 184 spatial configurations, were based on 36 occupied and virtual orbitals plus an additional He(1s) orbital taken from a separate atomic spin-coupled calculation.

The previous CIPSI calculations considered just six states, the highest of which corresponds at large nuclear separation to the 42nd root in our calculations. Nonetheless, we find excellent agreement between the asymptotic energies from the two sets of calculations. Indeed, the agreement remains good over the entire range of R, except, of course, in the regions of the additional avoided crossings with states neglected in the previous study.

The ability to describe consistently well such a large number of states of widely differing character over the entire range of R using such a compact wave function (184 spatial configurations) is of considerable importance. In particular, the calculation of accurate matrix elements of $\partial/\partial R$, required for quantal scattering calculations, becomes essentially routine.

The most straightforward evaluation of these nonadiabatic couplings is by numerical differentiation. Separate SCVB calculations are carried out for nuclear separations $R + \delta$ and $R - \delta$, and the overlap integrals between GTO's (calculated for the mean nuclear separation, R) are then used to form the quantity

$$\frac{\langle \Psi_i(\mathbf{r}|R-\delta)|\Psi_j(\mathbf{r}|R+\delta)\rangle}{2\delta} \qquad (32)$$

This simple approximation to $\langle \Psi_i|\partial/\partial R|\Psi_j\rangle$ neglects the changes to the basis functions; calculations which included also this term suggest that its contribution is small, at least for NHe^{5+}, but that it can make this procedure numerically unstable. One criterion for the consistency of the central difference scheme embodied in eq 32 is the equality

$$\langle \Psi_i|\partial/\partial R|\Psi_j\rangle = -\langle \Psi_j|\partial/\partial R|\Psi_i\rangle \qquad (33)$$

which is typically satisfied in our calculations to four or five significant figures. Typical values of δ for NHe^{5+} lie in the range 2×10^{-3} to 2×10^{-4} bohr, and the optimum value of δ remains constant over a wide range of R, so that the calculations are very straightforward.

In those cases for which the potential energy curves from the SCVB and CIPSI calculations are very similar, we also find excellent agreement for the corresponding matrix elements of $\partial/\partial R$, and this gives us great confidence in our very inexpensive central difference scheme. The nonadiabatic coupling show significant differences in the neighborhood of interactions with states not considered in the earlier CIPSI study. Analogous SCVB calculations of potential energy curves and nonadiabatic couplings have also been completed for the N^{4+} + H system.

B. Triatomic Systems

We describe here SCVB results for a number of reactions between small ions, such as Be^+, B^+, and C^+, and molecular hydrogen. The reactions involving B^+ and C^+ have also been studied experimentally and, in particular, observations of chemiluminescence have shed much light on the mechanisms and on the electronic states involved.

Collisions of an atomic ion A^+ with H_2 can give rise to a number of products in different states. The reactive and charge-transfer channels of interest in such experiments include $A^+ + H_2$, $A + H_2^+$, $A - H^+ + H$, and $A - H + H^+$, where both the reactants and products may be in ground or excited states. It is necessary that the calculations determine the potential curves out to large interatomic distances, corresponding to all these different arrangements. In order to obtain a clear physical picture of how these reactions proceed, and of the processes of bond making and bond breaking in the different states, it is important to be able to describe accurately all of the relevant molecular states by using compact, easily interpreted wave functions.

In the case of the BeH_2^+ and BH_2^+ ions, it turned out to be appropriate to select very small, physically reasonable sets of virtual orbitals of both σ and π symmetry by using very simple rules. It is interesting to note that the virtual orbitals are fairly localized, but not necessarily on the same center as the corresponding occupied orbital. The configurations generated by single excitations into the σ virtual orbitals were found to provide good reference structures for the excited states; the role of the chosen π orbitals is to provide angular correlation. It is very easy to classify the various structures in terms of different physical processes, such as charge transfer or a local electronic excitation.

In the case of the reactions of Be^+ with H_2, we picked out for each occupied valence orbital both the lowest unoccupied orbital of the same symmetry (σ) and the lowest energy virtual orbital of different symmetry (both π_x and π_y).[64] We constructed an extremely compact set of 58 configurations (83 structures), in the manner described in section II.D. Computed energy separations were found to be within 0.3–0.4 eV of the experimental values, in spite of the use of a rather small GTO basis set.

The reactions involving B^+ have been studied[65] by employing a much larger GTO basis set: B(11s6p2d/9s5p2d), H(6s2p1d/4s2p1d). Diffuse functions on boron were needed to represent the B($2s^2 3s;^2S$) Rydberg state, which is a dissociation product of the $B^1\Sigma^+$ state of BH, and the 3d functions on hydrogen were included so as to improve the description of certain states of BH in which the hydrogen atom acquires significant H^- character. All the states lying within 13 eV of the BH^+ ($X^2\Sigma^+$) + H ground state were described well, and the calculated asymptotic energies were in good agreement with experimental values. The chief shortcoming of the calculation was a discrepancy of 0.3 eV for the energy of the charge-exchange process $B^+(2s^2;^1S) + H \rightarrow B(2s^2 2p;^2P) + H^+$.

The set of orbitals used in the SCVB calculations for the BH_2^+ ion consisted of the occupied orbitals plus two virtuals of σ and one of π symmetry (π_x and π_y) for each of the four valence electrons. The structures included in this case arise from single and double excitations from the original spin-coupled configuration and from the reference configurations for the excited states. The total number of configurations generated in this way was 400, corresponding to 592 structures. For any state, no more than about 10 structures make up ~95% of the wave function, so that the interpretation of the character of the various states is very straightforward.

This SCVB study of BH_2^+ concentrated only on the asymptotic regions of the potential surfaces. The two lowest $BH^+ + H$ and $BH + H^+$ states could be compared directly with earlier MCSCF and CASSCF calculations for the isolated BH^+ and BH species. The total SCVB energies turned out to be significantly lower, in spite of the use of a smaller basis set. In particular, the potential energy curve for the BH ($B^1\Sigma^+$) state, which features a double minimum, was well represented by the SCVB calculation, even though the relevant BH ($B^1\Sigma^+$) + H^+ state occurs as the sixth or the seventh root of the calculation, depending upon the nuclear geometry. The dipole moments from the SCVB study were found to agree very well with those from other theoretical studies.

The reactions of $C^+(^2P)$ with H_2 to produce CH^+ ($X^1\Sigma^+$) + H and $CH^+(A^1\Pi)$ + H are considered to proceed either through formation of an intermediate CH_2^+ complex or through a direct mechanism. An SCVB study has been carried out with the aim of shedding some light on the mechanism of these reactions.[66] Extensive regions of the potential energy surfaces have been mapped out at the spin-coupled level for the lowest $^2A_1$ and $^2B_1$ states of CH_2^+. Additional electron correlation was introduced for key regions using SCVB wave functions consisting of 181 configurations. The effect of these additional configurations was to provide a fairly uniform lowering of the surfaces, without altering the shapes of the surfaces or the character of the respective wave functions.

Minimum energy paths for the lowest $^2A_1$ and $^2B_1$ states were determined for the perpendicular approach of C^+ to H_2. Polarization forces between C^+ and H_2 were found to be responsible for the appearance of long-range wells. On both surfaces the minimum-energy path was associated with very rapid changes in the mode of spin coupling from that characteristic of the reagents, $C^+(^2P) + H_2$, to that of the CH_2^+ products. As the two fragments approach along this path, there is a saddle point in each potential energy surface, with barriers of 3.83 eV and of 2.03 eV for the $^2A_1$ and $^2B_1$ states, respectively. The absolute minimum for the $^2A_1$ state corresponds to a bond angle of 140° and to C–H bond lengths of 1.1 Å. The minimum in the $^2B_1$ state was located for a linear ($^2\Pi$ state) configuration with the same bond length. The overall results were in excellent agreement with previous extensive MO-CI studies.

Another representative example of the applications of SCVB theory is a study of the potential energy surfaces for several low-lying singlet and triplet states of the molecular dication H_2O^{2+}, which has been studied experimentally using a variety of techniques.[67] This species dissociates into $OH^+ + H^+$, $O + H^+ + H^+$ and $O^+ + H^+ + H$ in a variety of states. The SCVB calculations[68] used the same GTO basis of DZP quality as employed in an earlier MO-CI study of this system. Wide regions of the surfaces were studied, including the

TABLE X. Comparison of SCVB Results for CH_2 with the MO-CI Results of Bauschlicher and Taylor (ref 23)[a]

method[b]	ΔE, kcal/mol
1R-SCF	26.14
1R-SD-CI	14.63
spin-coupled	13.27
CASSCF	12.82
2R-SCF	12.73
1R-SD(Q)-CI	12.35
2R-SD-CI	12.20
SCVB	12.11
full CI	11.97

[a] ΔE is the $^3B_1$–$^1A_1$ splitting. The various calculations use the same geometries and the same basis set, except for the number of d components. [b] 1R single (reference) configuration for both states; 2R two (reference) configurations for $^1A_1$, but one for $^3B_1$.

various dissociation channels. The SCVB wave functions were constructed from a very small set of orbitals, namely the six spin-coupled orbitals for the valence electrons and the lowest unoccupied orbital from each of the six stacks. The configurations included correspond to single "vertical" excitations only, i.e. to the replacement of an occupied orbital by the first virtual orbital from the same stack. However, we also included all configurations in which one of the orbitals is doubly occupied, in order to provide for an improved description of the charge-transfer effects occurring in the excited states. The total set consisted of 187 configurations, giving rise to 395 structures for the singlet states and 603 structures for the triplet states. In spite of the very limited number of orbitals and of configurations, there was no ambiguity when correlating any of the *twenty* states which were examined. These states span a range of more than 30 eV. The agreement with other theoretical results employing the same basis set was quite striking. Analogous SCVB calculations have been carried out for the dications of methane and ammonia,[69] and also for triply charged molecular ions.

Certainly, it is true that a majority of the applications of the SCVB approach have been to ionic systems. This is purely a reflection of the type of system which is of greatest interest to us, rather than of any limitation of the method itself. We mention here, very briefly, just one SCVB study of a neutral triatomic system. The spin-coupled descriptions of the lowest singlet and triplet states of CH_2, and the consequences of these for understanding various reactions of methylene, have been described in section III.A. The SCVB calculations for this system[19] were carried out in much the same way as for H_2O^{2+}, but including now also the doubly excited configurations. The same list of 202 configurations was used for both spin multiplicities, corresponding to 738 and 470 structures for the $^3B_1$ and $^1A_1$ states, respectively. It is important to note that the singlet and triplet states are being treated in an identical fashion—the difference in the number of structures arises only because of the different values of f_S^N in the two cases.

We compare in Table X the SCVB estimate of the $^3B_1$–$^1A_1$ splitting with values obtained using different theoretical methods. All of these calculations used the same GTO basis set of DZ quality. In spite of the compactness of the wave functions, the SCVB calculations predict an energy difference which is very close to the corresponding full-CI result. The SCVB value is probably much more sensitive to the quality of the basis set than to the inclusion of further dynamical correlation effects. Certainly, analogous 202-configuration SCVB calculations, but now using a much larger basis set, yield a value for the $^3B_1$–$^1A_1$ splitting which is in fairly good agrement with the experimental value.

C. Molecular Properties

Since all the orbital coefficients $c_{\mu p}$ and the spin-coupling coefficients c_{Sk} in the spin-coupled wave function are fully optimized, it is straightforward to show that the expectation values of one-electron operators are given to "second-order" accuracy. The proof follows lines parallel to those for the Hartree–Fock SCF wave function. Provided that the basis set is sufficiently large and flexible, this means in practice that the errors in the computed values of properties such as electric dipole moments are typically ~5%, at least close to the equilibrium geometry.

The same is true of time-independent response functions, such as electric dipole polarizabilities and magnetic susceptibilities, which also involve one-electron operators. The determination of such properties from spin-coupled wave functions has only become possible very recently, and the number of applications is still relatively small. However, the "perturbed spin-coupled" programs are fairly general, and we intend to carry out many more such studies of this kind in the very near future.

The calculation of expectation values of one-electron operators over the spin-coupled wave function is entirely straightforward. The range of applications is limited only by the availability of the necessary "property integrals" in the AO (i.e. χ_p) basis. A particular advantage of spin-coupled wave functions is that the same level of accuracy is generally maintained over wide ranges of the internuclear distance, both for expectation values and for response functions.

The inclusion of additional structures, by means of nonorthogonal CI calculations, provides a quantitative refinement of the expectation values, but does not in general introduce any new qualitative features. Of course, such refinement is only worthwhile if the initial basis set is of sufficient quality: as is well known, this is not always easy to attain.

We consider first of all the dipole moment function $\mu(R)$ of the $^1\Sigma^+$ ground state of the LiH molecule.[70] The spin-coupled wave function for this system takes the form $\{\sigma_1\sigma_2\sigma_3\sigma_4\}$, in which the four distinct nonorthogonal orbitals have been labeled according to their symmetry properties. Calculations were carried out by using the same large UET basis set as for CH^{4+} (see section IV.A). Orbitals σ_1 and σ_2 are essentially Li(1s) core orbitals, with an overlap of $\Delta_{12} \approx 0.93$, which varies very little with internuclear distance. This suggests that the core correlation, in the spin-coupled context, remains constant to a very good approximation as the internuclear distance varies. Orbital σ_4 is almost entirely a hydrogen 1s function, and undergoes no more than minor changes as the two atoms approach. However, there are substantial changes in orbital σ_3: at long range, it takes the form of a Li(2s) orbital, but as the internuclear distance decreases, it shows considerable delocalization onto the H nucleus.

The variation of the calculated dipole moment function with R is shown in Figure 21, in which it is

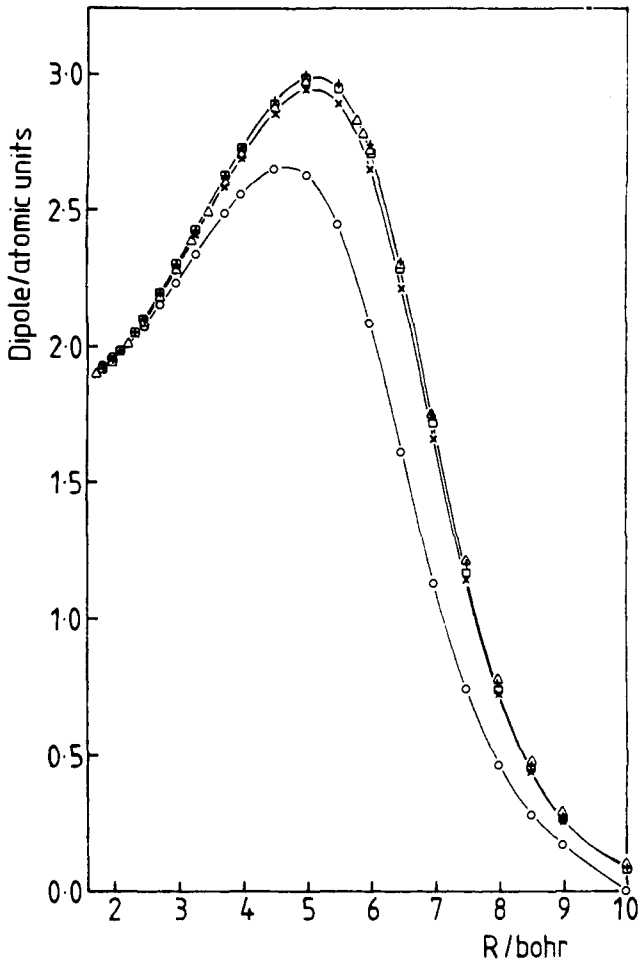

Figure 21. Dipole moment functions $\mu(R)$ for LiH ($X^1\Sigma^+$): ○, spin-coupled configuration; ×, 78 configurations, □, 127 configurations; +, 188 configurations, Δ, CI results from ref 71.

compared with values from the CI calculations of Partridge and Langhoff.[71] It is clear that the spin-coupled results for $\mu(R)$ possess the correct functional form, increasing in value from $R \approx 2$ bohr to a maximum around 5 bohr, and then falling to zero close to 10 bohr. In particular, the calculations provide accurate values of $d\mu/dR$ near the equilibrium internuclear distance, which determine the intensity of infra-red absorption.

Excited configurations were constructed exactly as described in section II.D, using the occupied orbitals plus virtual orbitals taken from the stacks arising from ϕ_3 and ϕ_4, and a series of SCVB calculations of increasing size were carried out. These calculations used the first n virtual orbitals of σ symmetry and the first n virtual orbitals of symmetries π_x and π_y: for $n = 2$ this gives rise to 78 configurations, for $n = 3$ to 127, and for $n = 4$ to 188. The resulting dipole moment functions are displayed in Figure 21. It is clear that this sequence of calculations, with 1, 78, 127, and 188 configurations, converges rapidly onto the results from the large CI calculations. Indeed, it becomes difficult to distinguish in Figure 21 between the different calculations.

The results of the 188-configuration SCVB study of the dipole moment function are compared in Table XI with those from the accurate CASSCF study of Roos and Sadlej,[72] who employed a polarized basis set especially suited to the calculation of electric multipole moments. The similarity between the two sets of values

TABLE XI. Comparison of Dipole Moment Functions $\mu(R)$ for LiH[a]

R, bohr	$\mu(R)$, au	
	CASSCF	SCVB
2.734	2.1813	2.194
2.965	2.2725	2.286
3.015	2.2921	2.306
2.065	2.3139	2.327
3.362	2.4422	2.456

[a] The different calculations are identified in the text. The SCVB values listed here were obtained by interpolation between the computed points.

is very satisfying, as is also the agreement of the vibrationally averaged results with experimental quantities (for $J = 1$).

In view of the large dipole moment for LiH, it is natural to expect that the corresponding negative ion will be stable with respect to electron detachment. LiH^- has never been observed experimentally, but various theoretical studies suggest that this anion possesses a stable ground electronic state. We find that the spin-coupled description of LiH^- ($X^2\Sigma^+$) is very similar to that described above for LiH ($X^1\Sigma^+$): the "extra" electron occupies a diffuse nonbonding sp^x hybrid orbital localized on lithium and directed away from the H atom. The anion is predicted to be bound, even at the spin-coupled level of theory, and it has proved possible to calculate accurate potential energy curves and vibrational constants using a compact SCVB wave function consisting of just 55 configurations.[73] Similarly, compact SCVB wave functions provide an accurate value for the electron affinity of the lithium atom.[74]

Molecular response functions can be determined for spin-coupled wave functions using the expression

$$\partial^2 E/\partial\lambda^2 = \Delta^{-1}\{\langle\Psi^{(1)}|H^{(1)}-E^{(1)}|\Psi^{(0)}\rangle + \langle\Psi^{(0)}|H^{(1)}-E^{(1)}|\Psi^{(1)}\rangle + \langle\Psi^{(0)}|H^{(2)}|\Psi^{(0)}\rangle\} \quad (34)$$

in which λ is the external perturbation (an electric or magnetic field), and

$$E^{(1)} = \partial E/\partial\lambda = \Delta^{-1}\langle\Psi^{(0)}|H^{(1)}|\Psi^{(0)}\rangle$$

$$H^{(1)} = \partial H/\partial\lambda$$

$$H^{(2)} = \partial^2 H/\partial\lambda^2$$

$$\Psi^{(1)} = \partial\Psi/\partial\lambda \quad (35)$$

For external electric fields, $H^{(2)}$ is zero. Other response functions, such as nuclear magnetic shieldings and chemical shifts, are given by mixed second derivative expressions of the form $\partial^2 E/\partial\lambda\partial\mu$, where λ and μ represent two distinct perturbations. In the case of nuclear magnetic shielding, for example, λ would be an external magnetic field and μ the internal field due to a nuclear magnetic moment.

In order to evaluate $\partial^2 E/\partial\lambda^2$ via eq 34, it is necessary to determine the first-order perturbed wave function $\Psi^{(1)} = \partial\Psi/\partial\lambda$. This in turn requires the determination of the derivatives of the spin-coupled orbitals, $\phi_\nu^{(1)} = \partial\phi_\nu/\partial\lambda$, since

$$\Psi^{(1)} = \sum_{\nu=1}^{N} \{\phi_1\phi_2\cdots\phi_\nu^{(1)}\cdots\phi_N\} \quad (36)$$

The $\phi_\nu^{(1)}$ are obtained from equations of the general type

$$\sum_{\nu=1}^{N} G(\mu,\nu)\phi_\nu^{(1)} = \Delta^{-1}b_\mu \quad (37)$$

where the elements of the vector **b** are determined by the particular perturbation of interest. For real perturbations, such as an external electric field, the $G(\mu,\nu)$ are obtained directly from the corresponding block of the second derivative or hessian matrix, **G**, described in section II.C. For an external magnetic field, $G(\mu,\nu)$ is somewhat different, and must be constructed separately. In the case of a magnetic field, both $\phi_\nu^{(1)}$ and b_μ are pure imaginary.

The procedure just outlined is a fully coupled "perturbed spin-coupled" theory.[75] The essential step is the determination of the $\phi_\nu^{(1)}$ from eq 37, followed by the evaluation of $\partial^2E/\partial\lambda^2$ in eq 34. The computation is very rapid and a wide range of different response functions can be studied, provided that the various property integrals are available.

A simple but nontrivial test case is that of the H_2 molecule in its $X^1\Sigma^+$ ground state, for which it is possible to compare with extremely accurate theoretical values of the electric dipole polarizability α and the magnetic susceptibility κ over a wide range of internuclear distances. Figure 22b shows α_{zz}, α_{xx}, and $\bar{\alpha}$ as functions of R, as determined by Rychlewski[76] using a wave function of the Kołos-Wolniewicz type; these results are essentially exact. The analogous quantities from the perturbed spin-coupled approach, determined by using a [2s2p] basis set on each center, are shown in Figure 22a. It can be seen that the two sets of results are very close. The asymptotic value of the polarizability for H_2 is 9 atomic units, and that given by the spin-coupled calculation is 8.45 atomic units.

The determination of the magnetic susceptibility as a function of R throws into sharp focus questions of completeness of the basis set, and the associated gauge dependence. The $H^{(1)}$ terms in eq 34 give rise to the paramagnetic contribution to the total susceptibility, κ^p, and $H^{(2)}$ to the diamagnetic contribution, κ^d. As R increases, it is clear that these two contributions must undergo extensive cancellation, since the atomic susceptibilities are purely diamagnetic. The terms $\kappa_{xx}^p = \kappa_{yy}^p$, for example, increase sharply with R, whereas the diamagnetic parts $\kappa_{xx}^d = \kappa_{yy}^d$ decrease. The behavior of κ as a function of R constitutes a sensitive test of the completeness of the basis set; unless the basis set is effectively complete, a "magnetic catastrophe" will eventually occur, with the perpendicular part of κ tending toward $\pm\infty$.

Figure 23b shows the behavior of the different components of κ as determined by Rychlewski and coworkers,[77] again using a wave function of the Kołos-Wolniewicz type. The analogous quantities from the spin-coupled calculation are shown in Figure 23a. The two sets of results are very similar.

The polarizability and the magnetic susceptibility of LiH ($X^1\Sigma^+$) have been calculated with the perturbed spin-coupled method using a [8s5p/8s5p] basis set due to Roos and Sadlej.[72] We find that no "magnetic catastrophe" occurs when using this basis set. The

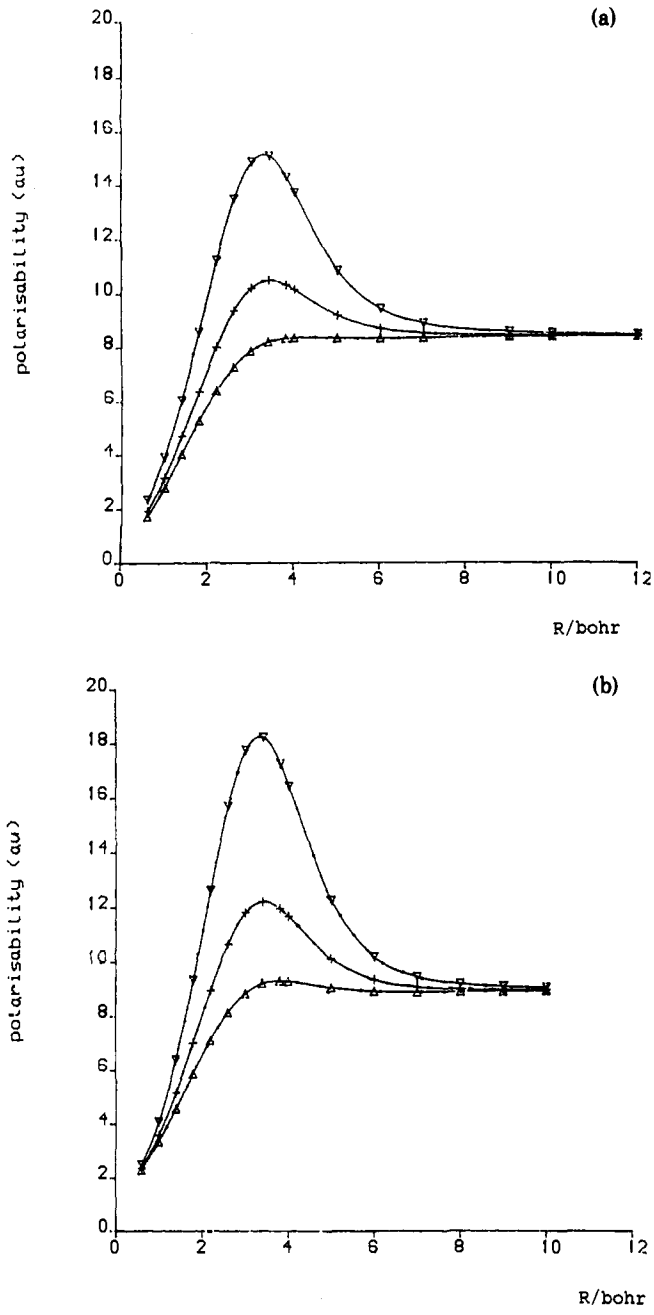

Figure 22. Variation with R of the polarizability of H_2 ($X^1\Sigma^+$). The quantities shown are α_{zz} (▽), $\alpha_{xx} = \alpha_{yy}$ (△) and $\bar{\alpha}$ (+): (a) spin-coupled calculation and (b) essentially exact results from ref 76.

variation of the different components of α with R is displayed in Figure 24. A recent calculation by Sasagane et al.,[78] using a time-dependent multiconfiguration method, leads to results which closely resemble those from the spin-coupled calculation for all values of R. Values have also been determined in a CASSCF calculation using a finite field:[79] the general shapes of the curves are similar to those from the spin-coupled calculations and to those reported by Sasagane et al., but the numerical values differ somewhat. The CASSCF calculation gives an asymptotic value of 152 atomic units, to be compared with 175 atomic units from the spin-coupled calculation, and with the known values of 168 atomic units for Li(^{2}S) plus 4.5 atomic units for H(^{2}S).

Preliminary spin-coupled calculations of the magnetic properties of benzene reproduce the expected anisot-

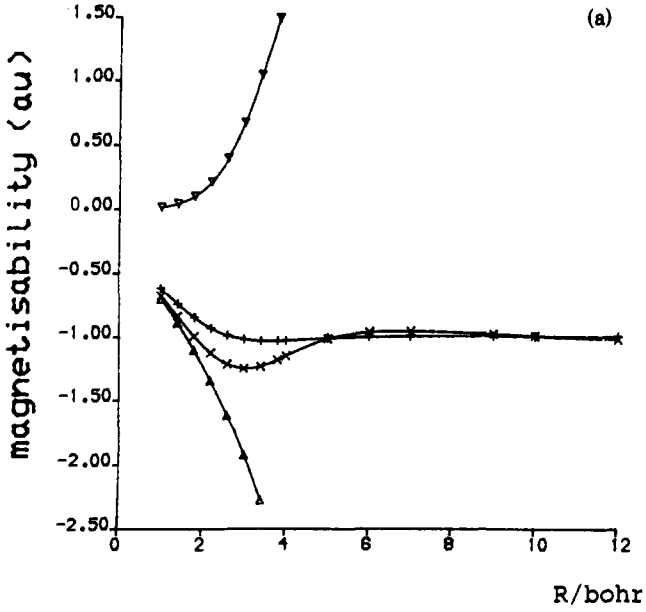

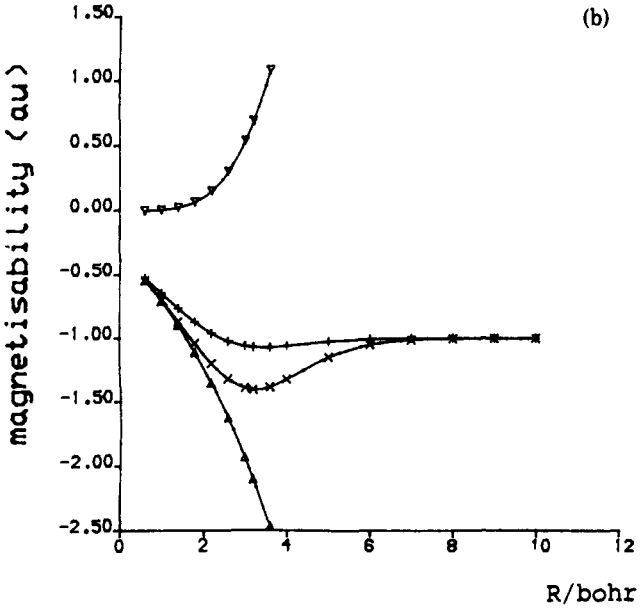

Figure 23. Variation with R of the magnetic susceptibility of H_2 ($X^1\Sigma^+$). The quantities shown are κ^d_{zz} (+), $\kappa^d_{xx} = \kappa^d_{yy}$ (△), $\kappa^p_{zz} = \kappa^p_{yy}$ (▽) and $\kappa_{xx} = \kappa_{yy}$ (×): (a) spin-coupled calculation; and (b) essentially exact results from ref 77.

ropy in the magnetic susceptibility. It is already clear that the spin-coupled description of this phenomenon must differ significantly from the conventional "ring current" model.

The examples described here demonstrate that spin-coupled wave functions can provide computed values of molecular properties to a very useful accuracy over a wide range of nuclear geometries, a feature which is not generally available from other methods. There are many possible directions for further progress in this aspect of spin-coupled theory, such as the determination of time-dependent response functions, which could be carried out by using methods similar to those outlined here. In view of the emphasis placed in the spin-coupled model on the different modes of spin coupling, a particularly promising direction for future development is the determination of spin-dependent properties, such as nuclear spin–spin coupling constants.

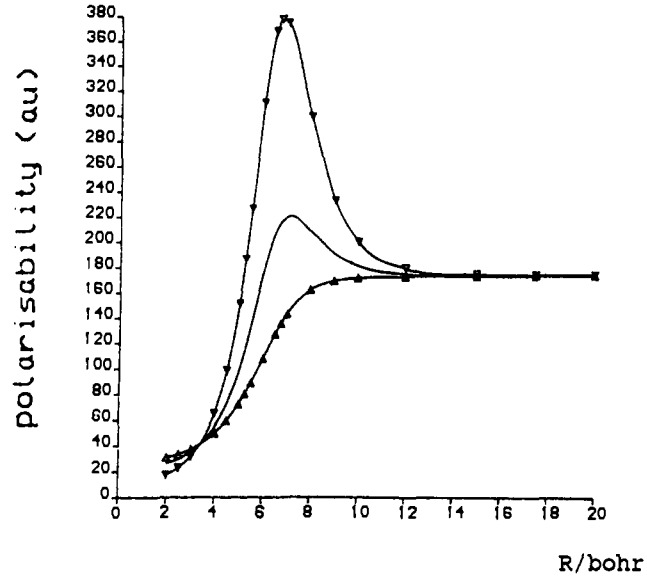

Figure 24. Variation with R of the polarizability of LiH ($X^2\Sigma^+$). The quantities shown are α_{zz} (▽), $\alpha_{xx} = \alpha_{yy}$ (△), and $\bar{\alpha}$ (—).

V. Conclusions

Spin-coupled valence bond theory is a sophisticated ab initio approach to molecular electronic structure which takes into account, from the outset, the chemically most important effects of electron correlation. The approach is based on the spin-coupled wave function, which consists of an antisymmetrized product of distinct, singly occupied, nonorthogonal orbitals and of all the allowed modes of coupling together the individual electron spins. Each of the orbitals is fully optimized without preconceptions as to the degree of localization and it is allowed to overlap freely with each of the others. In many cases, the optimal orbitals are found to be highly localized with obvious parentage in terms of deformed atomic functions. Familiar concepts, such as localized directed covalent bonds, arise naturally, simply by minimizing the energy.

The single-configuration spin-coupled wave function provides a highly visual model of the behavior of correlated electrons, and it is an excellent starting point for multiconfiguration calculations. Nevertheless, this quantitative refinement of the spin-coupled configuration does not lead to any significant change in the essential physical picture. Thus, the SCVB method provides accurate descriptions of molecular processes, while retaining a chemically appealing representation of the wave function in terms of simple orbital pictures and in terms of the different ways of pairing-up the electron spins.

Various representative applications have been described in this Review, indicating both the simplicity and utility of the descriptions that arise from applications of spin-coupled theory and the accuracy which can be achieved in SCVB (multiconfiguration) calculations. Whole areas of current activity have not been described here, such as the study of intermolecular forces (see for example ref 80) and the calculation of interionic potentials in solids.

The outlook for SCVB theory is very bright, both in terms of the development of improved algorithms and

in terms of extensions to the range of systems which can be studied. Concerning the first point, a generalization to the nonorthogonal problem of the unitary group algorithms used in state-of-the-art CASSCF codes looks particularly promising. Concerning the second, we are currently investigating, for example, the implications of the conclusions from "small molecule" studies for the electronic structure of crystalline solids.

Valence bond theory has come of age.

References

(1) Heitler, W.; London, F. *Z. Phys.* **1927**, *44*, 455.
(2) Coulson, C. A.; Fischer, I. *Philos. Mag.* **1949**, *40*, 386.
(3) Cooper, D. L.; Gerratt, J.; Raimondi, M. *Adv. Chem. Phys.* **1987**, *69*, 319.
(4) Cooper, D. L.; Gerratt, J.; Raimondi, M. *Int. Rev. Phys. Chem.* **1988**, *7*, 59.
(5) Cooper, D. L.; Gerratt, J.; Raimondi, M. *Top. Curr. Chem.* **1990**, *153*, 41 (*Advances in the Theory of Benzenoid Hydrocarbons*; Gutman, I., Cyvin, S. J., Eds.).
(6) Gerratt, J.; Cooper, D. L.; Raimondi, M. In *Valence bond theory and chemical structure*; Klein, D. J., Trinajstič, N., Eds.; Elsevier: Amsterdam, 1990.
(7) Cooper, D. L.; Gerratt, J.; Raimondi, M. *Mol. Simulation* **1990**, *4*, 293.
(8) (a) Werner, H.-J.; Knowles, P. J. *J. Chem. Phys.* **1985**, *82*, 5053. (b) Knowles, P. J.; Werner, H.-J. *Chem. Phys. Lett.* **1985**, *115*, 259.
(9) Pauncz, R. *Spin Eigenfunctions*; Plenum Press: New York, 1979.
(10) (a) Verbeek, J. Doctorate thesis, University of Utrecht, 1990. (b) van Lenthe, J. H.; Verbeek, J.; Pulay, P. The convergence and efficiency of the VBSCF method. *Mol. Phys.*, to be published.
(11) Gerratt, J. *Adv. Atom. Mol. Phys.* **1971**, *7*, 141.
(12) Sironi, M.; Cooper, D. L.; Gerratt, J.; Raimondi, M. To be published.
(13) Goldfeld, S. M.; Quandt, R. E.; Trotter, H. F. Research Memorandum No. 95 1968, Econometric Research Program, Princeton University.
(14) Gerratt, J.; Raimondi, M. *Proc. Roy. Soc. (Lond.) A* **1980**, *371*, 525.
(15) Coulson, C. A. *Valence*, 2nd edition; Oxford University Press, Oxford: 1961, p 162.
(16) Pauling, L. *Proc. Natl. Acad. Sci. U.S.A.* **1928**, *14*, 359. Pauling, L. *J. Am. Chem. Soc.* **1931**, *53*, 1367.
(17) Raimondi, M.; Campion, W.; Karplus, M. *Mol. Phys.* **1977**, *34*, 1483.
(18) Penotti, F.; Gerratt, J.; Cooper, D. L.; Raimondi, M. *J. Mol. Struct. (THEOCHEM)* **1988**, *169*, 421.
(19) Sironi, M.; Raimondi, M.; Cooper, D. L.; Gerratt, J. *J. Chem. Soc., Faraday Trans. 2* **1987**, *83*, 1651.
(20) Wright, S. C.; Cooper, D. L.; Sironi, M.; Raimondi, M.; Gerratt, J. *J. Chem. Soc., Perkin Trans. 2* **1990**, 369.
(21) (a) Skell, P. S.; Woodworth, R. C. *J. Am. Chem. Soc.* **1956**, *78*, 4496. (b) Skell, P. S.; Garner, A. Y. *J. Am. Chem. Soc.* **1956**, *78*, 5430. (c) Etter, R. M.; Skovronek, H. S.; Skell, P. S. *J. Am. Chem. Soc.* **1959**, *81*, 1008.
(22) Sironi, M.; Cooper, D. L.; Gerratt, J.; Raimondi, M. *J. Am. Chem. Soc.* **1990**, *112*, 5054.
(23) Bauschlicher, C. W.; Taylor, P. R. *J. Chem. Phys.* **1986**, *85*, 6510.
(24) Sironi, M.; Raimondi, M.; Cooper, D. L.; Gerratt, J. *J. Mol. Struct. (THEOCHEM)* **1991**, *229*, 279.
(25) Hiberty, P. C.; Shaik, S. S.; Lefour, J.-M.; Ohanessian, G. *J. Org. Chem.* **1985**, *50*, 4657.
(26) (a) Cooper, D. L.; Gerratt, J.; Raimondi, M. *Nature* **1986**, *323*, 699. (b) Gerratt, J. *Chem. Brit.* **1987**, *23*, 327. (c) Cooper, D. L.; Wright, S. C.; Gerratt, J.; Hyams, P. A.; Raimondi, M. *J. Chem. Soc., Perkin Trans. 2* **1989**, 719.
(27) Sironi, M.; Cooper, D. L.; Gerratt, J.; Raimondi, M. *J. Chem. Soc., Chem. Commun.* **1989**, 675.
(28) (a) Cooper, D. L.; Wright, S. C.; Gerratt, J.; Raimondi, M. *J. Chem. Soc., Perkin Trans. 2* **1989**, 255. (b) Cooper, D. L.; Wright, S. C.; Gerratt, J.; Raimondi, M. *J. Chem. Soc., Perkin Trans. 2* **1989**, 263.
(29) (a) Wright, S. C.; Cooper, D. L.; Gerratt, J.; Raimondi, M. *J. Chem. Soc., Chem. Commun.* **1989**, 1489. (b) Wright, S. C.; Cooper, D. L.; Gerratt, J.; Raimondi, M. The spin-coupled description of cyclobutadiene and 2,4-dimethylenecyclobutane-1,3-diyl: anti-pairs. To be published.
(30) (a) Norbeck, J. M.; Gallup, G. A. *J. Am. Chem. Soc.* **1973**, *95*, 4460. (b) Norbeck, J. M.; Gallup, G. A. *J. Am. Chem. Soc.* **1974**, *96*, 3386. (c) Gallup, G. A.; Norbeck, J. M. *J. Am. Chem. Soc.* **1975**, *97*, 970.
(31) Hiberty, P. C.; Cooper, D. L. *J. Mol. Struct. (THEOCHEM)* **1988**, *169*, 437. See also: Penotti, F. E. G.; Cooper, D. L.; Gerratt, J.; Raimondi, M. *J. Chem. Soc., Faraday Trans. 2* **1989**, *85*, 151.
(32) Garratt, P. J.; *Aromaticity*; John Wiley: New York, 1986; Chapter 11.
(33) (a) Davidson, E. R.; Borden, W. T.; Smith, J. *J. Am. Chem. Soc.* **1978**, *100*, 3299. (b) Du, P.; Hrovat, D. A.; Borden, W. T. *J. Am. Chem. Soc.* **1989**, *111*, 3773.
(34) (a) Feller, D.; Davidson, E. R.; Borden, W. T. *J. Am. Chem. Soc.* **1982**, *104*, 1216. (b) Budzelaar, P. H. M.; Krakar, E.; Cremer, D.; Schleyer, P. v. R. *J. Am. Chem. Soc.* **1986**, *108*, 561. (c) Snyder, G. J.; Dougherty, D. A. *J. Am. Chem. Soc.* **1989**, *111*, 3942.
(35) Li, X.; Paldus, J. Valence bond approach to the Pariser–Parr–Pople hamiltonian and its application to simple π-electron systems. *J. Mol. Struct. (THEOCHEM)*, in press.
(36) (a) Cooper, D. L.; Gerratt, J.; Raimondi, M.; Wright, S. C. *Chem. Phys. Lett.* **1987**, *138*, 296. (b) Cooper, D. L.; Gerratt, J.; Raimondi, M. *J. Chem. Soc., Perkin Trans. 2* **1989**, 1187.
(37) Pauling, L. *The nature of the chemical bond*, 3rd edition; Cornell University Press: Ithaca, NY, 1948; p 187.
(38) Koutecký, J.; Fantucci, P. *Chem. Rev.* **1986**, *86*, 539.
(39) (a) Fantucci, P.; Koutecký, J.; Pacchioni, G. *J. Chem. Phys.* **1984**, *80*, 325. (b) Boustani, I.; Pewestorf, W.; Fantucci, P.; Koutecký, J.; Bonačič-Koutecký, V. *Phys. Rev. B* **1987**, *35*, 9497.
(40) Rao, B. K.; Jena, P. *Phys. Rev. B* **1985**, *32*, 2058.
(41) Ray, A. K.; Hira, A. S. *Phys. Rev. B* **1988**, *37*, 9943.
(42) McAdon, M. H.; Goddard, W. A. *J. Phys. Chem.* **1987**, *91*, 2607.
(43) (a) McAdon, M. H.; Goddard, W. A. *Phys. Rev. Lett.* **1985**, *55*, 2563. (b) McAdon, M. H.; Goddard, W. A. *J. Non-Cryst. Solids* **1985**, *75*, 149.
(44) Lepetit, M. B.; Malrieu, J. P.; Spiegelmann, F. *Phys. Rev. B* **1990**, *41*, 8093.
(45) Tornaghi, E.; Cooper, D. L.; Gerratt, J.; Raimondi, M.; Sironi, M. To be published.
(46) Dunning, T. H.; Hay, P. J. In *Methods of electronic structure theory*; Schaefer, H. F., Ed.; Plenum: New York, 1977.
(47) Hehre, W. G.; Radom, L.; Schleyer, P. v. R.; Pople, J. A. *Ab initio molecular orbital theory*; Wiley Interscience: New York, 1986.
(48) (a) Gatti, C.; Fantucci, P.; Pacchioni, G. *Theor. Chim. Acta* **1978**, *72*, 413. (b) Cao, W. L.; Gatti, C.; MacDougall, P. J.; Bader, R. F. W. *Chem. Phys. Lett.* **1987**, *141*, 380. (c) Cioslowski, J. *J. Phys. Chem.* **1990**, *94*, 5496. (d) Cooper, D. L. *Nature* **1990**, *346*, 796.
(49) (a) Kleier, D. A.; Halgren, T. A.; Hall, J. H.; Lipscomb, W. N. *J. Chem. Phys.* **1974**, *61*, 3905. (b) Switkes, E.; Lipscomb, W. N.; Newton, M. D. *J. Am. Chem. Soc.* **1970**, *92*, 3847. (c) Epstein, I. R.; Marynick, D. S.; Lipscomb, W. N. *J. Am. Chem. Soc.* **1973**, *95*, 1760.
(50) Cooper, D. L.; Gerratt, J.; Raimondi, M. *J. Mol. Struct. (THEOCHEM)* **1991**, *229*, 155.
(51) Pipek, J.; Mezey, P. G. *J. Chem. Phys.* **1989**, *90*, 4916.
(52) Sironi, M.; Cooper, D. L.; Gerratt, J.; Raimondi, M. The electronic structure of diborane and $B_3H_8^-$: B–H–B bridges and closed BBB bonding. *J. Phys. Chem.*, in press.
(53) Greenwood, N. N.; Earnshaw, A. *Chemistry of the elements*; Pergamon Press: Oxford, 1984; p 175.
(54) (a) Loades, S. D.; Cooper, D. L.; Gerratt, J.; Raimondi, M. *J. Chem. Soc., Chem. Commun.* **1989**, 1604. (b) Cooper, D. L.; Loades, S. D.; Allan, N. L. *J. Mol. Struct. (THEOCHEM)* **1991**, *229*, 189. (c) Loades, S. D.; Cooper, D. L.; Gerratt, J.; Raimondi, M. To be published.
(55) (a) Chong, D. P.; Langhoff, S. R.; Bauschlicher, C. W.; Walch, S. P.; Partridge, H. *J. Chem. Phys.* **1986**, *85*, 2850. (b) Langhoff, S. R.; Pettersson, L. G. M.; Bauschlicher, C. W.; Partridge, H. *J. Chem. Phys.* **1987**, *86*, 268. (c) Pettersson, L. G. M.; Bauschlicher, C. W.; Langhoff, S. R.; Partridge, H. *J. Chem. Phys.* **1987**, *87*, 481.
(56) Loades, S. D.; Cooper, D. L.; Gerratt, J.; Raimondi, M.; Sironi, M. To be published.
(57) Barnes, L. A.; Bauschlicher, C. W. *J. Chem. Phys.* **1989**, *91*, 314.
(58) Cooper, D. L.; Gerratt, J.; Raimondi, M. *Mol. Phys.* **1985**, *56*, 611.
(59) Cooper, D. L.; Ford, M. J.; Gerratt, J.; Raimondi, M. *Phys. Rev. A* **1986**, *34*, 1752.
(60) Barnard, S. A.; Ford, M. J.; Cooper, D. L.; Gerratt, J.; Raimondi, M. *Mol. Phys.* **1987**, *61*, 1193.
(61) (a) Gargaud, M.; Hanssen, J.; McCarroll, R.; Valiron, P. *J. Phys. B: At. Mol. Phys.* **1981**, *14*, 2259. (b) Valiron P. Private communication.
(62) (a) Gargaud, M.; McCarroll, R.; Valiron, P.; Zannoli, G. *ICPEAC*, **1985**. (b) Valiron, P. Private communication.
(63) (a) Bacchus, M. C. Private communication. (b) Bacchus-Montabonel, M. C. *Phys. Rev. A* **1987**, *36*, 1994.

(64) Raimondi, M.; Gerratt, J. *J. Chem. Phys.* **1983**, *79*, 4339.
(65) Cooper, D. L.; Gerratt, J.; Raimondi, M. *Chem. Phys. Lett.* **1986**, *127*, 600.
(66) Walters, S. G.; Penotti, F.; Gerratt, J.; Raimondi, M. *Mol. Phys.* **1987**, *61*, 1341.
(67) Richardson, P. J.; Eland, J. H. D.; Fournier, P. G.; Cooper, D. L. *J. Chem. Phys.* **1986**, *84*, 3189.
(68) Cooper, D. L.; Gerratt, J.; Raimondi, M.; Sironi, M. *J. Chem. Phys.* **1987**, *87*, 1666.
(69) Sironi, M.; Cooper, D. L.; Gerratt, J.; Raimondi, M. *Mol. Phys.* **1988**, *65*, 251.
(70) Cooper, D. L.; Gerratt, J.; Raimondi, M. *Chem. Phys. Lett.* **1985**, *118*, 580.
(71) Partridge, H.; Langhoff, S. R. *J. Chem. Phys.* **1981**, *74*, 2361.
(72) Roos, B. O.; Sadlej, A. *Chem. Phys.* **1985**, *94*, 43.
(73) Ford, M. J.; Cooper, D. L.; Gerratt, J.; Raimondi, M. *J. Chem. Soc., Faraday Trans. 2* **1989**, *85*, 1713.
(74) Cooper, D. L.; Gerratt, J. *J. Phys. B: At. Mol. Phys.* **1983**, *16*, 3703.
(75) Hyams, P. A.; Cooper, D. L.; Gerratt, J.; Raimondi, M. To be published.
(76) Rychlewski, J. *Mol. Phys.* **1980**, *41*, 833.
(77) Rychlewski, J.; Raynes, W. T. *Mol. Phys.* **1980**, *41*, 843.
(78) Sasagane, K.; Mori, K.; Ichihara, A.; Itoh, R. *J. Chem. Phys.* **1990**, *92*, 3619.
(79) Roos, B. O.; Sadlej, A. *J. Chem. Phys.* **1982**, *76*, 5444.
(80) Raimondi, M. *Mol. Phys.* **1984**, *53*, 161.
(81) Moore, C. E. *Atomic Energy Levels*, National Bureau of Standards Reference Data System No. 35; U.S. Department of Commerce: Washington, DC, 1971 (and supplements).